

MASTER OF SCIENCE THESIS

# Exploration into the mechanisms that govern the stability of an Xbloc<sup>+</sup> v1 armour unit

by

A.B. Vos



August 14, 2017

Thesis Committee:	Prof.dr.ir. S.G.J. Aarninkhof	TU Delft, Chair
	Ir. H.J. Verhagen	TU Delft
	Dr.ir. B. Hofland	TU Delft
	Ir. B. Reedijk	BAM Infraconsult bv
	Ir. R. Jacobs	BAM Infraconsult bv

Master program:	Hydraulic Engineering
Section:	Coastal Engineering and Hydraulic Structures





---

List of trademarks used in this thesis:

- Delta Marine Consultants is a registered trade name of BAM Infraconsult bv, the Netherlands
- Accropode is a registered trademark of Artelia (Sogreah Consultants), France
- A-jack is a registered trademark of Armourtec, United States of America
- Basalton is a registered trademark of Holcim betonprodukten bv, Aalst, Netherlands
- Core-loc is a registered trademark of US Army Corps of Engineers, United States of America
- Crablock is a registered trademark of AM Marine Works, United Arab Emirates
- Cubipod is a registered trademark of S.A. Trabajos y Obras (SATO), Spain
- Haro is a registered trademark of NV Haecon, Belgium (until 2008)
- Hillblock is a registered trademark of Hill Innovations bv, Netherlands
- HydroBlock betonzuilen is a registered trademark of Betonfabriek Haringman, Goes
- Ronaton is a registered trademark of Altenagroep, 't Harde, Netherlands
- Xbloc is a registered trademark of Delta Marine Consultants, the Netherlands

The use of trademarks in any publications of Delft University of Technology does not imply any endorsement or disapproval of this product by the University.

---

**Master student**

Amber Balou Vos

Schieweg 86A  
3038BA, Rotterdam  
(+31)06-37373176  
amberbvos@gmail.com

**Thesis Committee**

Prof.dr.ir. S.G.J. Aarninkhof  
Ir. H.J. Verhagen  
Dr.ir. B. Hofland  
Ir. B. Reedijk  
Ir. R. Jacobs

TU Delft, Chair  
TU Delft  
TU Delft  
BAM Infraconsult bv  
BAM Infraconsult bv



**Delft University of Technology**

Faculty of Civil Engineering and Geosciences  
Stevinweg 1, Building 23  
2628 CN Delft / PO-box 5048  
The Netherlands  
(+31)015-2789802



**BAM Infraconsult bv**

H.J. Nederhorststraat 1  
2801 SC Gouda / PO-box 268  
The Netherlands  
(+31)0182-590510

# Preface

This is the final report written to obtain my Master's degree in the track Coastal Engineering, a specialization of the master Hydraulic Engineering at Delft University of Technology. An experimental study was performed in which the stability mechanisms of a new concrete armour unit were explored.

Physical model tests were carried out in the wave flume of the coastal department of BAM Infraconsult bv, also known as Delta Marine Consultants. Analysis of the results was mostly done at their main office in Gouda. The development of Xbloc<sup>+</sup> has created a lot of opportunities for MSc students, like me, to become familiar with the more practical side of Coastal Engineering, in particular, breakwater design. The experience gained by doing such practical work is, in my opinion, a most valuable tool in understanding the theory as tutored at the Faculty of Civil Engineering and Geosciences. I would like to thank BAM Infraconsult bv for making this possible.

My thesis committee is the second group of people who I'd like to thank. Each meeting they gave me something to think about which helped me to obtain a better understanding of the subject. Their readiness for answering questions, sometimes even when on holiday, is very much appreciated.

Thirdly I would like to thank the colleagues at Delta Marine Consultants for assisting me with valuable knowledge on the practical application and execution of model work. An extra thanks go out to Robert and Jay, who always made me laugh when they thought I wasn't listening and Mark who kept me grounded. Also a thank you goes out to the guys in the asphalt lab for help with the manual labour.

Lastly I would like to especially thank; Noor, who helped me coming to terms with the process and who was impressed when I wasn't, Huize Eende, who's inhabitants helped me to see that everything is relative, my parents and sis, who helped me see the subject through the eyes of non-civil engineers and gave me space when I needed to, and Bart, for without his continuous support and capability to make me laugh it all would have been a lot harder.

This report finalizes my years as a student, which I am quite sad about but it also ushers in the coming years of getting familiar with the work field of a Civil Engineer, which is something I'm looking forward to.

*Amber Balou Vos  
August 14, 2017*



# Summary

For the fortification of the Afsluitdijk, BAM Infraconsult bv proposed an armour layer design with Xbloc units. After evaluation it was concluded that, for aesthetic reasons, Xbloc units were only to be used when placed with uniform orientation. This is possible but causes the effectiveness per block to decrease by 30% which has to be compensated by increasing the concrete volume and, consequently, the design costs. As an alternative to Xbloc, a new concrete armour unit has been developed which is placed with a uniform orientation: Xbloc<sup>+</sup>. This thesis discusses the first version of this unit: Xbloc<sup>+</sup> v1. As this new block is still under development, insights are required on the performance under various conditions.

The main goal of this thesis is *'to find the failure mechanism(s) that dominate Xbloc<sup>+</sup> v1 and modify its shape such that an armour layer made out of Xbloc<sup>+</sup> v2 armour units will be more stable'* and the resulting main question reads *"how does the shape of the uniformly placed single layer concrete armour unit Xbloc<sup>+</sup> v1 affect the armour layer stability?"*. To answer the main question, the most important stability mechanisms and the response to wave loading were investigated. Two different type of model tests were performed to test both above-mentioned aspects: dry pull-out tests and 2D hydraulic physical model tests.

Based on knowledge of other blocks, a hypothesis was formed with respect to the stability mechanisms. It was expected that the stabilizing mechanisms of Xbloc<sup>+</sup> v1 consists of own weight, interlocking and friction, of which the first two would be the main mechanisms; and, furthermore, that the stability was increased for an increasing number of rows and a decreasing under layer roughness. Dry pull-out tests have been performed in which the extraction force as function of the unit weight was measured for small Xbloc<sup>+</sup> v1 units of 58 gr. This was done with smooth (plastic) as well as rough (concrete) model units for four different levels on the slope (5, 10, 15 and 20 rows below the top) and for two different force directions (under an angle of 45 degrees and perpendicular to the slope). In total, 23 pull-out tests on a 3:4 slope were conducted.

The pull-out tests showed that there is a large difference between the plastic and the concrete units for both pull-directions. For the 90° pull-direction the concrete units have on average 55% larger resistance against pulling out, for the 45° pull-direction this is on average 21%. Since in this model, the only difference between the units is their surface roughness, the friction mechanism contributes significantly to the armour layer stability. However, since friction cannot be scaled correctly this might not be the case in prototype. The interlocking mechanism contributes less than expected and is dependent on the force direction. Following the up-slope wave force, the force perpendicular to the slope is largest, followed by the down-slope force. It is concluded that, from the tested directions, the armour unit is least stable in a direction perpendicular to the slope.

Failure mechanisms and placing difficulties related to both pattern placed blocks and concrete armour units have been observed. To investigate if Xbloc<sup>+</sup> v1 behaves more like a pattern placed block or an armour unit, Xbloc<sup>+</sup> v1 and both armouring concepts have been compared based on the load factor. This showed that, although Xbloc<sup>+</sup> v1 experienced some pattern-placed characteristic problems, it is in fact a concrete armour unit.

Based on the obtained data, observations and conclusions from the pull-out tests, 2D hydraulic physical model tests were conducted in the wave flume of Delta Marine Consultants in Utrecht. A typical breakwater cross-section in deep water was subjected to a JONSWAP wave spectrum with constant wave steepness. The significant wave height and wave period were stepwise increased until failure occurred. With respect to wave action it was expected that there would be a large difference between the performance of the plastic and concrete armour units since in the absence of a strong interlocking mechanism friction plays a large role. Also, any surface profile irregularities could be an indication for weak spots as at those locations there is not enough surface contact to provide the friction needed.

---

Lastly, it was expected that the stability number of Xbloc<sup>+</sup> v<sup>1</sup> would be between 2.0 and 3.3 for failure.

The model had the following characteristics: a water depth of 50 cm, a slope angle of 3:4, model units with a width of 4.7 cm, a freeboard of 25 cm, an under layer with a median weight of  $1/11$  of the armour unit weight, a JONSWAP spectrum with  $\gamma = 3.3$ , a wave steepness of 4% and an initial step size of 2 cm with respect to  $H_s$ . The slopes were stable up until a stability number ( $\frac{H_s}{\Delta D_n}$ ) of 1.75. The start of damage has been observed at a stability number of 2.0 with 2.44 on average and the first failure at 2.25 with 2.59 on average. The stability, as measured in 1 preliminary test, could only be reproduced when comparing the concrete units using a stability number based on the extreme wave height  $H_{0.1\%}$  instead of the significant wave height  $H_s = H_{1/3}$ . This is because the preliminary test made use of a 1:30 foreshore and had shallow water ( $h < 2.5 \cdot H_s$ ) while the tests in the current study were conducted in deep water ( $h > 3.5 \cdot H_s$ ) without foreshore. The difference in geometrical configurations and armour unit specific characteristics, such as packing density, make it impossible to compare different units on a quantitative basis. Compared on a qualitative basis, Xbloc<sup>+</sup> v<sup>1</sup> is on the right track of becoming a good competitor.

Again, a difference between the performance of plastic and concrete units was observed. On the slopes with plastic units, elements were extracted earlier than on the slopes with concrete units. When the step size was decreased from 2 cm with respect to  $H_s$ , to 1 cm with respect to  $H_{0.1\%}$ , the slope was compacted by multiple lower runs. This resulted in an increase of stability such that the single plastic test with small step size performed similar to the concrete tests on average.

The 2D hydraulic physical model tests showed, in accordance with the pull-out tests, that the armour unit indeed depends mainly on friction and that the armour unit has a low interlocking mechanism. Armour units could be easily rotated during up-rush and, after losing their stable foundation on the under layer, would start to rock. When a large wave disintegrated on the slope and water flowed out of the structure, the rocking units were pulled out. This observation has been contributed to the combined influence of a low interlocking mechanism and low armour layer porosity.

It is recommended that for the design of Xbloc<sup>+</sup> v<sup>2</sup> the interlocking capacity is increased by rotating the chamfers such that they are almost vertical. Also, the permeability of the armour layer is too low, making the armour layer vulnerable to uplift. This can be counteracted by incorporating a hole through the armour unit, perpendicular to the slope. Another solution is to increase the gaps between the armour units, just as is done for Single Layer Cubes. Lastly it is advised that the friction mechanism is improved by rotating the friction surfaces such that they are perpendicular to the slope, just as they are for other uniformly oriented units and pattern-placed blocks like Haro, Single layer cubes and Basalton. Additionally this will also result in an easier to place armour unit. These alterations are expected to have a positive impact on the stability of the layer. Especially the increase of the interlocking mechanism is of importance as preventing rotation of a unit also prevents it to be extracted.

From both the pull-out and hydraulic model tests it was concluded that the surface roughness of the units has a large impact on the results. It has also been found that the smooth units can perform similar to the rough units if the wave load is slowly increased. For reference, pull-out and hydraulic tests for a simple reference case should be done with both concrete and plastic Crablock (uniformly placed but influenced by friction as well as by interlocking) and Xbloc (interlocking dominated) units. If there is a large difference between plastic and concrete in these tests, any hydraulic model tests executed with concrete units might have given an overestimation of the stability, both for friction and interlocking dominated armour units.

*NOTE: The armour unit discussed in this thesis is the first version of Xbloc<sup>+</sup>, namely the Xbloc<sup>+</sup> v<sup>1</sup>. The conclusions and recommendations from the practical work done for this thesis lead to alterations of the armour unit design. As this report was being written, physical model tests with the next version of Xbloc<sup>+</sup> were conducted by Rada [2017] and Moreno [2017], who focussed on stability and overtopping. The viewer is referred to these master theses for an evaluation of the most recent design.*



# Contents

<b>Preface</b>	<b>iii</b>
<b>Summary</b>	<b>v</b>
<b>Contents</b>	<b>ix</b>
<b>List of Symbols</b>	<b>x</b>
<b>Chapter 1 Introduction</b>	<b>1</b>
1.1 Positioning of the subject . . . . .	1
1.2 Incentive for this report . . . . .	1
1.3 Problem analysis . . . . .	2
1.4 Objective . . . . .	3
1.5 Approach . . . . .	4
1.6 Thesis Outline . . . . .	4
<b>Chapter 2 Background information</b>	<b>6</b>
2.1 Waves . . . . .	6
2.1.1 Wave characteristics . . . . .	6
2.1.2 Wave growth . . . . .	8
2.1.3 Wave height in deep and shallow water . . . . .	9
2.1.4 Waves on a slope . . . . .	11
2.2 Design of Armour layers . . . . .	11
2.2.1 Breakwaters in general . . . . .	11
2.2.2 Concrete armour units . . . . .	12
2.2.2.1 Stability . . . . .	14
2.2.2.2 Damage progression . . . . .	16
2.2.2.3 Failure mechanisms . . . . .	17
2.2.2.4 Influence of structural parameters on the armour layer stability . . . . .	17
2.2.3 Placed blocks . . . . .	19
2.2.3.1 Stability . . . . .	20
2.2.3.2 Failure mechanisms . . . . .	20
2.3 Model testing . . . . .	20
2.3.1 Scale rules . . . . .	21
2.3.2 Generally used method and scale-effects . . . . .	21
2.3.3 Physical models . . . . .	22
2.4 Xbloc <sup>+</sup> v1 . . . . .	23
2.4.1 Design process leading to Xbloc <sup>+</sup> v1 . . . . .	23
2.4.2 Characteristics . . . . .	24
2.4.3 Previous hydraulic model tests . . . . .	25
2.4.4 Comparable units . . . . .	26
2.4.4.1 Crablock . . . . .	26
2.4.4.2 Single Layer Cube . . . . .	27
<b>Chapter 3 Hypotheses</b>	<b>28</b>
3.1 Stabilising mechanisms . . . . .	28

3.1.1	Hypothesis . . . . .	29
3.2	Wave action . . . . .	29
3.2.1	Hypothesis . . . . .	30
<b>Chapter 4</b>	<b>Experiment set-up</b>	<b>31</b>
4.1	Pull-out tests . . . . .	31
4.1.1	Set-up and geometry . . . . .	31
4.1.2	Test program . . . . .	32
4.1.3	Methodology . . . . .	33
4.2	Hydraulic physical model tests . . . . .	34
4.2.1	Set-up . . . . .	34
4.2.2	Geometry . . . . .	35
4.2.3	Test program . . . . .	38
4.2.4	Methodology . . . . .	39
<b>Chapter 5</b>	<b>Analysis</b>	<b>40</b>
5.1	Pull-out tests . . . . .	40
5.1.1	Results . . . . .	40
5.1.2	Visual observations . . . . .	42
5.1.3	Analysis . . . . .	45
5.1.4	Reflection on hypothesis . . . . .	47
5.2	Hydraulic physical model tests . . . . .	48
5.2.1	Presentation of results . . . . .	48
5.2.2	Visual observations . . . . .	50
5.2.3	Analysis . . . . .	52
5.2.3.1	Comparison with preliminary test . . . . .	52
5.2.3.2	Friction properties . . . . .	54
5.2.3.3	Step size . . . . .	55
5.2.3.4	Concrete armour unit or Pattern placed block . . . . .	57
5.2.3.5	Slope angle . . . . .	59
5.2.4	Reflection on hypothesis . . . . .	60
<b>Chapter 6</b>	<b>Conclusions and Recommendations</b>	<b>61</b>
6.1	Pull-out tests . . . . .	61
6.1.1	Conclusions . . . . .	61
6.1.2	Recommendations . . . . .	62
6.2	Hydraulic physical model tests . . . . .	63
6.2.1	Conclusions . . . . .	63
6.2.2	Recommendations . . . . .	64
6.3	Final conclusions and recommendations . . . . .	64
6.3.1	Conclusions and recommendations . . . . .	64
<b>Bibliography</b>		<b>68</b>
<b>List of Figures</b>		<b>70</b>
<b>List of Tables</b>		<b>i</b>
<b>Appendix A</b>	<b>Model Units</b>	<b>ii</b>
<b>Appendix B</b>	<b>LSH Load Cell</b>	<b>iv</b>
<b>Appendix C</b>	<b>Under layer composition(s)</b>	<b>v</b>
<b>Appendix D</b>	<b>Photo series Pull-out tests</b>	<b>vi</b>
<b>Appendix E</b>	<b>Applicable wave theory</b>	<b>viii</b>

<b>Appendix F</b>	<b>Core Material</b>	<b>x</b>
F.1	Theory on Core Scaling . . . . .	x
F.2	Core composition . . . . .	xi
<b>Appendix G</b>	<b>Actual wave heights</b>	<b>xii</b>
<b>Appendix H</b>	<b>Log physical hydraulic model tests</b>	<b>xiii</b>
<b>Appendix I</b>	<b>Before and after photographs hydraulic physical model tests</b>	<b>xviii</b>

# List of Symbols

**Table 1:** List of Latin Symbols

Latin parameters	Explanation	Units
$A_c$	Eroded cross-sectional area	[m <sup>2</sup> ]
$B$	Berm width	[m]
$B$	Unit width	[m]
$B_a$	Armour layer width	[m]
$d$	1. Water depth 2. Stone diameter	[m] [m]
	3. Height of the structure	[m]
	4. Thickness of the blocks	[m]
$d_f$	Thickness of the filter layer	[m]
$d_{n50}$	Nominal median sieve diameter	[m]
$d_t$	Thickness of the top layer	[m]
$D$	Characteristic armour unit size	[m]
$D_{cu}$	Unit layer thickness	[m]
$D_n$	Nominal cubic unit diameter	[m]
$D_{n50}$	Nominal median unit diameter	[m]
$D_x$	Horizontal placing distance	[m]
$D_y$	Up-slope placing distance	[m]
$f$	Friction coefficient	[-]
$F$	(Pull) Force	[N]
$F_{down}$	Down-slope directed force	[N]
$F_{normal}$	Slope-normal directed force	[N]
$F_{up}$	Up-slope directed force	[N]
$F_{\perp}$	Measured maximum pull force perpendicular to the slope	[kg]
$Fr$	Froude number	[-]
$g$	Gravitational acceleration	[m/s <sup>2</sup> ]
$G$	Observed unit weight	[kg]
$h$	Water depth	[m]
$h_t$	Water depth at the toe	[m]
$H$	1. Actual wave height 2. Unit height	[m] [m]
$H_{1/x}$	Mean of the highest $1/x$ of the waves	[m]
$H_D$	Design wave height	[m]
$H_{max}$	Maximum wave height in a time series	[m]
$H_{m0}$	Significant wave height as obtained via spectral analysis	[m]
$H_{rms}$	Root mean square wave height, exceeded by 37% of all waves	[m]
$H_s$	Significant wave height: 1. Mean of highest $1/3$ of the waves obtained from a time series analysis 2. (Spectral) Significant wave height obtained from spectral analysis	[m] [m]
$H_{tr}$	Transitional wave height	[m]
$H_x$	Observed wave height	[m]
$H_{x\%}$	Wave height exceeded by $x\%$ of the waves	[m]
$I$	Horizontal pressure gradient	[-]
$k_f$	Permeability of the filter layer	[m <sup>2</sup> ]
$k_t$	Permeability of the top layer	[m <sup>2</sup> ]
$K_D$	Stability parameter	[-]

*Continued on next page*

Table 1 – Continued from previous page

Latin parameters	Explanation	Units
$L$	1. Wave length 2. Unit length	[m] [m]
$L_p$	Wave length based on peak wave period	[m]
$L_0$	Deep water wave length	[m]
$m_0$	Zero <sup>th</sup> order moment in the wave spectrum	[m <sup>4</sup> ]
$M$	Stone or unit mass	[kg]
$n$	porosity	[-]
$n_{lf}$	Load factor expressed in number of elements	[#]
$n_v$	Volumetric porosity	[-]
$N$	Number of waves	[#]
$N_{\#d}$	Number of units displaced more than $0.5D_n$	[#]
$N_{od}$	Number of displaced units	[#]
$N_s$	Stability number	[-]
$N_{Ursell}$	Ursell number	[-]
$P$	1. Exceedance probability 2. Notial permeability	[-] [-]
$R_c$	Relative freeboard	[m]
$R_{d,max}$	Maximum run down	[dm <sup>3</sup> /s]
$Re$	Reynolds number	[-]
$RPD$	Relative packing density	[-]
$s$	Wave steepness	[-]
$s_{0p}$	Fictitious wave steepness based on the deep water wave length	[-]
$s_{max}$	Maximum wave steepness	[-]
$S$	Dimensionless damage level	[-]
$SWL$	Sea Water Level	[-]
$t_a$	Thickness of the armour layer	[m]
$t_f$	Thickness of the under layer	[m]
$t_u$	Thickness of the filter layer	[m]
$T$	Wave period	[s]
$T_p$	Peak wave period	[s]
$U$	Flow velocity	[m/s]
$V$	1. Unit volume 2. Voltage	[ml] [V]
$W$	Stone or unit weight	[N]
$W_{50,under}$	Median weight of the under layer	[N]
$W_{armour}$	Armour unit weight	[N]
$W_{dry}$	Dry armour unit weight	[N]
$W_{sat}$	Saturated armour unit weight	[N]
$W_{wet}$	Wet armour unit weight	[N]
$x_{1\&2}$	Distance between wave gauge 1 and 2	[m]
$x_{1\&3}$	Distance between wave gauge 1 and 3	[m]

Table 2: List of Greek symbols

Greek parameters	Explanation	Units
$\alpha$	1. Slope angle 2. Grain shape coefficient in the pressure gradient formula	[°] [-]
$\alpha_f$	Foreshore slope angle	[°]
$\beta$	1. Unit rotation angle 2. Grading coefficient in the pressure gradient formula	[°] [-]
$\delta_s$	Band width of experimental data	[ ]

Continued on next page

Table 2 – Continued from previous page

<b>Greek parameters</b>	<b>Explanation</b>	<b>Units</b>
$\Delta$	Relative buoyant density	[-]
$\theta$	Pulling angle in dry pulling tests	[°]
$\Lambda$	Leakage length	[°]
$\nu$	Kinematic viscosity	[m <sup>2</sup> /s]
$\phi$	Internal friction angle	[°]
$\rho_c$	Density of concrete	[kg/m <sup>3</sup> ]
$\rho_{c,sat}$	Density of saturated concrete	[kg/m <sup>3</sup> ]
$\rho_r$	Density of rock	[kg/m <sup>3</sup> ]
$\rho_w$	Density of water	[kg/m <sup>3</sup> ]
$\xi$	Iribarren number	[-]
$\xi_{0p}$	Iribarren number based on the deep water wave length	[-]
$\xi_p$	Iribarren number based on peak period	[-]

# Chapter 1: Introduction

This chapter is the introduction to the presented research and serves as a guide for the rest of this report. Firstly, the importance of breakwater armour layer stability will be explained. After this, the new uniformly oriented single layer concrete armour unit called Xbloc<sup>+</sup> will be introduced. In the third section, a problem analysis is given that results in the objectives for this research being formed in the fourth section. Hereafter, the approach used for answering the main question is elaborated on. The chapter ends with an explanation on how this report should be read and interpreted.

## 1.1 Positioning of the subject

All across the world defences are built to give land and harbours shelter to wind-induced waves, erosion and sedimentation. In absence of land directly behind a defence, breakwaters are often built near the entrance of harbours where waves hinder the passing vessels. A breakwater literally brakes waves, thereby reducing the energy in the propagating waves such that its wave height and wavelength are reduced. It is part of a coastal defence system and should, therefore, have a high reliability. Failure of a breakwater may have serious consequences for the hinterland. Depending on the hinterland's economic value, breakwaters with varying failure probabilities are built. There are several types of breakwaters but this thesis will be limited to discussing rubble mound breakwaters, and specifically the stability of armour layers constructed of concrete armour units.

Originally, rubble mound breakwaters were constructed with rock of various size and shape which was strong enough to withstand wave action in small ports. As ports grew bigger, breakwaters were situated in deeper water, resulting not only in higher waves and larger stones but also in a greater amount of rubble needed to complete the structure. At some locations, the material demand could not be satisfied, either due to the absence of a quarry or through economical reasons due to the required stone size. As a solution, concrete armour units that could fulfil the same task were developed. The armour units could be made on site in any size, making them superior to rock. At first, they were placed similar application rules as for rock: an armour layer should have a thickness of at least two times the units nominal diameter. However, this requires a lot of concrete. The stabilising mechanism of these first blocks was based on the block weight and friction between blocks solely.

New armour units were developed such that a breakwater's main costs, the concrete usage, is decreased. In contrast to the earlier units, which were placed in a double layer, these units could be placed in a single layer. The stabilising mechanism for these blocks consisted of the combined influence of the weight of the block, friction between blocks and interlocking. Nowadays, armour units placed in a single layer are dominating breakwater design.

The main purpose of breakwaters is to reduce storm-impact on the protected area, for which its stability against wave-action is of great importance. Changing geometrical demands and more intense storm conditions lead to innovative breakwater design and, consequently, new concrete armour units. The most recent development is the design of a concrete armour unit by Delta Marine Consultants, namely the Xbloc<sup>+</sup>. This thesis will discuss the hydraulic stability of the first version of this block, the Xbloc<sup>+</sup> v1, under wave loading.

## 1.2 Incentive for this report

The most important defensive structure against water in the Netherlands is the Afsluitdijk. A design upgrade is planned in the near future since, at the moment, it does not meet the safety standards imposed by the government. In the new design, the Afsluitdijk has a steeper outer slope with a berm. For the outer slope protection, BAM Infraconsult made a suitable design with Xbloc units. The design was discussed and it was concluded that, for aesthetic reasons, Xbloc units were to be used only when

placed with uniform orientation. This is possible with Xbloc but causes the effectiveness per block to decrease by 30% which has to be compensated by increasing the concrete volume and, consequently, the design costs.

Next to the aesthetic drawback, Xbloc appears to also have a practical drawback. The main benefit of Xbloc is that the placement is very simple: the crane controller places the unit, hanging off a sling, with one of its four legs on a predefined staggered grid, as depicted in Figure 1.1a. By decreasing the tension on the sling, the Xbloc unit finds its most stable orientation on the slope. In practice, however, crane controllers feel inclined to give the units a little push to position them in a specific direction and speed up the placement process. This small manipulation leads to the formation of columns or loss of interlocking, resulting in a decreased stability of the slope. Correcting the manipulated orientation is time-consuming and could better be spent on placing other units.

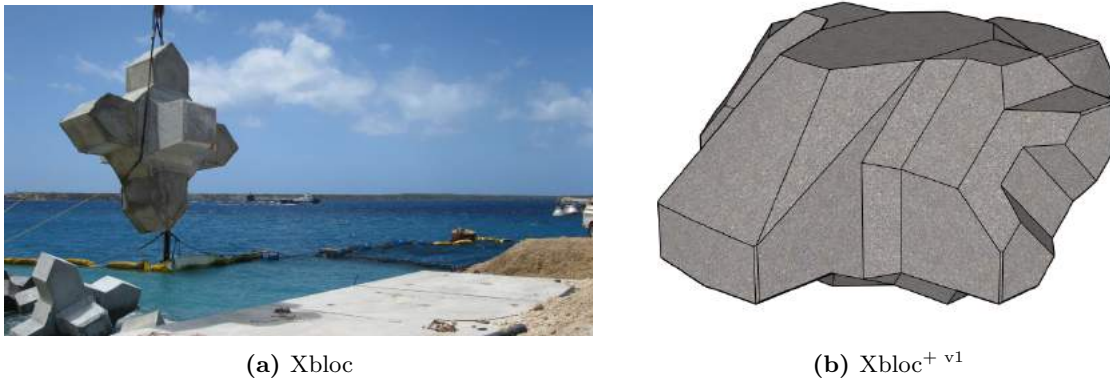


**Figure 1.1:** Difference between Xbloc and Xbloc<sup>+</sup>

With these two aspects in mind, the in-house engineering firm of BAM Infraconsult, Delta Marine Consultants (DMC), developed a new concrete armour unit that is placed with a uniform orientation: the Xbloc<sup>+</sup>. The first version of this armour unit, the Xbloc<sup>+ v1</sup>, is depicted in Figure 1.1b. Xbloc<sup>+ v1</sup> should be placed in a specific way enabling easy and quick placement, in contrast to other single layer concrete armour units that are usually placed on a staggered grid with random orientation. Due to the shape and placement of Xbloc<sup>+ v1</sup> a visually smooth slope is created, which is a desirable feature on a landmark like the Afsluitdijk.

There already is a great number of armour units to choose from including the Stabloc, Antifer Cube, Accropode, Crablock, Xbloc and Cube. Each armour unit has its own positive and negative attributes and is most suitable for a specific combination of situations and parameters. The process of choosing an armour unit is a consideration between costs, risk, ease of placement & monitoring, maintenance, and aesthetics. If research shows that Xbloc<sup>+ v1</sup> can compete with other units, or that it has properties that make it a good alternative, the development of this armour unit will be continued.

### 1.3 Problem analysis

The interactions between waves and an armour layer are complex; to a certain extent because the load on an armour layer is influenced by waves that vary in space, time, direction and size as well as the breakwater geometry itself. The structural parameters influence the wave field in front of the breakwater, which, sequentially, influences the stability of the armour layer. Common wave-structure interactions are wave reflection, wave run-up, overtopping and wave transmission. These interactions create extra inwards or outwards directed loads (or even a turning moment), all depending on parameters such as the unit geometry, the core composition and the slope angle. Also, for different elevations on the slope - below, around and above sea water level (SWL) - a different balance of forces is considered. For different elevation distinctive wave-structure interactions dominate the stability.

For the above reasons, all relationships and formulae used to design armour layers are based on (small)



physical model tests and are derived empirically. For each new situation, parameter combination and armour unit shape these relationships are redefined. Ever since the shift of breakwaters to deeper water, many formulae have been developed to compute the desired armour unit size. The one that is most widely used is the Hudson formula [US Army Corps of Engineers, 1984]:

$$\frac{H_s}{\Delta D_{n50}} = (K_D \cot \alpha)^{1/3} = N_s \quad (1.1)$$

In this formula  $H_s$  represents the significant wave height,  $\Delta (= \frac{\rho_r - \rho_w}{\rho_w})$  the relative density,  $D_{n50}$  the nominal stone size or  $D_n$  the nominal armour unit size,  $K_D$  the stability parameter and  $\alpha$  the slope angle. Lastly,  $N_s$  represents the stability number, which is a measure of the armour layer performance. The higher the stability number, the higher the acceptable wave load on an armour unit and the less material is needed in the design. In current design methodology,  $K_D$  is related to a general breakwater design with a specific armour unit. Deviations from the general design are accompanied by a factor on the armour unit size, for example a factor 1.5 in case the water depth is larger than  $2.5 \cdot H_s$  and a factor 2.0 in case the water depth is larger than  $3.5 \cdot H_s$ .

When designing a new concrete armour unit, there are many uncertainties in the way it will respond to wave loading. Based on knowledge of other blocks, the structural integrity of an armour layer with the new Xbloc<sup>+ v1</sup> unit can be estimated and various analyses will be conducted to gather information on its performance. The most important aspects to gain knowledge in are the range of application, the behaviour under different wave loads, the required under layer size, the influence of the placing accuracy, the damage progression and the ability to recover. When the influence of fore-mentioned aspects on the performance of Xbloc+ is mapped, the success of the design can be assessed.

In preliminary 2D physical model tests that were executed by Delta Marine Consultants [Jacobs, 2015], some observations were made with respect to the failure mechanisms. In subsequent tests, different packing densities and shape variations were tried to assess the (de-)stabilizing mechanisms governing the armour layer stability. After these tests, the shape was altered, resulting in the shape shown in Figure 1.1b, and new model tests were done. The results were promising but to get a full understanding of the processes governing stability of an armour layer of Xbloc<sup>+ v1</sup> units, more research should be performed. Based on this research, Xbloc<sup>+</sup> will be further developed.

## 1.4 Objective

The objective of this thesis is to get insight into the different variables and failure mechanisms that influence the stability of an Xbloc<sup>+ v1</sup> armour layer. This will be used to, thereafter, further develop the armour unit. The following **main question** to be answered in this thesis is:

*How does the shape of the uniformly placed single layer concrete armour unit Xbloc<sup>+ v1</sup> affect the armour layer stability?*

The envisioned **goal** is:

*To find the failure mechanism(s) that dominate Xbloc<sup>+ v1</sup> and modify its shape such that an armour layer made out of Xbloc<sup>+ v2</sup> armour units will be more stable.*

The stability of breakwaters can be split up into three main aspects, namely geotechnical, hydraulic and structural stability. The scope of this thesis will be the hydraulic stability of the armour layer. All failure mechanisms related to geotechnical instability (f.e. sliding and liquefaction of the subsoil) or structural strength of the concrete armour units will not be discussed.

## 1.5 Approach

To answer the main question, **two research questions** have been posed:

1. *How does Xbloc<sup>+ v1</sup> achieve its stability?*
2. *How does Xbloc<sup>+ v1</sup> respond to wave loading?*

To answer the first sub-question, knowledge has to first be gained on how armour units in general achieve their stability and what units are suitable as possible comparison to Xbloc<sup>+ v1</sup>. A literature study is, therefore, carried out to gain insight into the load exerted by waves, how stability is calculated and defined, how (geometrical) parameters influence the stability, what kind of failure mechanisms exist, how stability can be tested in models and how scaling should be executed. Also, the different concrete armour units and pattern-placed blocks available are discussed. Additionally, Xbloc<sup>+ v1</sup> and previous model tests are described in detail and two comparable units are elaborated on. A hypothesis for the research questions is formed based on the available literature and data.

To test the hypothesis, dry pull-out tests are carried out in which the extraction force as function of the unit weight is measured. This is done with smooth as well as rough model units (plastic and concrete) for four different levels on the slope and for two different directions of the force. The outcomes are compared to available data of other armour units and pattern-placed blocks to determine the important (de-)stabilizing mechanisms.

With the data, observations, conclusions and recommendations from the pull-out tests, a hypothesis is formulated on the stability of an Xbloc<sup>+ v1</sup> armour layer under wave action. 2D hydraulic physical model tests are conducted in the wave flume of Delta Marine Consultants in Utrecht to test the hypothesis. A typical breakwater cross-section in deep water is subjected to a JONSWAP wave spectrum with constant wave steepness. The significant wave height and wave period are stepwise increased until failure occurs. A longer-than-usual breakwater slope is used to prevent large waves passing over the crest. In this way, all energy is dissipated on the slope. The focus of these tests lies on registering the damage patterns, for example discovering where damage occurs on the slope (below, at or above the water level) and monitoring its development.

The data and observations resulting from the two model tests give a good overview of the overall stability of Xbloc<sup>+ v1</sup> and lead to conclusions and recommendations on how to modify the Xbloc<sup>+ v1</sup> shape such that an armour layer made from Xbloc<sup>+ v2</sup> armour units will be more stable.

## 1.6 Thesis Outline

The approach as described in the previous section deviates from the way this report is built up. Figure 1.2 shows a flow chart representing the outline of this thesis. All relevant literature needed to understand the basis of the model tests is gathered in Chapter 2: Background information. The next three chapters (Hypotheses, Experiment Set-up and Analysis) are each subdivided into two sections, one describing the pull-out tests and one describing the hydraulic tests. This is done so that all information on each topic can be gathered in one chapter: it prevents repetition of already explained concepts and geometry. Eventually, Chapter 6 concludes this research with both the conclusions and recommendations of each of the model tests, as well as the overall conclusions and recommendations with respect to the possible shape modifications increasing stability.

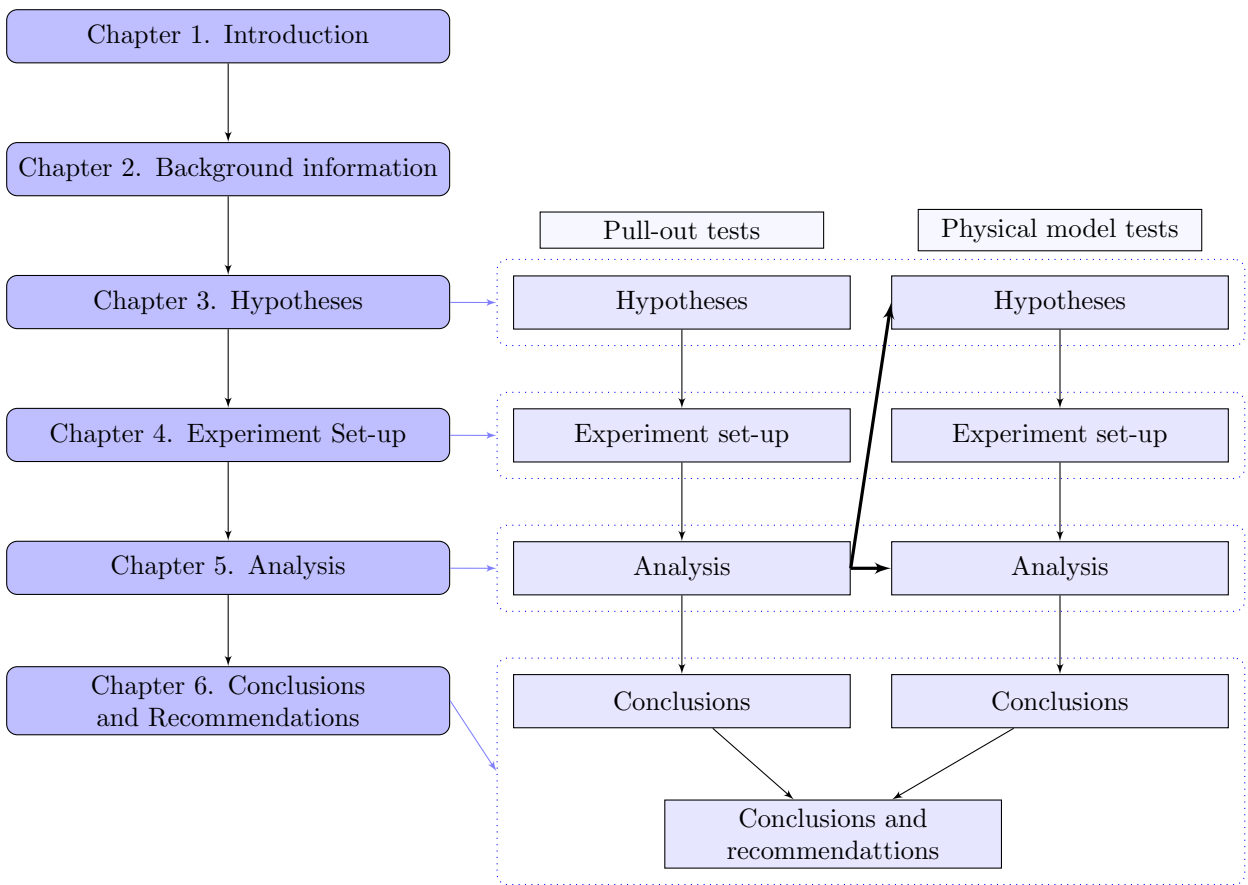


Figure 1.2: Thesis Outline

# Chapter 2: Background information

In this chapter, an overview of the available literature is given. The aim of this chapter is to introduce the concepts important for designing breakwater armour layers and validating these designs. Armour layer design is an extensive subject so to make this chapter readable some aspects are explained in detail and other aspects will only briefly be touched upon. In Section 2.1 the main concepts of Linear Wave Theory will be explained. Section 2.2 is dedicated to armour layer design and thereafter, Section 2.3 discusses how designs are validated. Finally, Section 2.4 explains the concepts of the Xbloc<sup>+</sup> v1 armour unit.

## 2.1 Waves

The design criteria determining the composition of a rubble mound breakwater are primarily governed by the sea state. Linear Wave Theory is used to describe the sea state by assuming waves as a summation of harmonic functions. Linear Wave Theory is applicable when "the water is assumed to be an ideal fluid with only the Earth's gravitation inducing the forces that control the motions of the water particles" [Holthuijsen, 2007]. Additionally, this theory requires that the wave height is small compared to its length or compared to the water depth, implying the condition of deep water. When waves become too steep and lose their continuous property due to breaking, or enter shallow water, non-linear phenomena occur and Linear Wave Theory no longer holds. However, when Linear Wave Theory becomes invalid it still gives a good estimate of the surface gravity waves and their propagation.

In the following paragraphs, the relationships that are most important for breakwater design will be touched upon. For now, Linear Wave Theory is valid, even though it is known that non-linear phenomena will occur. It has been checked if linear wave theory is applicable in Appendix E. For a full description of all relationships a formula applicable for oceanic and coastal waters the reader is referred to Holthuijsen [2007].

### 2.1.1 Wave characteristics

The hydraulic parameters needed for breakwater designs are the water depth  $h$ , the various wave heights  $H_s$ ,  $H_{1/x}$ ,  $H_{x\%}$  and  $H_{max}$ , the wave period  $T$ , the wavelength  $L$ , the deep water wave length  $L_0$ , the deep water wave steepness  $s_{0p}$  and the Iribarren number  $\xi_{0p}$ . Together they fully determine the hydraulic conditions atop and around a breakwater. The relationship between the wavelength and period is given by the dispersion relation, equation 2.1. The ratio of the wave height over the deep water wave length is called the fictitious wave steepness and is given by equation 2.2. Finally, the relation between the slope angle and the fictitious wave steepness determines the type of wave energy present in front of the breakwater. This relation is given by equation 2.3.

$$L = \frac{gT^2}{2\pi} \tanh \frac{2\pi h}{L} = L_0 \tanh \frac{2\pi h}{L} \quad (2.1)$$

$$s_{0p} = H_s/L_{0p} = \frac{2\pi H_s}{gT_{0p}^2} \quad (2.2)$$

$$\xi_{0p} = \frac{\tan \alpha}{\sqrt{s_{0p}}} \quad (2.3)$$

#### Dispersion relation

The dispersion relation describes the effect of dispersion on the properties of waves for varying frequencies and wave numbers. It is fully described by equation 2.1, which can be simplified in the case of shallow or deep water. In a dispersive wave field, each wave has its own velocity. Quicker waves will thus catch up on slower waves. All waves cluster together to what is called a wave group or wave train.

### Wave steepness

The wave shape, in this case meaning the wave steepness, is fixed in the relation between the wave height and the wave period. Therefore, through the dispersion relation the wave length is also fixed by this relation. When the wave height is increased without changing the wave length, the wave shape changes and becomes steeper. This relationship is described by the (fictitious) wave steepness, see Equation 2.2.

For a breakwater design, it is important to know the wave steepness during the significant storm in that area. Figure 2.1 shows the joint probability density function of the significant wave height and peak period (formed by combining two histogram plots with probability distributions for  $H_s$  and  $T_p$ ). The inner ring shows the combinations which have the highest probability of occurrence, with an increasing probability for each following ring. Along the exponential lines, the wave steepness remains constant. This is especially the case during storms.

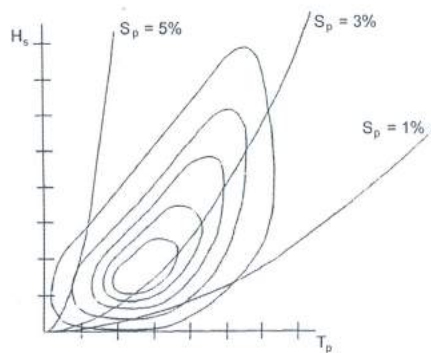


Figure 2.1: H/T diagram, d'Angremond et al. [2001]

In deep water, the maximum steepness,  $s_{max}$ , is determined by the wave crest velocity that cannot exceed the wave celerity, otherwise breaking the wave. The upper limit for a single wave is  $s_{max} = 0.142$ , also known as the deep-water break criterion by Miche, but waves often break partially before this limit is reached. In practice, values of  $s > 0.055$  are rarely seen and, according to d'Angremond et al. [2001], correspond typically to "one nearby wind field". The observed average wave steepness is 0.036 for non-breaking waves and 0.042 for breaking waves according to Holthuijsen and Herbers [1986]. When wave heights are small or wave periods are long, such as for swell, a value of around 0.01 is found. For breakwater design values between 0.02 and 0.06 (2% and 6%) are used.

### Surf similarity parameter

Battjes introduced the surf similarity parameter. This was based on the concepts of reflection and dissipation on steep and gentle slopes, developed by Ramon Iribarren Cavanilles. For this reason he called it, the Iribarren number or breaker parameter,  $\xi$ , which describes the type of wave breaking and the nature of the wave load on the structure. It is a dimensionless parameter which relates the slope angle of the structure to the fictitious wave steepness and its outcome indicates the state of the waves. Equation 2.3 displays the formula used to compute the breaker parameter. The subscript that is sometimes given to this parameter represents which wave period is used in, for example, the offshore wave period or a spectral wave period.

The value of  $\xi$  gives an indication of the wave-structure interaction such as absorption and reflection. There are roughly four breaker types; spilling, plunging, collapsing and surging for  $\xi$  increasing from 0 up to 5 and higher. The latter three are most common on breakwater slopes, and, according to Schiereck and Verhagen [2001], "stability relations show that collapsing breakers cause the most damage". A collapsing wave can be seen as the transition between a plunging ( $0.5 < \xi < 3$ ) and a surging ( $3 < \xi < 5$ ) breaker or the grey area between non-breaking and breaking waves: a wave on the verge of breaking has the highest energy possible. This means that all combinations of parameters that lead to a value of  $\xi \approx 3$  cause the most damage. All breaker types are depicted in Figure 2.2.

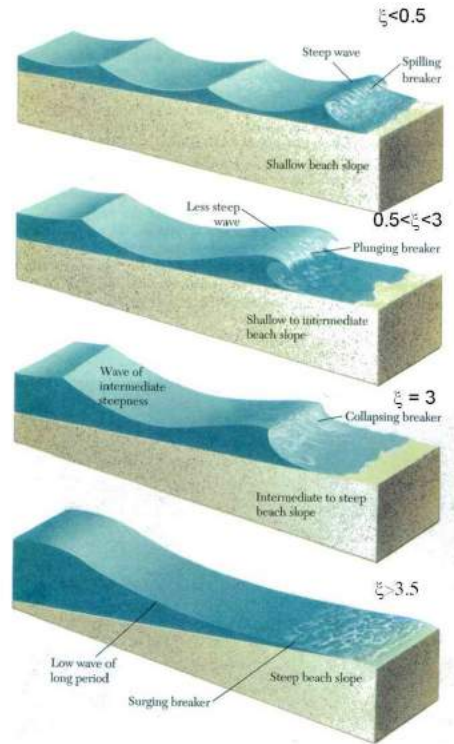


Figure 2.2: Breaker types as defined by the breaker parameter, Verhagen [2016]

## 2.1.2 Wave growth

Waves are formed by wind blowing over irregularities in the water surface. The energy that is put in by the wind is converted to wave growth. In an ideal situation, wind blows with a constant speed over an infinite stretch of water (called fetch). Waves then grow to their maximum height and break when they become too steep. But in a storm, due to the irregularity of wind fields, only a few waves will grow to their maximum form and most waves will stay small. The way to characterize the distribution of energy in a storm over the various wave frequencies (and thus over the various wave lengths) is with a wave spectrum: this relates the energy density to the wave frequencies.

### Wave spectra

The two most known spectra are the Pierson-Moskowitz spectrum and the JONSWAP spectrum. Without going into too much detail it can be stated that the Pierson-Moskowitz spectrum refers to a fully developed sea state, and the JONSWAP (Joint North Sea Wave Observation Project) spectrum refers to a young sea state. A fully developed sea state is when the wind has had enough time and space, for example, several days and hundreds of kilometres, to develop the waves to their fullest capacity. A young sea state is when the sea state hasn't fully developed. This has several reasons: storms do not always last several days, the fetch is often limited but also because interactions between waves re-distribute the energy over the spectrum. Even in hurricanes the latter holds. With help of observations it has been concluded that the JONSWAP spectrum is not only valid in the North Sea area, but also in many other parts of the world, making it the most relevant spectrum to use in the design and modelling of breakwaters.

The wave spectrum enables us to calculate several parameters, such as the zero<sup>th</sup> order moment,  $m_0$ , from which an estimation of the significant wave height,  $H_{m0}$ , can be computed through Equation 2.4.

$$H_s \approx H_{m0} = 4\sqrt{m_0} \quad (2.4)$$

### 2.1.3 Wave height in deep and shallow water

In deep water, the waves are distributed differently than in shallow water. This difference is mainly in the maximum wave height. In this section, both distributions are elaborated.

#### Deep water

The wave height distribution of irregular waves in deep water is described by a Rayleigh distribution (a Weibull distribution with shape parameter 2), Equation 2.5. The input for this distribution is the significant wave height and the root mean square wave height, for which there is a constant relation in deep water between both, see Equation 2.7. The significant wave height is either computed from a time series analysis or estimated from the JONSWAP spectrum. When a time series analysis is used, the significant wave height is defined as in Equation 2.6. When a spectral analysis is used, the significant wave height is referred to as  $H_{m0}$  and can be calculated through the zero<sup>th</sup> order moment as described in the previous section. For a narrow spectrum, these parameters correspond very well. The mentioned relations are constant in deep water conditions, therefore, for narrow spectra (such as a JONSWAP spectrum), the wave height distribution is known a priori and there is no need for a spectral analysis.

From the Rayleigh distribution, the exceedance probability of the various wave heights can be determined. It follows that the wave height exceeded by 0.1% of the waves,  $H_{0.1\%}$ , can be approximated by  $1.86H_s$  and the wave height exceeded by 1% of the waves,  $H_{1\%}$ , can be approximated by  $1.5H_s$ . Usually, the maximum wave height measured in deep water,  $H_{max}$ , is  $2H_s$ . The Rayleigh distribution with the discussed wave heights  $H_s$ ,  $H_{1\%}$  and  $H_{0.1\%}$  in dimensionless form, and their respective exceedance probabilities are depicted in Figures 2.3a and 2.3b.

$$P_{Rayleigh}(\underline{H} > H) = e^{-(\frac{H}{H_{rms}})^2} = e^{-2(\frac{H}{H_s})^2} \quad (2.5)$$

$$H_s = \text{average of highest one-third of the waves} = H_{1/3} \quad (2.6)$$

$$H_{rms} = \frac{1}{1.416} H_{1/3} \quad (2.7)$$

#### Shallow water

The Rayleigh distribution is valid for deep water: water depths larger than three times  $H_s$ . For smaller water depths a different distribution is used. Lower water depth induces wave breaking: the highest waves break and the energy is re-distributed into multiple lower waves. In this case, the relations between  $H_{1/3}$ ,  $H_{rms}$  and  $H_{max}$  are no longer constant and a different distribution should be used.

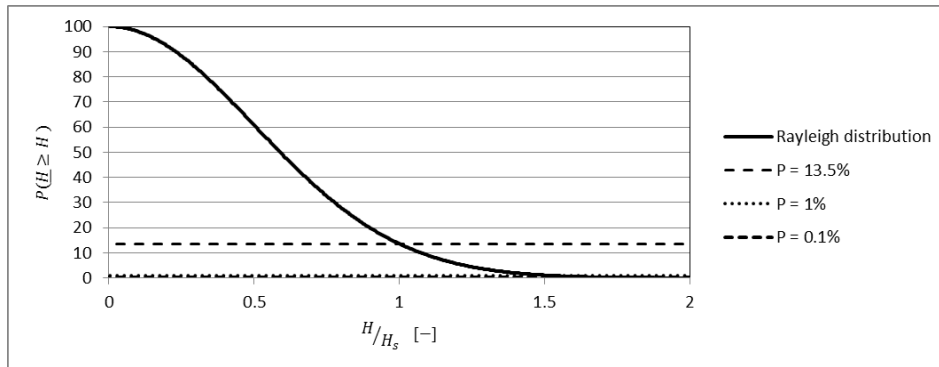
The distribution which is used in shallow water is called the Composed Weibull-distribution (CWD), formulated by Battjes and Groenendijk [2000]. For this distribution a transitional wave height,  $H_{tr}$ , and the root mean square wave height are used which are computed from the zero<sup>th</sup> order moment, water depth at the toe,  $h_{toe}$  and the foreshore slope angle,  $\alpha_f$ , see equations 2.8 through 2.10.

$$P_{BG}(\underline{H} \geq H) = \begin{cases} e^{-(\frac{H}{H_{rms}})^2}, & H \leq H_{tr} \\ e^{-(\frac{H}{H_{rms}})^{3.6}}, & H \geq H_{tr} \end{cases} \quad (2.8)$$

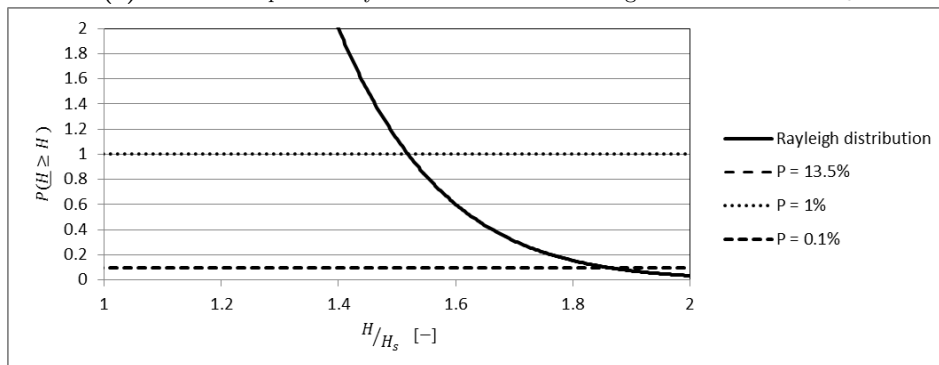
$$H_{tr} = (0.35 + 5.8 \tan \alpha_f) h_{toe} \quad (2.9)$$

$$H_{rms} = (2.69 + 3.24 \frac{\sqrt{m_0}}{h_{toe}}) \sqrt{m_0} \quad (2.10)$$

For the computation of the probability of exceedance of a wave height which is lower than the transitional wave height ( $H \leq H_{tr}$ ), the Rayleigh distribution is used. For wave heights higher than the transitional wave height ( $H \geq H_{tr}$ ) a Weibull distribution with a shape factor of 3.6 is used. The value for the transitional wave height is dependent on the water depth at the toe, and consequently, there is no constant ratio between the maximum and the significant wave height. Battjes and Groenendijk overcame this nuisance by normalising all wave heights with respect to the root mean square wave height. Then, they formulated a large table with the normalised transitional wave height and all accompanying values. The values in this table have been interpolated and the formula is rewritten such that the relation between the water depth at the toe and the maximum wave height, both made dimensionless by their significant wave height, could be sketched. In Figure 2.4 this relation is specified



(a) Exceedance probability of the observed wave height  $H$  for  $0 < H < 2H_s$



(b) Exceedance probability of the observed wave height  $H$ , for two different statistical definitions of  $H_{max}$ :  $H_{1\%}$  and  $H_{0.1\%}$

**Figure 2.3:** Rayleigh distribution for deep water

for the case of a 1:30 foreshore and without foreshore. Also plotted in this figure is the deep water theory as described by the Rayleigh distribution, valid for  $h_t > 3 \cdot H_s$ .

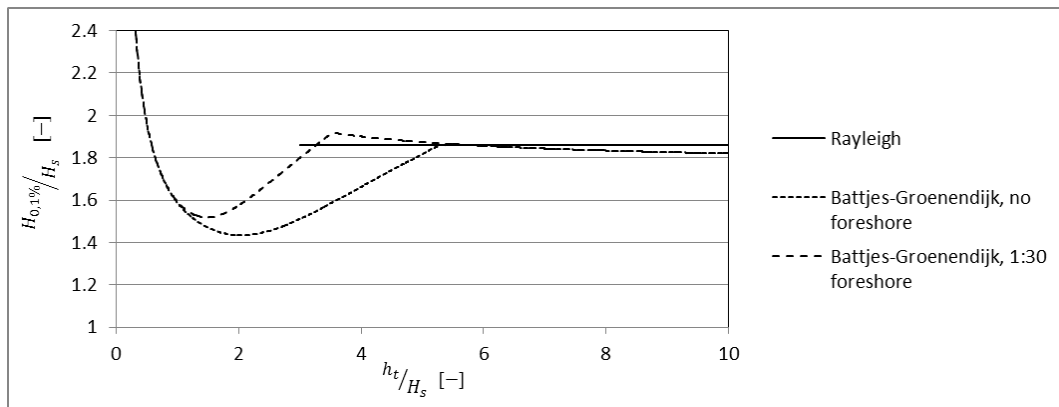


**Figure 2.4:** Relation between  $H_{0.1\%}$  and  $h_t$  made dimensionless by  $H_s$

Both the Rayleigh distribution and the Composed Weibull distribution are used to describe the short-term statistics, valid for f.e. a single storm. In the design process of breakwaters, appropriate values for the water depth at the toe and the significant wave height should be taken into account. This can be done by using a long-term wave height distribution, in which the significant wave height for the "once in x year storm" is computed.



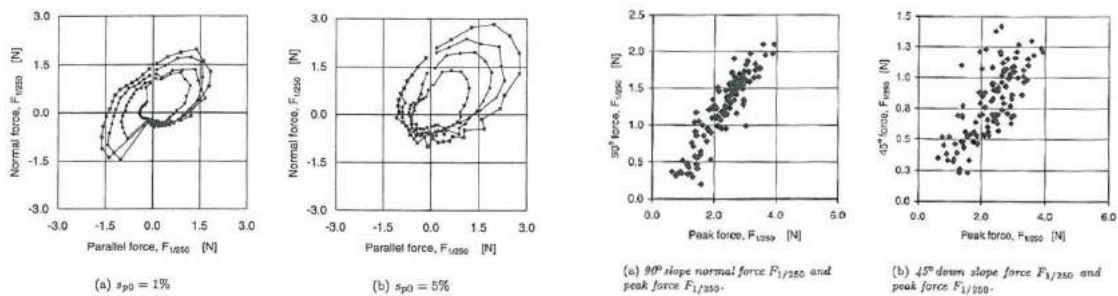
### 2.1.4 Waves on a slope

The interactions between waves and an armour layer are complex. The loads on an armour layer are determined by waves, which vary in space, time, direction and size, as well as by the breakwater design. The structural parameters influence the wave field in front of the breakwater, which, in its turn, influences the stability of the armour layer. Common wave-structure interactions are; wave reflection, wave run-up, overtopping and wave transmission. Loads can be inwards or outwards directed, or they can even create a turning moment. This depends on parameters such as the geometry of the units, the core design and the slope angle. A different balance of forces is considered for each location on the slope, for example, below, around and above sea water level, since different wave-structure interactions play a dominant role. The loads exerted by the waves consist of:

- The quasi-hydrostatic load: the presence of water on the slope, this load increases for every wave crest and decreases for every wave trough. This force is directed inwards.
- Wave velocities: the velocity of the wave exerts drag, lift and shear forces on the stones during uprush and downrush.
- The wave impact: the force a wave exerts when plunging on the slope, a short but high pressure. This force is directed inwards.
- Uplift: force due to the difference in water level inside and outside the breakwater. The permeabilities of the armour layer, under layer and core determine the force magnitude. This force is directed outwards.

The last 3 forces are the most important for breakwater design. How these influence the stability of an armour unit will be discussed in the next section.

In his PhD, Hald [1998] among other things looked at the direction and magnitude of wave induced forces on natural armour stones. By applying a force transducer to a single stone on the slope, the strain in two cross-sections was measured, enabling mapping of the wave forces in hodographs, depicted in Figure 2.5a. He stated that the 3 most destabilizing forces (for the initiation of movement of a stone out of the armour layer) were; the peak force, the 90° force and the 45° force, which represent the lifting as well as the up and down movement of the waves. Analysis of his wave data resulted in the conclusion that the peak force acts almost vertically upwards with a small tendency to act up-slope (115°-165° with 90° being the slope normal) and that the 90°-force and the 45°-force have relative magnitudes of 45% and 35%, see Figure 2.5.



(a) Force hodographs for tests with varying steepness. (b) Relation between Peak force and both the 90° and the 45° Constant slope of 1 : 1.5,  $H = 0.5m$  and  $\gamma = 3.3$  force

Figure 2.5: Experimental data on wave induced loading by Hald [1998]

## 2.2 Design of Armour layers

### 2.2.1 Breakwaters in general

All over the world breakwaters are built to shelter land and harbours from wind-induced waves, unwanted erosion or sedimentation. A breakwater is part of a coastal defence system. They can

be subdivided into 4 categories: rubble mound structures, monolithic structures, composite structures and special structures. Drawings and more detailed information on these breakwater categories can be found in d'Angremond et al. [2001, chapter 2]. In this thesis, the discussion will be limited to the topic of rubble mound breakwaters, and specifically to the stability of armour layers designed with concrete armour units.

### History

Originally, rubble mound breakwaters were built with rubble: rocks of various sizes and shapes. These were strong enough to withstand the wave action in small ports. Breakwaters like this date back as far as 2000 BC up until the 19th century. As ports grew bigger, the breakwaters were situated in deeper water, which meant not only higher waves (in other words larger stones) but also a greater amount of rubble needed to complete the structure. At some locations, the demand for rubble could not be satisfied (either due to the absence of a quarry or economically; due to the size of stones required) so engineers developed concrete armour units that could fulfil the same task. The armour units could be made on site and in any size, making them superior to rock. At first, they were placed with the same rules for application as rock: an armour layer should have a thickness of at least two times the nominal diameter of the blocks. This double layer needed a lot of concrete. The stabilising mechanism of these first blocks was based on the weight of the block and friction between blocks solely (interblock friction).

New armour units were developed such that the main cost of a breakwater, the concrete usage, was decreased. In contrast to the earlier units, which were placed in a double layer, these units could be placed in a single layer. The stabilising mechanism for these blocks consisted of the combined influence of the weight of the block, friction between blocks and interlocking. Nowadays, armour units that are placed in a single layer are dominating breakwater design.

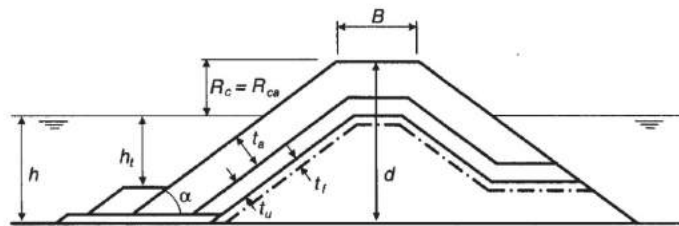


Figure 2.6: Important structural parameters in breakwater design [CIRIA et al., 2007]

### Elements of a rubble mound breakwater

The main components of a rubble mound breakwater, from the middle of the structure outwards, are the core, the filter layer, the under layer and the armour layer, Figure 2.6. The core usually consists of material with a wide stone grading, such as 1-500 kg. The under layer and filter layer have the function of preventing core material from being displaced through the armour layer. At the same time, they should be open enough for water to penetrate into the core because, in this way, energy is dissipated. Geometrical parameters to describe a rubble mound breakwater are:  $\alpha$ , the angle of the slope,  $d$ , the height of the structure,  $h$ , the water depth,  $h_t$ , the height of the water level above the toe,  $R_c$ , the crest height or freeboard (often expressed relative to the significant wave height),  $B$ , the berm width,  $t_a$ ,  $t_u$  and  $t_f$ , the thickness's of armour layer, under layer and filter layer respectively.

### 2.2.2 Concrete armour units

As has been explained in 2.2.1 the design of breakwaters has changed considerably over the last century. Where the concrete armour unit (the first design was a cube) first was used as a substitution for rock it eventually became an element of commercial rivalry. Elements in two layers got their stability mainly from weight and interblock friction. The main cost of an armour unit was, of course, the material so units which could be placed in a single layer were developed. These elements were based on the stability mechanism interlocking.























Manufactures proceeded to design increasingly slender elements with increasingly higher interlocking capacity. Scale model tests proved the high stability of these blocks and so they were used on breakwater

slopes. What was not taken into account in these studies were the tensile stresses occurring due to rocking elements. Concrete armour units do not have reinforcement (corrosion will occur when cracks are formed, which will damage the armour unit from the inside) and, therefore, have no capability to absorb tensile stresses. In a short period, on a large number of breakwaters, rocking of slender elements caused failure of the structure. The most known failing breakwater was the breakwater in the port of Sines, Portugal, in 1978 [d'Angremond et al., 2001]. After these failures, emphasis was laid on higher safety margins for the hydraulic design.

Prefabricated elements can be divided into 4 type of categories (after PIANC, WG36 [2005]):

- Layer thickness: Single layer, double layer or multiple layers
- Orientation: Randomly orientated or uniformly orientated
- Geometric: Blocky units, bulky units (no or marginally protruding elements), slender units (slender protruding elements) or multi-hole cubes
- Stabilising mechanism: Own weight, interlocking or friction

Nowadays there is a tendency towards designing bulkier armour units like Accropode, Core-loc and Xbloc which have a high structural integrity. An overview of the most used armour units, supplemented with 3 recently developed armour units (Cubipod, Crablock and the subject of this thesis: Xbloc<sup>+ v1</sup>), is given in Figure 2.7. In total there are over 100 different armour units, which only shows how much is still unknown about the processes influencing stability.

Randomly oriented armour units				Uniformly oriented armour units	
Double layer		Single layer			
Own weight		Own weight and Interlocking		Friction	
Cube 	Tetrapode France, 1950 	Accropode France, 1980 	Cob UK, 1969 		
Modified Cube USA, 1959 	Akmon NL, 1962 	Core-loc <sup>®</sup> USA, 1996 	Diahtis Ireland, 1998 		
Antifer Cube France, 1973 	Tribar USA, 1958 	A-Jack USA, 1998 	Seabee Australia, 1978 		
Haro Belgium, 1984 	Stabit UK, 1961 	Xbloc NL, 2003 	Shed UK, 1982 		
Tripod NL, 1962 	Dolos South Africa, 1963 	Cubipod Spain, 2007 	Single layer Cube, 1999 		
		Crablock UAE, 2009 			
		? Xbloc <sup>+ v1</sup> NL, 2015 			?

**Figure 2.7:** Overview of the most used armour units, supplemented with Cubipod, Crablock and Xbloc<sup>+ v1</sup>, after [Muttray and Reedijk, 2008]

As can be seen in Figure 2.7, after 1978 only single layer armour units have been developed. The 2 concepts are: *randomly oriented interlocking armour units* and *uniformly oriented friction based armour units*. Both have a bulky shape and the uniformly placed units all have one or multiple holes. The three exemptions are the single layer cube, which doesn't have a hole in it, the Crablock, which relies on interlocking but can be placed uniformly as well as randomly, and the Xbloc<sup>+ v1</sup>, for which it is not yet known what the main stabilising mechanism is. A detailed explanation of all units, including a timeline with design considerations, is given in the paper written by Muttray and Reedijk [2008].

### 2.2.2.1 Stability

As noticed by d'Angremond et al. [2001]: "It must be kept in mind that loss of stability is not a clearly defined phenomenon. Some subjectivity is involved, in particular, because the loss of the first stones cannot always be entirely attributed to wave action since it may at least in part, be due to the (random) position of the stone after construction". This citation perfectly sums up why there is still so much debate on the topic of stability. This section will discuss how stability is dealt with in armour layer design.

#### Armouring concepts

As discussed in the previous section, nowadays there are two basic concepts for armour units. Both concepts depend on different stabilizing mechanisms. Randomly oriented armour units all have in common that they gain extra stability from a mechanism that is called interlocking. The protruding elements of these armour units interlock so that when a load is exerted on an area of, for instance, 1 m<sup>2</sup>, an area much larger than 1 m<sup>2</sup> is activated to withstand the wave force. In this way, a stable slope can be acquired with little material. For these armour units, it is important that there are enough contact points with the under layer as well as with their neighbouring units. When one of these units is extracted from the armour layer the surrounding units usually show some rearrangement to fill up the gap.

Uniformly oriented armour units all have in common that they dissipate energy by a high slope roughness due to the big voids in these blocks. At the same time, their weight is a large contributor to the stability so the blocks have a cubelike shape, reducing the area they are placed on. The blocks remain stable due to the friction between them so it is paramount that all blocks are tightly fitted and all surfaces connect. The Rock Manual states: "If such close placement is not achieved, the stability of the entire layer is compromised." Also, special attention should be paid to the toe design to ensure that the first row can be placed accurately. In short, there is little room for error. These blocks are characterized by a high porosity.

#### Stability number

The parameter that describes the interaction of waves on a slope is called the stability number. Very bluntly said: the higher the stability number before failure occurs, the more effective an armour unit is.

$$\frac{H_x}{\Delta D_{n50}} = N_s \quad (2.11)$$

Equation 2.11 represents the balance between:

- The observed wave height  $H_x$ , which can be the average of the highest one-third of the waves,  $H_{1/3}$ , the highest 1% of the waves,  $H_{1\%}$ , or even lower percentages.
- The relative buoyant density, representing the fact that for submerged rock or concrete a lower density should be taken into account when computing stability. Submerged armour units experience an uplift force from the water surrounding them. The relative buoyant density is described by dividing the density of the submerged and saturated armour layer material by the density of water:  $\frac{\rho_{c,sat} - \rho_w}{\rho_w}$
- The characteristic armour stone diameter. For rock breakwaters this is the nominal median sieve diameter,  $d_{n50}$ , and for breakwaters, with concrete armour units this is the equivalent cubic diameter of the unit (since all units are of the same size), which is defined as the cubic root of the block volume:  $D_n = \sqrt[3]{V} = \sqrt[3]{\frac{M}{\rho_c}}$

#### Formulae

A number of formulae have been developed to express the right side of Equation 2.11. They were considered in the theory by Iribarren. In 1938, he proposed Equation 2.12, which describes the relationship between the wave-exerted forces (drag, lift, shear) and resisting forces (weight, friction) on an element, expressed in stone mass,  $M$ . He also included a correction for the slope angle, implemented by the coefficient  $\alpha$ . However, this equation doesn't state the exact relation.

$$M \propto \frac{\rho_s H^3}{\Delta^3 (\tan \phi \cos \alpha \pm \sin \alpha)^3} \quad (2.12)$$

In time, data generated from physical model tests were scrutinized to formulate an exact relation. Each test was done under different circumstances, with a different water depth, scale or procedure of documenting damage and failure. Each formula is only valid under certain circumstances and, partly because of this, it is difficult to decide which one is best. Some formulae are very straight-forward but could, therefore, be deemed too simple. Some formulae are quite elaborate but have other drawbacks.

The two most widely used formulae that describe the stability of a mound type of structure are the Van der Meer formula and the Hudson formula, that will be discussed below. Both were derived from different conditions, have a different applicability and take different parameters into account. A complete overview of all stability formulae can be found in the PhD thesis of Hald [1998].

#### Hudson

Hudson conducted physical model tests in 1953 to formulated coefficients for Equation 2.12. He eventually decided on another formula, Equation 2.13, based on the same principles. It takes the slope angle into account directly. All other influences were grouped in a "dustbin" parameter, the stability parameter  $K_D$ , as described by Equation 2.14. In this formula, each  $i$  represents the influence of some parameter. What this means in practice is that for each armour unit a basic, safe, value of  $K_D$  is formulated for a general breakwater design ( $H_s < h < 2H_s$ ,  $H_s < R_c < 1.5H_s$ , slope of 3V:4H,  $B = 3D_n$ ). For each deviation from this design, for example  $h > 2H_s$  or  $R_c < H_s$ , a multiplication factor on the nominal stone diameter is advised by the manufacturer. These multiplication factors are derived empirically. An example of the relation between the stability parameter and stability number for Xbloc is depicted in Figure 2.8.

$$N_s = (K_D \cot \alpha)^{1/3} \quad (2.13)$$

$$K_D = \prod_{\substack{1 < i < n \\ \alpha < j < \nu}} K_i^j \quad (2.14)$$

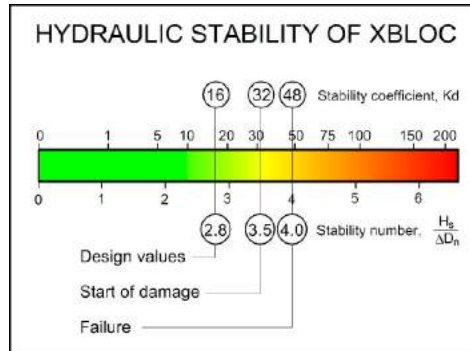


**Figure 2.8:** Relation between  $K_D$  and  $N_s$  for a safe design, start of damage and failure [Bakker et al., 2005]

#### Van der Meer

The Van der Meer formula, Equation 2.15, was formulated as improvement of the drawbacks of the Hudson formula, following the failure of several breakwaters. It is an empirically derived formula which takes into account the slope angle, the wave period, the number of waves, the damage level and the notial permeability. The first three are easily defined. The damage level is defined by Equation 2.16 where  $S$  is the dimensionless damage level and  $A_e$  is the eroded cross-sectional area [van der Meer, 1987]. The notial permeability is a vaguely defined parameter since the only documentation on it exists of four drawings indicating four type of armour layers (armour on a impermeable layer, armour on a filter layer on the core, armour directly on the core, only an armour layer so basically a heap of stones)

with corresponding values of 0.1 to 0.6.

$$N_s = \begin{cases} 6.2P^{0.18} \left(\frac{S}{\sqrt{N}}\right)^{0.2} \xi^{-0.5}, & \text{plunging breakers} \\ 1.0P^{-0.13} \left(\frac{S}{\sqrt{N}}\right)^{0.2} \xi^P \sqrt{\cot \alpha}, & \text{surging breakers} \end{cases} \quad (2.15)$$

$$S = \frac{A_e}{D_{n50}^2} \quad (2.16)$$

Compared to the Hudson formula the Van der Meer formula is quite elaborate. The main advantage of this formula is that it specifically takes into account five parameters that are known to influence the armour layer stability. The disadvantage is the vague formulation of the notial permeability and the way the damage level is defined. Van der Meer is especially good to use when the damage progression on the slope is gradual, that is, when the eroded area grows somewhat linearly. For relatively permeable cores, as well as for  $\pm 2000$  waves, both formulae give almost the same result. As we will see in the next section, for concrete armour units there is more a sudden type of failure and, therefore, the Hudson formula is more appropriate.

### 2.2.2.2 Damage progression

For Van der Meer, the start of damage is defined as  $2 < S < 3$  and the slope is considered failed for  $5 < S < 10$ . At this point many stones are removed and the under layer is visible. Hudson is unclear on the acceptable damage but, according to Schiereck and Verhagen [2001], the damage percentage  $D$  is supposed to be 5%. The damage percentage as defined by US Army Corps of Engineers [1984] is: "The normalized eroded volume in the active zone, from the middle of the crest down to  $1H_s$  below still water level". For concrete armour units, damage is defined differently since the damage progression is not a gradual process and it is difficult to define the surface profile. A comparison of the damage progression for breakwaters with a rock armour layer (rubble mound) and an armour layer of concrete units is depicted in Figure 2.9.

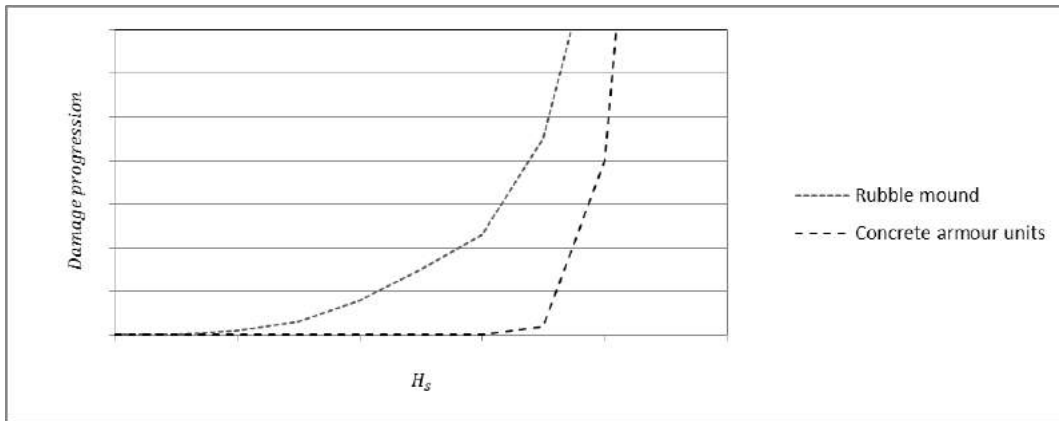


Figure 2.9: Damage progression for increasing wave height

For concrete armour units, damage is usually expressed in the "number of displaced units",  $N_{od}$ , which relates the number of units that were displaced out of the armour layer,  $N_{\#d}$ , to the width of the armour layer as a multiple of the nominal diameter of the armour stone,  $B_a/D_n$ . It can also easily be expressed as a percentage (the number of displaced units divided by the total number of units). The dimensionless damage level, as described by Van der Meer, is approximately two times larger than the number of displaced units [d'Angremond et al., 2001]. These relationships are depicted in Equations 2.17 and 2.18. When a stone is moved less than  $0.5D_n$  from its original position, it is considered to be "moved". When a stone is moved more than  $0.5D_n$  out of its original position it is considered to be "displaced".

$$N_{od} = \frac{N_{\#d}}{B_a/D_n} \quad (2.17)$$

$$S \approx 2N_{od} \quad (2.18)$$

For concrete armour units in a double layer, the accepted value for  $N_{od}$  is larger than that for a single layer since there is no risk for immediate failure. Extraction of 1 unit on a single layer is already a big problem as they no longer form a connection layer and loose units will collide with other units. The Rock Manual (CIRIA et al. [2007]) states that for single layer interlocking armour units, zero damage ( $N_{od} = 0$ ) is allowed for the design conditions (and only minor rocking). The armour layer may show limited damage during overload conditions of 20%. When  $N_{od} > 0.5$  the slope is classified as failed (for single layer cubes a stricter value of 0.2 is used). For each armour unit the range of stability numbers related to the 'no damage' and 'failure' criteria is different.

### 2.2.2.3 Failure mechanisms

Breakwaters can fail in more than one way. Failure is considered when a system no longer fulfils its function. The failure mechanisms relevant for this research are depicted in red in Figure 2.10 and includes:

- Berm and toe erosion
- Filter instability
- Erosion or breakage of the armour

The berm stability and the toe speak for themselves: the absence of a stable base construction will undermine the stability of the whole structure. The stability of a filter and an armour layer depend on multiple parameters and, therefore, are less straight-forward. Other failure mechanisms that consider overtopping and settlement are not discussed in this research.

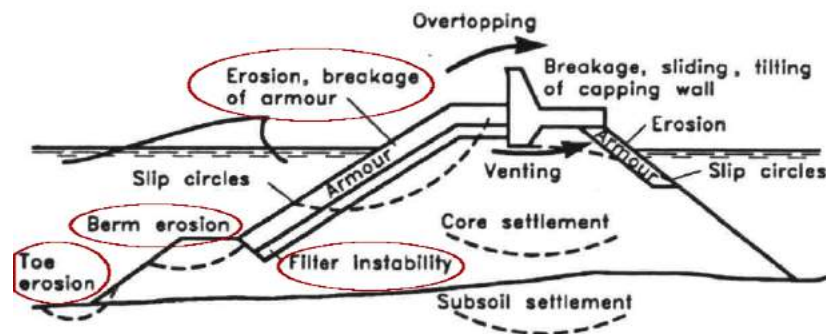


**Figure 2.10:** Possible failure mechanisms with red failure mechanisms being most important for this research [Burcharth, 1992]

### 2.2.2.4 Influence of structural parameters on the armour layer stability

Over the last decades a lot of research has been performed on the influence of structural parameters on the armour layer stability. A summary of this research is given below.

#### Foreshore steepness

Hovestad [2005] investigated the influence of the foreshore steepness on the stability of an Xbloc armour layer for a gentle (1:30) and steep (1:8) foreshore for comparable wave conditions offshore and comparable wave conditions near the structure. His conclusions were that equal offshore wave conditions, as well as equal near-structure wave conditions, resulted in more damage for the situation with a steep foreshore. He concluded that, since for the near-structure situation the wave heights and wave spectra were equal, it is not only the wave height that has an influence on the stability but also the wave steepness. On the steep foreshore, the shape of the wave became steeper which may explain the higher damage, together with other non-linear effects like wave asymmetry and peakedness.

The research by Hovestad has also served as basis material for several other papers by, for example, Muttray, Verhagen and Reedijk.

Oortman [2006] investigated why steep foreshores cause larger damage. He concluded that the difference in damage (up to 30% in some cases) was caused by increased velocities and acceleration during up- and downrush.

#### **Uplift: porosity and permeability**

As has been described in Section 2.1.4, the porosity and permeability have a large impact on the uplift forces. If the porosity of the structure is low with respect to the wave length, the phreatic surface in the structure cannot follow the instantaneous water level outside the structure. This leads to large head differences and, therefore, pressure from the inside which could lift the armour layer off. The structural sensitivity for this kind of failure mechanism can be indicated by the leakage length,  $\Lambda$ , Equation 2.19. It relates the permeability of the top and filter layer,  $k_T$  and  $k_F$ , to the thickness of these layers,  $d_T$  and  $d_F$  respectively. This formula was developed for dike revetments (which have an impermeable or low permeable core) but the general relations hold for concrete armour units on breakwaters as well and can serve as a tool to determine the influence of the porosity of the armour layer.

$$\Lambda = \sqrt{\frac{k_F d_F d_T}{k_T}} \quad (2.19)$$

For  $\Lambda \ll L$  the water level inside the structure can follow the instantaneous water level with ease and there are no differences across the top layer. This is the case for materials such as rock and armour units. For  $\Lambda \approx L$  the water level inside the breakwater has difficulties following the instantaneous water level. This is usually the case for pattern-placed blocks, which will be discussed in Section 2.2.3. If the core is permeable, the leakage length for a pattern-placed block will be lower and, therefore, uplift will be less of a problem.

The core permeability has been subject of research and debate since the 90's and is still not fully understood. During the design phase a permeable core is assumed but sometimes it is economically more attractive to use a geotextile container filled with, for example, dredged material as a core. As we have already seen in Equation 2.15 a higher permeability leads to a higher stability. This is because the energy in waves that penetrate the structure is dissipated by turbulent flow [Reedijk et al., 2008]. If the core is less permeable, waves reflect and hence exert an additional load on the armour layer. Research by Reedijk et al. [2008] has shown that an additional factor with a value of 1.4 should be applied on the stone diameter for waves with a period below 10 seconds when comparing an impermeable core with a permeable core. For larger wave periods this factor becomes even higher, up to 1.9 for waves of 16 seconds.

#### **Under layer**

The function of the under layer is two-fold: it has to transfer the loads to the core and it has to prevent fine material from exiting the core. As stated before, the under layer should be permeable, implying a narrow grading. At the same time, the material should be big enough so that it is not washed out through the armour layer. The Rock Manual suggests a median weight of  $1/10$  of the armour stone and minimum and maximum weights of 7% and 14% for single layer interlocking armour units. For single-layer Cubes and double-layer armour units, different requirements hold. The manufacturer states which requirements are applicable to their unit. The layer thickness is generally  $2D_{n50}$  that is allowed to deviated with a maximum of  $0.5D_{n50}$ .

In his MSc thesis, Brouwer [2013] investigated the influence of a deviation of the under layer profile for Xbloc armour units. He concluded that a tolerance larger than  $0.5D_{n50}$  leads to larger damage. This is especially the case for concave shaped slopes. Convex shaped slopes showed less damage for the same tolerance.

#### **Placement**

The accuracy of placement is of great importance for uniformly placed armour units due to the friction mechanism, as stated before in Section 2.2.2.1. For randomly orientated units some variation is possible.

Uniformly oriented units are placed according to a fixed pattern and randomly oriented units are placed on a predefined staggered grid for which the horizontal distance between the blocks,  $D_x$ , and the up-slope distance between the blocks,  $D_y$ , are specified. Special attention is paid to the transition



between two sizes of armour units and the placement on bends and roundheads. The horizontal and up-slope distance between the blocks together formulate the packing density. Randomly oriented units *can* also be placed uniformly but will reduce the stability due to less interlocking.

ten Oever [2006] conducted research on the influence of placement for Xbloc armour units (by varying the grid as well as the placement technique) and concluded that both have an influence on the quality of placement. A too low or too high packing density will result in a decrease of stability because either there is not enough material on the slope to create an interlocking layer, or there is so much material on the slope that the porosity is decreased.

### Additional influences

There are many other structural and hydraulic parameters that influence the stability but in view of readability, these will not be discussed in detail. The most important ones to mention are:

- **Rocking:** Even though the rocking of armour units is an unwanted phenomenon, it also indicates that the structure is close to being damaged. During the 80's extensive research has been done by all major research facilities in the Netherlands and one of the results was that the difference between the stability numbers for rocking and damage is approximately 0.5 [van der Meer and Heydra, 1991]. It can thus be seen as a warning phenomenon.
- **Crest height:** The higher the crest, the more interlocking and friction there is around the still water level, resulting in a stable armour layer. But the presence of a high crest also means that no energy can be dissipated via overtopping: all wave force is concentrated on the slope.
- **Wave height distribution:** Zwanenburg [2012] investigated what wave criterion is best used to describe the stability of single layer concrete armour units. In the present design,  $H_s$  is used as the design wave height, and the criterion is "no damage during design conditions and only minor displacements" but her research pointed out that this might not be a good design strategy. She investigated stability based on the number of rocking units instead of the number of displaced units, as is common. The conclusions included that different type of wave heights can be held accountable for different types of movement. The  $H_{2\%}$  shows to be the best design parameter for a rocking-based stability relationship and the extreme or maximum wave height shows to be the best design parameter for an extraction-based stability relationship. In shallow water with steep foreshores, however, it is better to use the significant wave height as a design parameter.

### 2.2.3 Placed blocks

The type of structure used to protect the outer slope of dikes (which have an impermeable core) is called a revetment. The main functions of a revetment are to protect the slope and to reduce run-up and overtopping. They can be constructed with small rocks called rip-rap or with pattern-placed blocks, an overview of the most used blocks is given in Figure 2.11. Just like the uniformly placed concrete armour units, these blocks obtain their stability from their own weight and interblock friction, and the accuracy of placement determines the strength of the slope. Placed blocks can have an interlocking mechanism but most do not. A placed-block revetment is a lot less permeable than a rip-rap revetment or breakwater concrete armour layer.



**Figure 2.11:** Examples of placed blocks: Basalt, Basalton, Ronaton, Verkalit (interlocking), Hillblock and Hydroblok

### 2.2.3.1 Stability

Compared to breakwaters, the wave load on dikes is different and much lower, therefore, the size of placed blocks is also much smaller (block heights are in the order of 0.5m compared to 2m and larger for concrete armour units). As has been described in Section 2.1.4, the main wave load components for breakwater slopes are the quasi-hydrostatic load, the wave velocities, the wave impact and the uplift. The surfaces of placed blocks are much smoother than those of concrete armour units, therefore waves exert less drag force. Due to the impermeable core, the last force is most important for the stability of placed block revetments.

A tight placement increasing interlocking effects: the uplift forces are resisted by clamping. Nevertheless, cracks will always be present and large differences in strength along the slope have been measured in the field. The strength of a revetment can be multiple times larger than the weight of a single element. A formula has been derived to describe the stability against uplift as the balance between the submerged weight of the revetment and the outward pressure due to the head difference across the revetment due to the run-down of waves, Equation 2.20. In this formula,  $d$  represents the block thickness. Unfortunately, this is only a guesstimate since the formula does not take into account the leakage length, the interblock friction or the clamping effect.

$$\frac{H_s}{\Delta d} = \frac{3 \cos \alpha}{\xi_p} \quad (2.20)$$

Little is known about the exact strength and stability of pattern-placed blocks. Simultaneously with the finishing of this report a PhD thesis on the "Design of Pattern-placed Revetments" is finished by Peters [2017]. In his thesis, he also investigated the stability of several elements of this kind of structure. In total ten propositions were given of which the first three are repeated here:

1. Pattern-placed revetments attain stability above the self-weight of the single revetment elements, due to the permeability properties and frictional interlocking.
2. Steep revetment slopes more strongly benefit from frictional interlocking than gentle slopes, if the toe is sufficiently resistant to deformation.
3. Pattern-placed revetments gain stability after every storm survived, provided that the revetment is supported by a strong and not deformable toe structure.

### 2.2.3.2 Failure mechanisms

Uplift can cause two main types of failure, depicted in Figure 2.12: the piston type of failure and beam-failure. In the first failure mechanism the water pressure pushes a single block, pressure can then easily be released and, depending on the shape and pattern of the block, damage progresses slowly. The second failure mechanism causes several blocks to fail at the same time and the damage can progress rapidly. The figure also depicts other failure mechanisms. The vulnerability of a placed block revetment with respect to uplift is expressed by the leakage length (Equation 2.19), however, it doesn't take into account the increased strength due to friction and clamping.

## 2.3 Model testing

There are many types of armour units and placed blocks that all have their own properties and stability mechanisms. Since they are all used in different areas around the world and each location has its own boundary and storm conditions, each structure requires a one-of-a-kind design. A lot is still unknown about the wave-structure interactions, which is exemplified by the numerous stability formulae, sometimes even element-specific, with many empirical coefficients having been developed over the years. For these reasons, each breakwater design is validated with help of a model to evaluate the stability under design conditions. Since often no numerical data is available, physical model tests will be done to obtain this data. The costs of such model tests may seem large but are insignificant relative to the costs of repair that would have to take place in case of damage or failure.

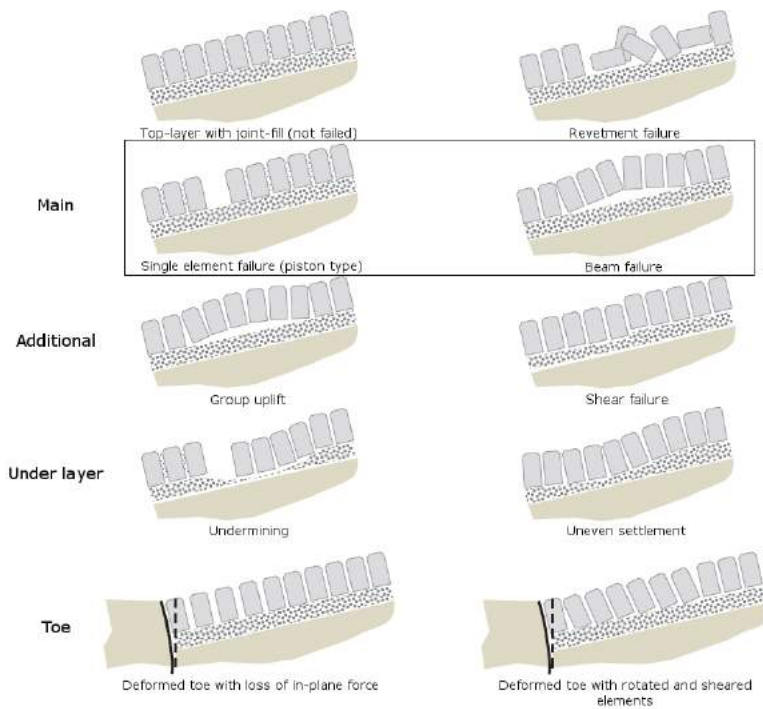


Figure 2.12: Failure mechanisms of pattern-placed blocks, after Peters [2017]

### 2.3.1 Scale rules

In the case of large constructions, it is impossible to perform full-scale model tests. For breakwaters, the general modelling steps are to first conduct small-scale 2D model tests after which, for a satisfactory design, the switch to 3D models can be made. The model should be a near-exact representation of the prototype. The scaling of a design is not as simple as the scale of, for example, a photograph. Not only geometric scaling, also the important kinematic and dynamic processes should be scaled such that they take place in the same manner in the model as in prototype. This implies that there should be similarity of fluid particle motions and similarity of vectorial forces. Hughes [1993] has stated that for hydraulic model tests the main problems arise with the scaling of the viscous forces and gravitation, which do not allow scaling. To compensate for this, other parameters need to be scaled in such a way that the model represents the prototype correctly. He stated that equal Reynolds and Froude numbers, Equations 2.21 and 2.22, for model and prototype would overcome this problem. In these equations,  $U$  represents the flow velocity,  $d$  represents the stone diameter,  $\nu$  is the viscosity of water ( $1.1 \cdot 10^{-6} m^2/s$ ) and  $L$  is the length scale.

$$\text{Re} = \frac{Ud}{\nu} \quad (2.21)$$

$$\text{Fr} = \frac{U}{\sqrt{gL}} \quad (2.22)$$

### 2.3.2 Generally used method and scale-effects

A scale model should be as close to the actual situation as possible but will always be an approximation. Therefore, scale-effects will always be present. For small-scale models Froude scaling is generally applied because waves interacting with the structure are gravity dominated. This implies linear geometric scaling, therefore, elasticity, surface tension and viscosity cannot be scaled correctly. As long as the wave lengths stay longer than 0.25 seconds, the influence of surface tension is negligible,

according to Holthuijsen [2007]. The scaling of viscosity, or to be more exact: the presence of laminar or turbulent flow, does become a problem. The flow through the layers and core of a breakwater in the prototype is turbulent. In a scale model, flow velocities through the armour and under layer are usually high enough to result in turbulent flow. When water has to flow through a geometrically scaled core it becomes laminar. The way to counteract this is to use a lower scale for the stone diameter in the core. Burcharth et al. [1999] proposed that "the diameter of the core material in models is chosen in such a way that the Froude scale law holds for a characteristic pore velocity." Appendix F.1 gives a detailed explanation of this approach and the problems it encounters.

Another important scale effect is friction. The difference in surface roughness is, unfortunately, a factor for which a method or design practice has not been developed. For armour units that obtain their stability from interlocking, this does not pose a serious problem. For friction-based stability mechanisms, this phenomenon should be kept in mind. When small-scale model tests are conducted with interlocking units made of concrete, the units are often spray-painted to reduce the surface roughness. Another practice is to use plastic model units instead. For friction-based armour units (uniformly placed concrete armour units and pattern-placed blocks) it is advised to keep the scale model as large as reasonably possible.

### 2.3.3 Physical models

The stability of armour layers can be tested by simulating the loads exerted on armour units in pull-out tests, or by applying the actual loads in hydraulic physical model tests.

#### Pull-out tests

Pull-out tests are conducted on concrete armour units when the initial stability of the armour unit needs to be tested. It is a quick, relatively easy and cheap method to gain insight into the stability mechanisms, especially when it can be done on a small scale. For placed blocks, these tests have to be done on (nearly) full scale since friction cannot be scaled down. Neither can the sub-layer be scaled down since sub-layers of placed blocks consist of fine to coarse material. An example of a full-scale pull-out test on placed blocks is depicted in Figure 2.13.



**Figure 2.13:** Full-scale pull-out test on Verkalit interlocking placed block, chronological sequence [Gier et al., 2012]

Price [1979] was the first to conduct several pull-out tests for concrete armour units and accumulated data for the well-known graphs that describe the total stability as the summation of own weight, friction and interlocking, for varying slope angle, Figure 2.14. His main conclusions were that compaction of the slope and the number of rows above the observed unit influence the stability of the slope greatly. In tests that were conducted with Dolos armour units, compaction of the slope by loading it without creating damage increased the stability with 31% to 36% while it decreased the covered area by 5%: "This demonstrates that if a Dolosse slope 'as laid' has not been bedded down by a favourable wave climate before it is caught by storm then it could be vulnerable. How long this compaction takes depends on the time/intensity of wave action and on the roughness of the underlayer which controls the ability of the Dolosse to slide down the slope and compact", [Price, 1979].

The stability against extraction of a block is expressed as the force needed to pull a block out, made dimensionless by the weight of the block:  $\frac{F}{W}$ . Especially for pattern-placed revetments these forces can become very large, such that, for example, the pull-out force is  $100 \cdot W$ . For these values, it is debatable if the expression of force as multiple of the own weight is still a good representation. This is motivated by that fact that the weight is clearly not the governing factor in stability anymore. For multiples larger than 10, caution should be paid to the interpretation of the results. A different expression for stability against extraction could be a good idea.

The measured spread in pull-out tests is often very high so many tests are needed to relate quantitative conclusions to the numbers. It also illustrates the distribution of strength over the slope: there will be elements with virtually no extra stability than their own weight but there will also be elements with much higher stability. The recently graduated Dr.ir. Peters made an effort to gather information on all pull-out tests for pattern-placed blocks, which can be found in Appendix C of his report [Peters, 2017].

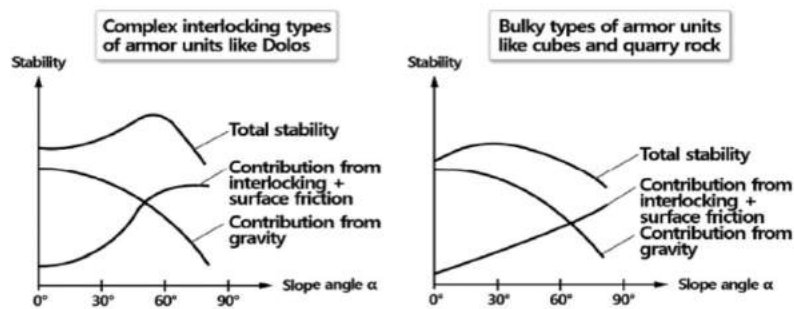


**Figure 2.14:** Influence of the slope angle on stabilisation mechanisms for complex interlocking units and bulky type of units, after Price [1979]

### Hydraulic physical model tests

In hydraulic model tests the structure to be tested, the prototype is scaled down to obtain an easy to handle structure, the model, on which measurements can be done. The generally used method is presented in the previous section. Hydraulic physical models are a very effective way to investigate the interaction between structure and waves for a specific set of parameters and conditions. They can be executed to test a design or to learn more about the armour unit (such as in this research).

## 2.4 Xbloc<sup>+</sup> v1

In this section, the development and characteristics of Xbloc<sup>+</sup> v1 as a solution to the drawbacks of Xbloc are discussed.

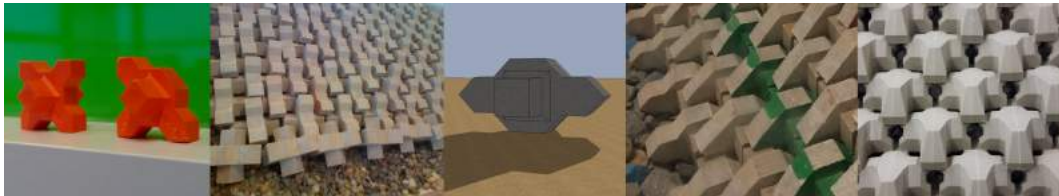
### 2.4.1 Design process leading to Xbloc<sup>+</sup> v1

As explained in detail in Chapter 1, there are two drawbacks with the design of Xbloc. Xbloc can be placed with uniform orientation but this results in an increase of 30% in material costs, which is unfavourable from a financial point of view. Additionally, it has turned out that the placement method of Xbloc, which is supposed to be extra easy, poses a problem for some contractors. It was looked at how the shape of Xbloc could be modified to obtain a more regular looking slope while providing the same amount of protection with the same quantity of material. The first modification was done by removing one leg to obtain Ybloc. Model tests concluded that there was a lot to be optimized. A second leg was removed, resulting in Ibloc.

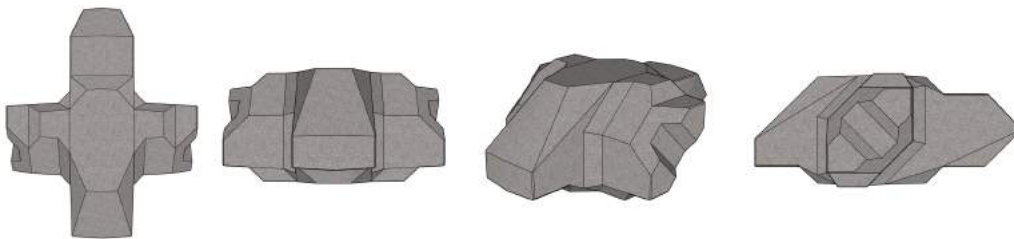
In preliminary 2D physical model tests done by Jacobs [2015] some observations were made with respect to the failure mechanisms and with respect to the influence of the shape on failure. Three tests were done in which different packing densities and shapes were tested. During the first two tests, rocking and extraction were observed. For the third test, the shape of Ibloc was altered to decrease the lift on the nose (Ibloc<sup>+</sup>), after which minimal rocking was observed. Lastly, several types of wings

were designed in which the balance between porosity, stability and concrete usage was optimized. These last design changes resulted in  $Xbloc^{+v1}$ .

Single layer concrete armour units are usually placed on a staggered grid with random orientation, but with  $Xbloc^{+v1}$  there is only one way to place the unit; uniformly. Due to the shape and placement of  $Xbloc^{+v1}$  a smooth looking slope is created, which is a desirable feature on a landmark like the Afsluitdijk.



(a) Design process from Xbloc to  $Xbloc^{+v1}$ , f.l.t.r.: Xbloc, Ybloc, Ybloc slope, Ibloc, slope with Ibloc as toe and Ibloc<sup>+</sup> subsequent rows, slope with  $Xbloc^{+v1}$



(b)  $Xbloc^{+v1}$ , f.l.t.r.: top view, front view, diagonal view and side view

**Figure 2.15:** Becoming familiar with  $Xbloc^{+v1}$

## 2.4.2 Characteristics

The new armour unit can be described by 3 geometric parameters;  $D$ ,  $L$  and  $H$ ; width, length and height. Furthermore, 5 area's can be discerned; the nose, the tail, the right and left wing and the core of the armour unit. The sloping surfaces from wing and tail to top and bottom of the core are called chamfers. These definitions are displayed in Figure 2.16.

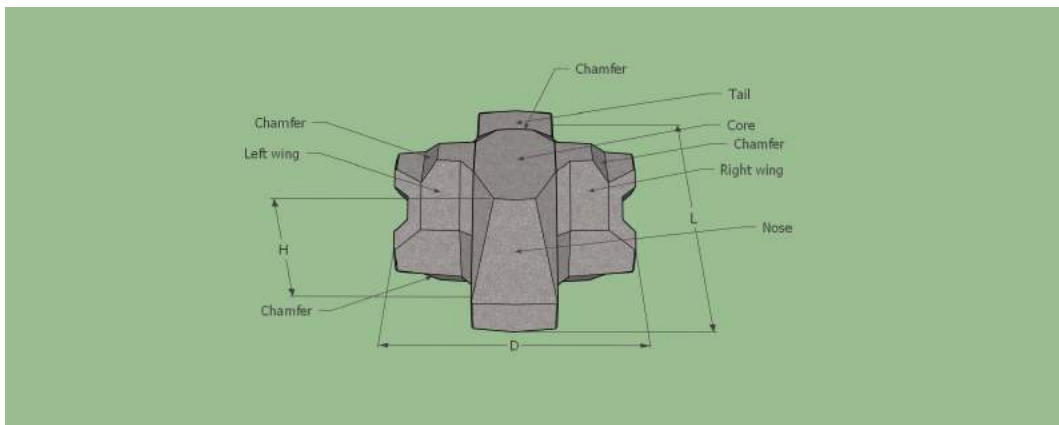


**Figure 2.16:** Definitions  $Xbloc^{+}$

Apart from the standard dimensions, the following characteristics can be defined: the nominal diameter  $D_n$ , the concrete usage per unit surface area or in other words the concrete volume expressed as layer thickness  $D_{cu}$  (also depicted in Figure 2.17), the actual layer thickness  $t_a$ , the horizontal placing distance  $D_x$ , the up-slope placing distance  $D_y$ , the relative packing density  $RPD$ , the volumetric porosity  $n_v$ , the design stability parameter  $K_D$  and lastly the material needed for protection against



the same wave. The characteristics as function of the armour unit size have been established in Table 2.1, in which the characteristics of Xbloc are also displayed for comparison.

**Table 2.1:** Characteristics Xbloc<sup>+</sup> v1 and Xbloc expressed as function of the unit size

Parameter	Xbloc <sup>+</sup> v1	Xbloc
D [m]	$D_{x+}$	$D_x$
L [m]	$1.27 \cdot D_{x+}$	$D_x$
H [m]	$0.50 \cdot D_{x+}$	$D_x$
$D_n$ [m]	$0.62 \cdot D_{x+}$	$0.69 \cdot D_x$
$D_{cu}$ [m]	$0.33 \cdot D_{x+}$	$0.40 \cdot D_x$
$t_a$ [m]	$0.80 \cdot D_{x+}$	$0.97 \cdot D_x$
$D_x$ [m]	$1.11 \cdot D_{x+}$	$1.32 \cdot D_x$
$D_y$ [m]	$0.63 \cdot D_{x+}$	$0.63 \cdot D_x$
RPD [units/m <sup>2</sup> ]	$1.43 / D_{x+}^2$	$1.2 / D_x^2$
$n_v$ [-]	0.583	0.587
$K_D$ [-]	12 (estimated)	16
Material quantity [%]	103	100

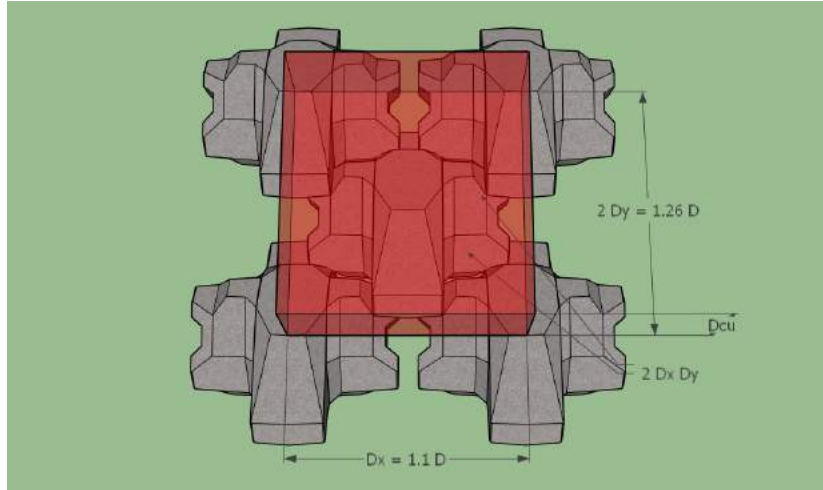


**Figure 2.17:** Definition of  $D_{cu}$

When the armour units are placed such that the top of the core, wings and tail are horizontal oriented, a slope under and angle of  $35.3^\circ$  is formed. This is just between a 2:3 and 3:4 slope that have an angle of  $33.7^\circ$  and  $36.8^\circ$  respectively. For a 2:3 slope the units will slant slightly backwards and for a 3:4 slope they will slant slightly forward. When the units are placed perfectly, all units have 9 contact area's, 8 of these area's make contact with other armour units (2 below the nose, 1 below and above each wing, 2 on top of the tail) and below the tail 1 area makes contact with the under layer.

### 2.4.3 Previous hydraulic model tests

In preliminary 2D physical model tests done by Delta Marine Consultants on the first version of Xbloc<sup>+</sup>, called Ibloc [Jacobs, 2015], some observations were made with respect to the failure mechanisms and with respect to the influence of the shape on failure. Three tests were done in which different packing densities and shapes were tested. During the first two tests, rocking and extraction were observed. For the third test, the shape of Ibloc was altered to decrease the lift on the nose, after which minimal rocking was observed. A wave height = 13.2 cm was reached without extractions and the armour layer failed before reaching a wave height of = 15.1 cm. Compaction of the armour layer was observed in all tests but this did not lead to loss of interlocking of the top rows. A fourth test was done to investigate damage progression.

A single test with the current shape of Xbloc has been conducted by Jacobs, showing a wave height up to  $H_s = 12.5\text{cm}$  before failure occurred. Rocking as well as extraction were observed. All runs were done with a JONSWAP spectrum and a 1:30 foreshore, causing the highest waves to break before reaching the structure, where the depth above the toe was 0.25m. The results of this test haven't been lined up in a document, therefore it will simply be referred to as "the preliminary test by Jacobs".

## 2.4.4 Comparable units

Two units will be discussed in further detail: Crablock and Single Layer Cube. Both units are placed with a uniform orientation but the first relies mainly on interlocking and the second relies mainly on inter-block friction.

### 2.4.4.1 Crablock

Crablock is a relatively new block designed in the United Arab Emirates. The block is similar to other interlocking armour units except for the fact that this block can be placed with a random orientation as well as with a uniform orientation in a diamond or rectangular grid (Figure 2.18). Recent master theses on the stability of these single layer armour units were done by Bonfantini [2014], Salauddin [2015] and Broere [2015].

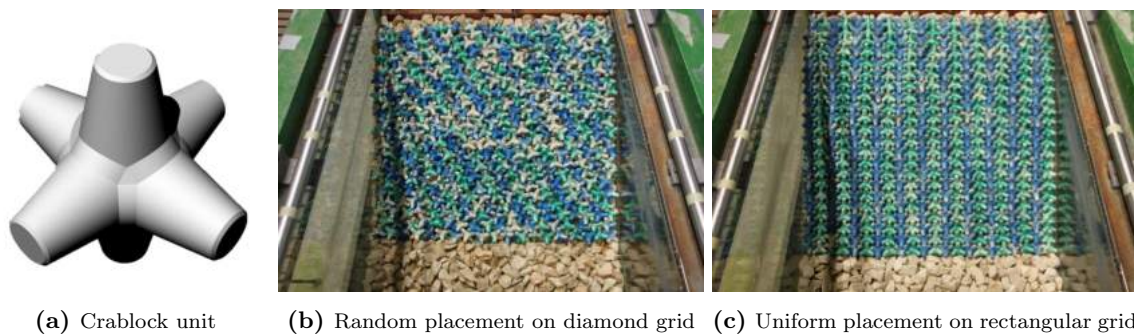


Figure 2.18: Introduction to Crablock

Eight out of the ten physical model tests done by Salauddin can be used as comparison material: the model units were placed on a rectangular grid with uniform orientation, use was made of a 1:30 foreshore slope and runs were increased with  $\pm 4$  cm in significant wave height. In these tests, the packing density ( $\frac{0.63}{D_n^2}$ ,  $\frac{0.66}{D_n^2}$  and  $\frac{0.69}{D_n^2}$ ), the crest height (0.14m and 0.185m) and the wave steepness (0.02 and 0.04) were altered. Unfortunately, the combination of a diamond grid together with uniform orientation wasn't tested.

The criterion for "no rocking" was set at  $N_{or} = 0.2$  to eliminate the influence of inaccurately placed units. This criterion was fulfilled up until a value of  $\frac{H_s}{\Delta D_n} = 4$  for the most densely packed slope. The slopes with lower packing density showed rocking in an earlier stage (for stability numbers of 3 and 2 respectively).

"Displacement" was defined as movement  $> 0.75D_n$ . A few tendencies can be concluded from the data presented by Salauddin:

- The larger crest height results in larger movement, especially for exceedance of the design wave height.
- The less steep waves result in earlier movement (between a stability number of 3 and 4.5), and the steeper waves result in almost no movement.
- For these steeper waves tests were limited to a stability number of 4.8 for which only 1 out of 4 slopes showed movement.



#### 2.4.4.2 Single Layer Cube

Initially, the cube was only used in a double layer but it wasn't easy to place them with a random orientation: the shape of cube makes that they want to be placed in one layer. Investigation into the stability of cubes in a single layer has been going on since 1998. The first conclusions of tests on a 2:3 slope in 1999 was: "In comparison with double layers the performance of single top-layers of Cubes is remarkably good and considered as a feasible and cost-saving alternative for traditional slope protections", van Gent et al. [1999]. In these tests, the units were placed irregularly and, next to stability, the tests focussed on the influence of the packing density, filter material, wave steepness, toe depth and crest elevation. In later tests also regular placement was explored. All tests were conducted on a 2:3 slope with an 1:30 foreshore and JONSWAP spectrum.

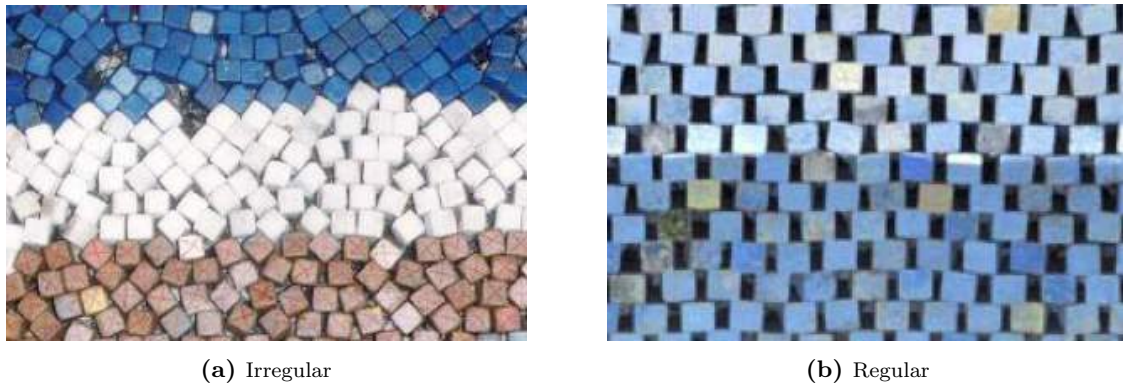


**Figure 2.19:** Pattern placement of cubes in a single layer [van Gent and Luis, 2013]

The more recent paper by van Gent and Luis [2013] gathers all results so far, of which the most important ones are presented here:

1. The stretching bond pattern (regular) has a higher stability number for start of damage.
2. The armour layer should be placed with 25% porosity to reduce settlement.
3. The mass ratio of cube over under layer should be 10 to prevent out-wash and enable smooth placement.
4. The weight of the armour layer is mainly transferred to the toe, therefore the toe should have sufficient rock material to provide a stable base or it should extend to within the seabed.
5. Start of damage occurs at stability numbers between 2 and 3, failure occurs at stability numbers between 3 and 3.5 in which failure is defined as  $N_{od} > 0.2$ .
6. Single layer cubes obtain their stability from a combination of their own weight, inter-block friction and reduced wave attack due to a smoother slope.

# Chapter 3: Hypotheses

In this chapter, the two research questions as presented in chapter 1 are discussed and a hypothesis is formed for both. These hypotheses give direction to the different model tests that have been performed and its focus areas. The two research questions are presented again below:

1. *How does Xbloc<sup>+ v1</sup> achieve its stability?*
2. *How does Xbloc<sup>+ v1</sup> respond to wave loading?*

## 3.1 Stabilising mechanisms

Section 2.2.2 states that armour units that are randomly oriented usually rely on a combination of their own weight and interlocking to be stable. Armour units that are uniformly oriented usually rely on a combination of their own weight and inter-block friction. In that view, Xbloc<sup>+ v1</sup> is expected to derive its stability from a combination of own weight and inter-block friction. However, there are some large differences between the uniformly placed units discussed in Section 2.2.2 and Xbloc<sup>+ v1</sup>.

### Own weight and friction

The discussed units all have a blocky type of shape:  $B \cdot L \cdot H = D \cdot D \cdot D$ . If the shape deviates from a cubic type it is to become a column type, increasing the weight per unit slope area:  $B \cdot L \cdot H = D \cdot D \cdot c_1 D$ . Xbloc<sup>+ v1</sup> doesn't have a cubic nor a column shape. If a box were placed around it, it would have the following dimensions:  $B \cdot L \cdot H = D \cdot 1.27D \cdot 0.50D$ . Additionally, all other blocks have a hole in it which can be seen in Figure 3.1. Cube is the only exception but is placed in such a way that large voids are created.

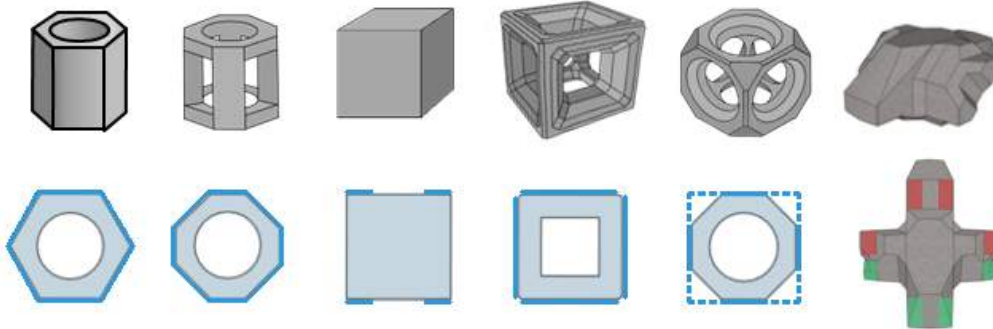


**Figure 3.1:** 3D and topview of SeaBee, Diahitis, Cube, Cob, Shed and Xbloc<sup>+ v1</sup>. Indication of colours: blue = vertical friction plane ( $\perp$  to slope), red = horizontal friction plane atop ( $\parallel$  to slope), green = horizontal friction plane below ( $\parallel$  to slope)

Taking into account that the surface area spanned by the extremities of Xbloc<sup>+ v1</sup> also includes parts of other units, and because of the absence of a hole, it is estimated that the stabilising mechanism "own weight" has a relatively large influence compared to the other units.

The wave load acts predominantly perpendicular to the slope (see Section 2.1.4), creating friction on planes which are oriented perpendicular to the slope. The surfaces which cause friction between the Xbloc<sup>+ v1</sup> units (red and green in Figure 3.1) have a different orientation than those of the blocky units, which are perpendicular to the slope (blue in Figure 3.1). The wave load doesn't act solely in perpendicular direction so some friction will be generated. For this reason it is expected that inter-block friction contributes to the stabilization of Xbloc<sup>+ v1</sup>, but to a far lesser extent than is typical for uniformly oriented single layer units.

**Interlocking**

The units are placed in stretching bond, overlapping each other. The chamfers from core and both wings of an observed  $Xbloc^{+v1}$  prevent the neighbouring units and the units a row above from being displaced in horizontal direction. At the same time, part of the weight of the two units from a row above rests on the observed unit, increasing the units resistance against movement. It is expected that the interlocking mechanism contributes largely to the stabilization of  $Xbloc^{+v1}$ .

**Number of rows**

It is expected that units high on the slope will be easy to pull out. For an increasing number of rows above the observed block, an increasing pull-out force will be found. An equilibrium will be formed concerning the transfer of forces to lower rows and under layer, therefore the pull-out force will converge to a constant value for an increasing number of rows. These were relations also found by Price [1979] and van de Koppel [2012].

**Under layer**

Randomly oriented armour units require a relatively coarse under layer to prevent washing out of material but uniformly oriented armour units require a relatively fine under layer so that the units can be placed tightly together. It is expected that, due to the uniform placing of the armour unit, a finer sub-layer will lead to a more stable construction.

**3.1.1 Hypothesis**

The hypothesis for the first research question is:

*The stabilizing mechanisms of  $Xbloc^{+v1}$  will consist of own weight, interlocking and friction, of which the first two will be the main mechanisms; furthermore, the stability is increased for an increasing number of rows and a decreasing under layer roughness.*

To test this hypothesis and get a better understanding on the stabilizing mechanisms, pull-out tests have been carried out. The set-up of these model tests and a more elaborate explanation of the expectations are explained in Section 4.1, the results in Section 5.1 and the conclusions and recommendations in Section 6.1.1. How the outcome of these model tests should be interpreted can only be fully understood when also hydraulic tests have been done. The combination of the results will give a better understanding of the stabilizing mechanisms than either of the tests alone.

**3.2 Wave action**

The pull-out tests gave insight into the stabilising mechanisms of  $Xbloc^{+v1}$ . This information, together with the information presented in this section and Sections 2.4.3 and 2.4.4 leads to the hypothesis for the second research question.

**Armour unit roughness**

The main conclusions from the pull-out tests were that the interlocking mechanism of  $Xbloc^{+v1}$  is low and that the armour unit is sensitive to small deformations and settlements in the under layer. The low interlocking capabilities result in a large contribution of friction to the armour layer stability. When units are placed in water, friction between the units becomes less. This is both due to a film layer of water around the unit, decreasing the roughness, and the buoyant forces on the unit. Since the plastic units are already smooth, the presence of water will have the most influence on these armour units.

**Placement**

Any units that do not make contact with other units on all 9 points are less stable. However, placement will become easier; the under layer can be compacted due to the presence of a core instead of a rigid board. It is expected that instabilities will occur due to difficulties with aligning a unit such that nose, wings and tail are secured.

**Previous model tests**

Based on previous model test by Jacobs in which a significant wave height of 12.5 cm resulted in failure, a stability number of  $\pm 3.3$  can be calculated. These tests were conducted on a 3:4 slope with a 1:30 foreshore and a water depth of 0.25m. The geometry of the model is conform the general breakwater design.

Single layer cubes under 4% wave steepness reached stability numbers between 2 and 3 for start of damage and between 3 and 3.5 for failure. These tests were conducted on a 2:3 slope without a foreshore and water depth of 0.50m ( $\approx 2.5 \cdot H_s$ , indicating relatively deep water and thus the possibility of larger waves). It is expected that Xbloc<sup>+ v1</sup> will respond similarly to waves as Single layer cubes due to the smooth surfaces and the relatively large contribution of friction. Based on the previous model test by Jacobs it is expected that the stability number will remain below 3.3 since a larger water depth is used, allowing for larger extreme waves (see also 1.3).

**3.2.1 Hypothesis**

The hypothesis for the second research question is:

*There will be a large difference between the performance of the plastic and concrete armour units since, in the absence of a strong interlocking mechanism, friction plays a large role. Any irregularities in the surface profile can be an indication for weak spots; at those locations there is not enough surface contact to create the needed friction. The stability number of Xbloc<sup>+ v1</sup> will be*

$$2.0 < \frac{H_s}{\Delta D_n} < 3.3 \text{ for failure.}$$

To test this hypothesis, hydraulic model tests have been performed. The set-up of these model tests and a more elaborate explanation of the expectations are explained in Section 4.2, the results in Section 5.2 and the conclusions in Section 6.2. Based on the combined results, conclusions and recommendations of the pull-out tests and hydraulic model tests, the final conclusions and recommendations have been formed. These are presented in Section 6.3.

# Chapter 4: Experiment set-up

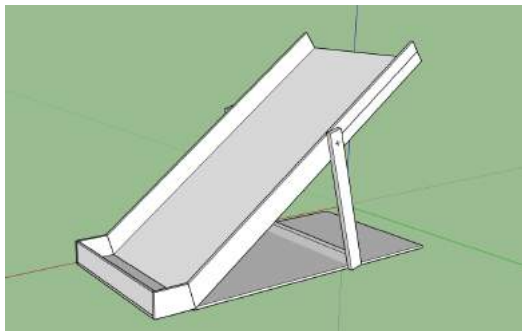
The hypotheses stated in Chapter 3 was tested by conducting pull-out tests and hydraulic physical model tests, which will be described in this chapter. Based on these tests conclusions and recommendations will be given to optimize the shape of Xbloc<sup>+</sup> v1.

## 4.1 Pull-out tests

The performed pull-out tests consist of measuring the force required to extract a unit from the armour layer. The set-up, used test program, methodology and expectations are discussed in this section.

### 4.1.1 Set-up and geometry

No test facilities were available for this kind of dry model tests so a construction was built, this was done in such a way that it can also be used in later studies (so it was made extra long, small enough to be put in the flume as well and adjustable for 3 slope angles). The construction is made out of wood, hinges and wire mesh. First, a wooden box is constructed on which the wire mesh is nailed. The wire mesh is needed to increase the roughness of the board, making it possible for small rocks to stay in place on the slope. The short edge of the box is secured to a heavy plate by a hinge, facilitating rotation of the box around the short edge. At approximately 2/3 of the box length, a frame is secured to the sides of the box with bolts. Lastly, some pieces of wood are screwed into the base plate such that the frame can support the box for slope angles 1:2, 2:3 and 3:4. The box was designed to hold at least 30 rows with alternating widths of 10 and 9 units respectively. Figure 4.1 depicts the design of the slope.



(a) Design



(b) Reality

Figure 4.1: Model set-up

The model units that were used for this research, as well as for the hydraulic model tests, have the following dimensions:  $D = 4.8\text{cm}$ ,  $L = 5.9\text{cm}$ ,  $H = 2.9\text{cm}$ ,  $D_n = 2.9\text{cm}$  and weighing 58 gr on average. Appendix A gives a detailed description of the characteristics of the model units.

The slope angle determines how much of the weight of each block is transferred to under layer or blocks on lower rows. For a steep slope more force is transferred to the blocks, increasing interlocking and friction forces. Additionally, most breakwaters are built with a 3:4 slope to reduce the amount of material and space needed in the design. For these reasons pull-out tests were conducted on a 3:4 slope.

Under layers were applied with a thickness of  $2 \cdot D_{n50}$ , just as would be applied for a prototype breakwater. Sieve curves of the under layer material are enclosed in Appendix C.

### 4.1.2 Test program

In total 22 tests were conducted in which the parameters were varied accordingly table 4.1. Each test consisted of 8 samples: 2 samples pulled out 20 rows from the top, 2 samples 15 rows from the top, 2 samples 10 rows from the top and 2 samples 5 rows from the top. Additionally, some initial tests were carried out to determine the appropriate methodology with respect to the modelling of the wave force. The force pulls on the centre of gravity of the unit in a uniform direction so it should be applied in the model in the same way. Usually, a hole is drilled into the core of a model unit, but for these small units this is not possible without destroying it. Several methods of securing fishing line to the model unit were tested. Methods "Simple" and "3 loops" lead to an asymmetrical application of the force so eventually the method "Cross" was chosen, see Figure 4.2. On 8 predefined locations on the slope, sample blocks with fishing line around them and numbered from 1 through 8 were placed, Figure 4.3a. An LHS Load Cell (of which the specifics are included in Appendix B) and the software package DasyLab were used for measuring.

**Table 4.1:** Test program pull-out tests

Series number	Test number	Material	$W_{50,under}$	$\theta$
1	1	Concrete	$\frac{1}{6} \cdot W_{armour}$	90°
2	2 and 3	Plastic	$\frac{1}{6} \cdot W_{armour}$	90°
3	4 through 9	Plastic	$\frac{1}{11} \cdot W_{armour}$	90°
4	10 through 14	Concrete	$\frac{1}{11} \cdot W_{armour}$	90°
5	15 through 18	Concrete	$\frac{1}{11} \cdot W_{armour}$	45°
6	20 through 23	Plastic	$\frac{1}{11} \cdot W_{armour}$	45°



**Figure 4.2:** Methods of securing fishing line: "Simple", "3 loops" and "Cross"

Since friction cannot be scaled down correctly, as discussed in Section 2.3.2, both plastic and concrete blocks were used. The difference in surface roughness may lead to a larger force for one of the units. For both units statistics on width, weight and density have been determined and enclosed in Appendix A.

The model units used in this research have the following general dimensions:

- $D = 4.7$  cm
- $L = 5.9$  cm
- $H = 2.4$  cm
- $D_n = 2.9$  cm
- $D_x = 1.1D = 5.17$  cm
- $2 \cdot D_y = 2 \cdot 0.63D = 5.92$  cm
- $D_{cu} = \frac{\text{Concrete volume}}{\text{Covering area}} = \frac{2D_n^3}{D_x 2D_y} = 1.56$  cm

At first an rather coarse under layer was used, which resulted in a very slow placement process. Even though the surface profile was measured and approved according to the methodology stated in the next section, the under layer was too rough for the units to be placed accurately. The switch to an

under layer with a median weight of  $1/11$  times the weight of the armour unit resulted in a faster and more accurate placing sequence.

Lastly, the direction of pulling was varied. Based on Hald [1998] (see section 2.1.4) both the  $90^\circ$  and  $45^\circ$ , resembling the outward flow force, will be tested (Figure 4.3b). The up-slope directed force is of least interest since it is obvious from the Xbloc<sup>+</sup> v1 shape that the slope will have a high resistance against this force.

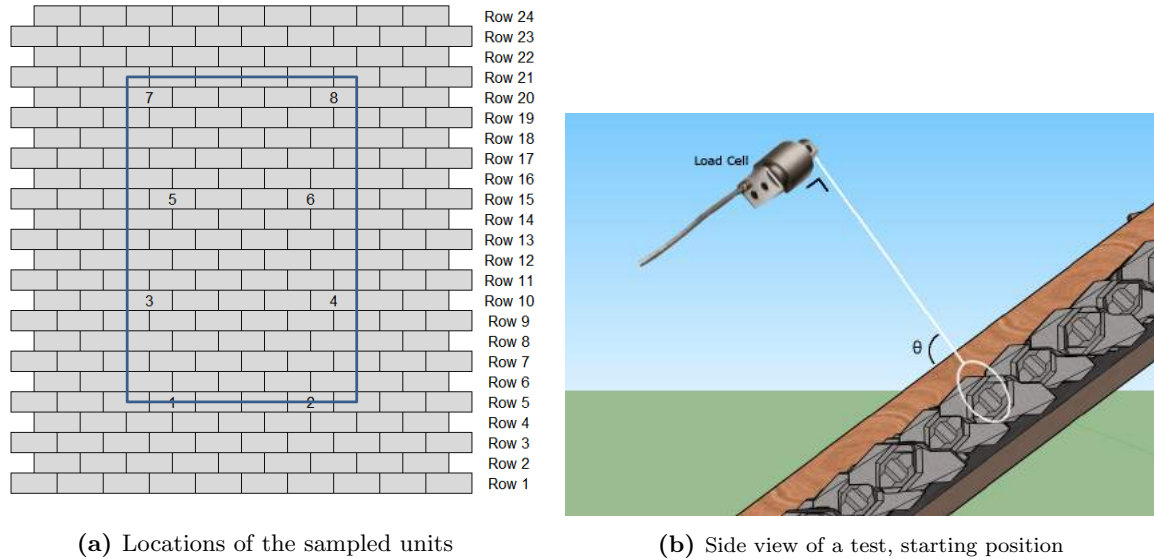


Figure 4.3: Measuring method

### 4.1.3 Methodology

A methodology was established to assure that each test would be conducted in the same manner:

1. Clear all material of the slope and load it (again) until a thickness of approximately  $2 \cdot D_{n50}$  is reached. Flatten the slope using a trowel, check if the slope is level everywhere and there are no elements protruding out of the under layer. Adjust if needed.
2. Confirm the smoothness of the under layer by applying the foot staff method as recommended by CIRIA et al. [2007] (using a probe with a spherical foot with a diameter of  $0.5D_{n50}$  to measure the surface profile of the under layer). A grid of  $5\text{cm} = 3.66D_{n50}$  was used in contrary to the advised  $0.75D_{n50}$  grid in view of time (108 instead of 3171 grid points).
3. Place the first row of blocks accordingly the advised horizontal placement distance of  $1.1 \cdot D$ , checking if every block is placed firmly onto the under layer. As discussed in Chapter 2 the toe structure has a rather large influence on the armour layer stability for all types of units.
4. Place all subsequent rows, checking if each unit has at least 4 out of 5 contact points (1 beneath each wing, 2 beneath the nose and 1 beneath the tail). Secure the sides of the armour layer with excess under layer material.
5. On the 5th, 10th, 15th and 20th row 2 sample units should be placed such that there are 20, 15, 10 and 5 rows above each 2 units respectively. There should be at least 2 units between the edge of the slope and the sampled unit, as well as between two consecutive sampled units to eliminate boundary effects.
6. Check the packing density for each slope by measuring the up-slope distances between units 3 through 8 (counted from left to right) on rows 5 and 20, and the horizontal distances between units 3 and 8 on rows 5, 7, 9, ..., 21. This reference area is also depicted in Figure 4.3a by the blue box. Slopes with packing density below 98% or above 105% of the theoretical packing density should be rebuild.



7. Write down observations with respect to the state of the slope, any details out of the ordinary should be noted.
8. Calibrate the LHS Load Cell
9. Create a new file in DasyLab (in which the recordings are saved for each individual measurement, so 8 files per slope). Secure the load cell to the sample unit and hold the device at a 90°-angle with the pull direction to create an artificial reference point for the start of the test. Start the test at location 1, hold the load cell in the starting position (Figure 4.3b) for a few seconds before gradually building up force.
10. After the unit has been pulled out check if there was loss of contact for any of the other locations. Continue until all locations are sampled and repeat the sequence for each test.

## 4.2 Hydraulic physical model tests

The observations and conclusions of the pull-out tests lead to a number of questions with respect to the influence of various parameters on the armour layer stability. Due to time restrictions, it was not possible to investigate all combinations of parameters, therefore, the decision was made to execute a simple test program. The sections below will discuss how the research was executed.

The hydraulic physical model tests consisted of observing the armour layer stability against wave action. To help achieve this, a scale model was built in the wave flume of DMC in Gouda, in total 10 tests were conducted which can be subdivided into 5 series. The aim of these tests was to find the weak and strong points in the design, as well as to verify the conclusions of the pull-out tests. The tests started with a low significant wave height of  $\pm 6$  cm and the wave load on the model was increased stepwise until failure occurred.

### 4.2.1 Set-up

This section will elaborate on the set-up *around* the structure.

#### Wave flume and gauges

The model tests were conducted in the wave flume of Delta Marine Consultants in Gouda which is 60 cm wide, 100 cm high and has a length of 25 m, Figure 4.4a. The maximum water level in the flume is 70 cm for which a maximum wave height of 30 cm can be reached. The flume has a piston-type wave board which is capable of producing very specific spectra due to its reflection compensation system. Several meters behind the wave generator 3 gauges were placed, as well as directly in front of the breakwater toe. The incoming and reflected waves will be analysed in the program Wavelab with the method of Mansard and Funke [1980] which also prescribes the distances between the first, second and third wave gauge as depicted in Equations 4.1 and 4.2. The parameter  $L_p$  is the wave length based on the peak wave period  $T_p \approx 1.15T_{mean}$ .

$$x_{1\&2} = \frac{L_p}{10} \quad (4.1)$$

$$\frac{L_p}{6} \leq x_{1\&3} \leq \frac{L_p}{3}, \quad x_{1\&3} \neq \frac{L_p}{5}, \quad x_{1\&3} \neq \frac{3L_p}{10} \quad (4.2)$$

The waves in this research had a length ranging between 1.7 m and 2.8 m, leading to values for the wave gauge distances as shown in Table 4.2. It can be concluded that there is no combination possible that adheres to the prescribed standards, therefore the generally used distances of  $x_{1\&2} = 0.3$  and  $x_{1\&3} = 0.7$  were used, Figure 4.4b.

**Table 4.2:** Required distances for wave gauges

	$L_p$	$1/3L_p$	$1/6L_p$	$1/10L_p$	$1/5L_p$	$3/10L_p$
<b>Min</b>	1.70	0.57	0.28	0.17	0.34	0.51
<b>Max</b>	2.83	0.94	0.47	0.28	0.57	0.85



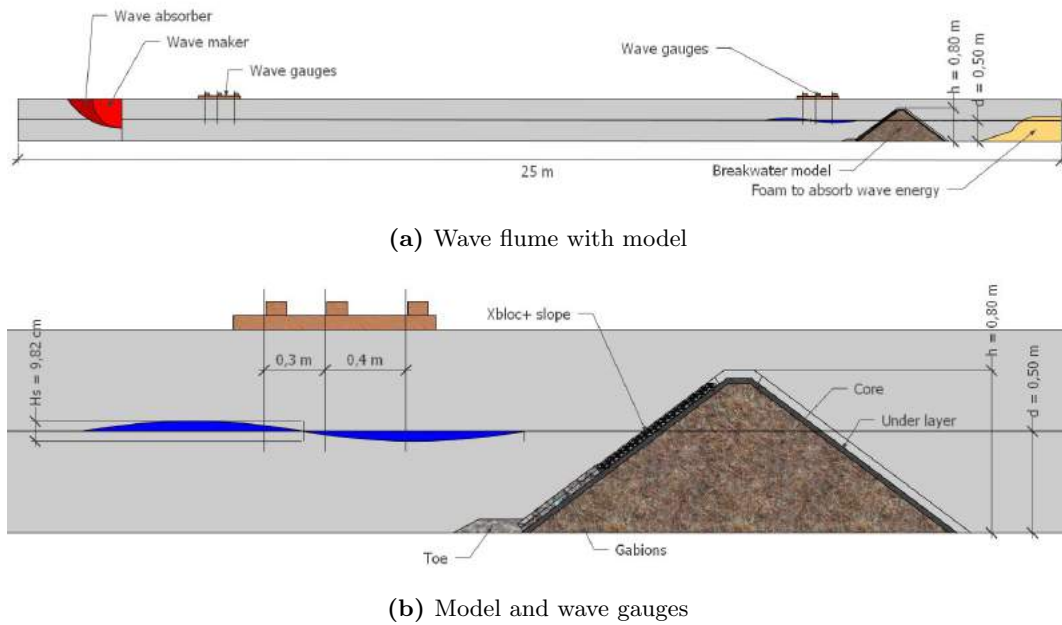


Figure 4.4: Overview of the model set-up

### Documenting

The armour layer stability was documented by 2 video cameras on tripods. One camera was mounted on the wave flume, directed perpendicular to the slope and one camera was placed in front of the structure on the right side of the flume, creating an oblique view of the structure. With the camera in this specific set-up, any form of damage was recorded. The camera on top was used to take photographs of each slope before and after a run. Additionally, visual observations with respect to rocking units were written down in a log since the processing of video material to obtain information on rocking is very time-consuming. In Appendix D a photo series is enclosed that shows each slope at the start of a test and after failure. The log of the hydraulic model tests can be found in Appendix H.

### 4.2.2 Geometry

Since these are the first test series with Xbloc<sup>+</sup> v1 the geometry is designed in such a way that an undesirable set of parameters is obtained with respect to the exerted wave loads. The *armour layer* in these test series is intended to be loaded until failure occurs so a general impression of the stability and failure mechanisms can be formed. Table 4.3 shows an overview of all elements and their contribution to the degree of conservativeness of the model. The next paragraphs will give a description of the most important parameters. Figure 4.5, together with Figures 4.4a and 4.4b show a full description of the model set-up and geometry. The cross-section as depicted in Figure 4.5 was drawn on the glass of the wave flume as a blueprint for the construction of the model.

Table 4.3: Overview of model elements

Model element	Conservative/Optimistic
Slope + Wave steepness	Conservative
Spectrum	Normal
Wave height + Step size	Conservative
Waterdepth + Foreshore	Conservative
Freeboard	Conservative
Number of rows	Normal
Toe construction	Optimistic
Under layer	Normal/Conservative
Core	Conservative

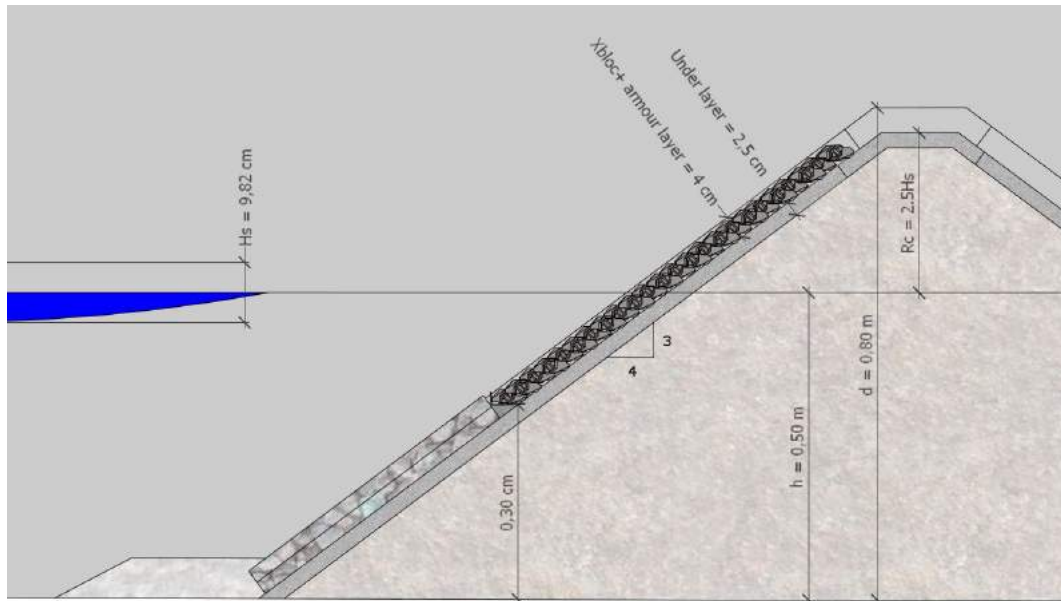


Figure 4.5: Overview breakwater set-up

### Slope

Most breakwaters have a 2:3 or 3:4 slope to prevent the construction getting wide. The pull-out tests were executed with a 3:4 slope, consequently, the hydraulic physical model tests were also executed with a 3:4 slope.

### Wave steepness

In Section 2.1.1 it is shown that a steepness of 4% is the most natural value. Additionally, for a breakwater slope of 3:4 this will result in the lowest stability number: the interaction between the incoming and reflected waves creates a wave field with breakers in between plunging and surging, this relation is also depicted in Figure 4.6.

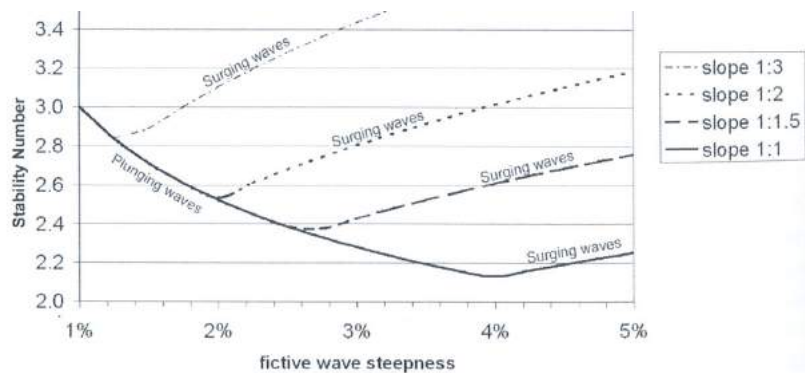


Figure 4.6: Relation between wave steepness and stability number for varying slopes [d'Angremond et al., 2001]

### Spectrum

A JONSWAP spectrum with  $\gamma = 3.3$  was chosen to be most suitable for general breakwater design, simulating a young sea-state. Per test run 1000 waves were exerted, simulating a storm of 3 hours in which the mean wave period is 10.8 seconds. The duration of a test will, therefore, be  $\pm 15$  minutes.

### Wave height

As discussed in Chapter 2, Xbloc<sup>+</sup> v1 is based on the Xbloc. The hydraulic physical model test of Jacobs showed that, compared to Xbloc, the unit performs approximately the same. Based on this

information a range of  $6 \text{ cm} \leq H_s \leq 16 \text{ cm}$  was chosen to be suitable. A step size of 2 cm per run was chosen to prevent a lot of runs without any disturbances. During the first run, the armour layer gets the opportunity to settle and compact, creating a more stable construction. This is comparable with reality since the chance of a significant storm event taking place directly after (or during) construction is very small.

### Water depth

The water depth in the flume should be at least 3 times the significant wave height to accommodate these waves implying a water depth of at least 45 cm. Additionally, the wave paddle needs at least 40 cm water depth to operate correctly and performs best from 50 cm upwards. A water depth of 50 cm was used. No use has been made of a foreshore since this filters out the higher or extreme waves and, as has been established in 2.2.2.4, these are the typical waves which determine rocking and extraction.

### Relative freeboard

The shape of Xbloc<sup>+</sup> v1 makes it such that the topmost armour unit should be high enough above the waves to prevent movement. This means that the model needs to have a large relative freeboard. The number of rows above the waterline has both positive and negative effects on the armour layer stability: the more rows above a block, the higher its resistance against extraction (this was also concluded from the pull-out tests, see Section 6.1.1) but since no wave energy is dissipated via overtopping the load is also higher. To prevent this extra mass benefiting the results in terms of stability too much,  $R_c$  can not be too high. A relative freeboard of  $2 \cdot H_s$  was used.

### Number of rows

Since the total height of the model,  $50 \text{ cm} + 2 \cdot H_s$ , was quite large, gabions secured by a rock toe were used to bridge the first part of the slope. The damage was expected to be concentrated between  $1.5 \cdot H_s$  below SWL and  $0.5 \cdot H_s$  above, therefore the gabions were placed until a depth of 30 cm (from the bottom upwards). The rest of the slope was covered with armour units, which resulted in a total of 23 rows per slope (this was also the maximum number of rows that could be placed with the available units).

### Toe

From the pull-out tests it, has been concluded that this armour unit is vulnerable to toe instability and that a stable and horizontal placement of the first row is of great importance for the stability of subsequent rows. The scope of this research is the armour layer stability so a toe failure is undesirable. As a solution, an aluminium toe-beam (Figure 4.7) was hand-made and placed just above the gabions. The toe-beam insured the stability of the first row such that only failure due to extraction or settlement could occur.



(a) Distance between units is exactly  $1.1 \cdot D_{n50}$

(b) Close-up: extra plates provide solid foundation

Figure 4.7: Toe-beam

### Under layer

As concluded from the pull-out tests, the under layer used in those tests was a bit coarse but it was

also less stable due to difficulties with transferring forces to the wooden slab and sometimes acted more like a sandy layer than an under layer. In prototype and in a breakwater model this problem will not arise. Since one of the objectives of the hydraulic model tests is to verify the results of the pull-out tests, the grading of the under layer will be kept the same. The under layer was placed in a thickness of minimally  $2 \cdot D_{n50}$ .

### Core

The scaling of core material has been done according to the method presented in Burcharth et al. [1999]. The  $D_{n50}$  was determined to be 8.8 mm, see also Appendix F.2 and Figure F.1 for a graphic representation (of both the core for this research and the core used by Jacobs). It is estimated that this core is less permeable than an average core since a grading around the  $D_{n50}$  was used.

### 4.2.3 Test program

In total 10 tests were conducted in which the parameters were varied accordingly table 4.4. Just like the test program of the pull-out tests, this program includes both plastic and concrete units. All tests were conducted on the  $1/11$  under layer.

During the course of the test program, it was noticed that rocking occurred very early, sometimes as early as the end of run 1 or the beginning of run 2. It was therefore decided that, keeping in mind the main conclusions of Price [1979], compaction of the slope by exerting a favourable wave climate should be tested as well. The step size of the last 3 tests was decreased to investigate if the armour layer became more stable when given the time to get accommodated to the wave load.

**Table 4.4:** Test program hydraulic model tests

Test number	Material	$W_{50,under}$	Step size
1, 5, 6 and 7	Plastic	$1/11 \cdot W_{armour}$	large
2, 3 and 4	Concrete	$1/11 \cdot W_{armour}$	large
8 and 9	Plastic	$1/11 \cdot W_{armour}$	small
10	Concrete	$1/11 \cdot W_{armour}$	small

Table 4.5 additionally shows the target significant wave height ( $H_s = H_{1/3}$ ) and the peak period per test run. In each run the construction was submitted to a JONSWAP spectrum with  $\gamma = 3.3$  for 1000 waves with a steepness of 4%.

**Table 4.5:** Targeted significant wave height and peak period per test run

Test number	Run	$H_s$ [m]	$T_p$ [s]
1 through 4	1	0.0673	1.04
	2	0.0898	1.2
	3	0.1122	1.34
5 through 7	1	0.0589	0.97
	2	0.0786	1.12
	3	0.0982	1.25
8 through 10	1	0.0589	0.97
	2	0.0688	1.05
	3	0.0737	1.09
	4	0.0786	1.12
	5	0.0835	1.16
	6	0.0884	1.19
	7	0.0933	1.22
8	0.0982	1.25	
9	0.1031	1.29	
10	0.1080	1.32	

#### 4.2.4 Methodology

A methodology was established to assure that each test would be conducted in the same manner:

1. Drain the flume and clear all armour units of the slope. Make sure the gabions are well-secured by the rock toe. In its turn, the toe-beam should be kept in place by the gabions in front of them (see also Figure 4.5). Check if the toe-beam is slanted slightly forward.
2. Flatten the slope using a trowel, check if the slope is level everywhere and there are no elements protruding out of the under layer. Adjust if needed. Check a second time if the toe-beam is secure.
3. Place the first row of armour units on the toe beam, make sure their tails all make contact with the under layer
4. Place all subsequent rows, checking if each unit has at least 4 out of 5 contact points (1 beneath each wing, 2 beneath the nose and 1 beneath the tail). Secure the sides of the armour layer with excess under layer material.
5. After having placed row 10, check from the side of the flume if the armour layer is being built according to the blueprint sketched on the glass, any obvious convex or concave slopes should be rebuilt.
6. When all 23 rows are placed, secure the top row with coarse material so that overtopping cannot result in removed units.
7. Write down observations with respect to the state of the slope, any details out of the ordinary should be noted.
8. Take 2 photographs before filling the flume. Fill the flume to 50 cm. Take 2 photographs.
9. Calibrate the wave gauges
10. Start both video recordings with showing the number of the test, number of the run and the wave height. Start the run.
11. Write down observations. After the run is completed, stop the recordings. Wait until the water level has found an equilibrium again before taking 2 photographs.
12. Check if the wave gauges are still calibrated, re-calibrate if necessary.
13. Repeat last 3 steps. If during a run a unit is moved or displaced from the layer the run can be continued provided that the armour layer is still functioning (for the definitions of moved and displaced Section 2.2.2.2 applies). If 3 or more units are displaced on the slope the armour layer no longer functions and the under layer will start to erode, which results in a time consuming build-up for the next test. At this point the slope has failed and the test has to be stopped. Repeat the sequence for next runs and tests.

# Chapter 5: Analysis

In this chapter the results of the pull-out and hydraulic model tests will be discussed, as well as the observations that were done during these tests. Each section will be concluded with an analysis of the combination of the background literature, the results and observations. Sections 5.1 and 5.2 will conclude with a short reflection on the hypotheses as stated in Chapter 3.

## 5.1 Pull-out tests

In total 22 pull-out tests were conducted which were subdivided into 6 series. The first two series were executed on a very coarse under-layer of which the median weight was  $\frac{1}{6}$  of the armour weight. Series 3 through 6 were conducted on an  $\frac{1}{11}$  under layer. In series 3 and 4, model units were pulled out at a  $90^\circ$  angle with the slope and in series 5 and 6 this angle was  $45^\circ$ . In half of series 3 through 6, concrete units were used and the other half was executed with plastic model units. The results of series 3 through 6 were processed and are presented in the next section. Hereafter these results will be substantiated by visual observations.

### 5.1.1 Results

Figures 5.1 and 5.2 show the required pull-out force per unit as a function of its elevation on the slope. On the horizontal axis the number of rows from the top is shown in which 5 rows from the top corresponds to samples 7 and 8 (see the previous chapter), 10 rows from the top to samples 5 and 6, etcetera. The column at 0 rows from the top corresponds to an extra set of units that were sampled without any restrictions from the rows above. The vertical axis shows the maximum pull-out force measured for each sample, normalised by the weight of the observed unit,  $G$ . Each series comprised at least 4 tests, so at least 8 samples with the same number of rows from the top. The maximum pull-out force of these 8 samples were analysed and grouped into boxplots which show the minimum, 25<sup>th</sup> percentile, average, 75<sup>th</sup> percentile and maximum values of the required force. In both figures, the plastic series is depicted by the green boxplots and the concrete series are depicted by the blue boxplots. Table 5.1 shows the corresponding values.

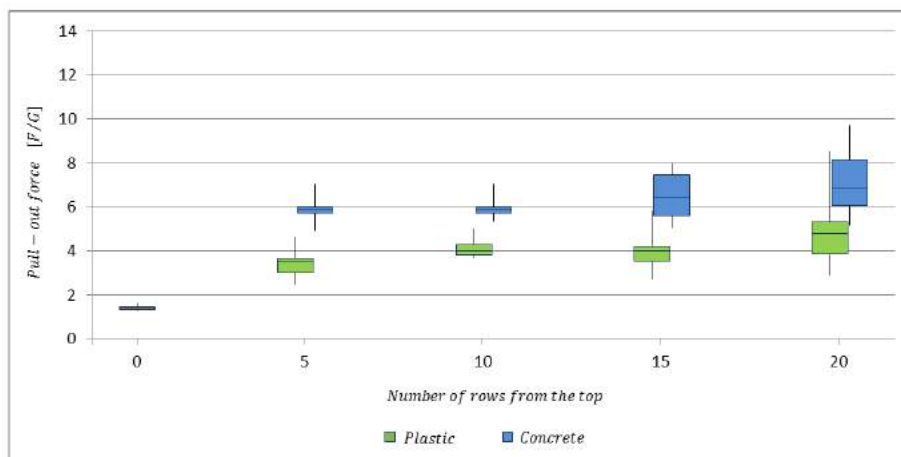


Figure 5.1: Results pull-out series 3 and 4,  $\theta = 90^\circ$ , 3:4 slope,  $\frac{1}{11}$  under layer

The first thing to notice immediately from looking at Figure 5.1 is the increasing strength with the number of rows and the difference between the plastic and the concrete armour units. For the  $90^\circ$ -tests almost every concrete sample required a larger pull-out force than the plastic sample at the same location on the slope. The 25<sup>th</sup> percentile of the concrete samples is always larger than the 75<sup>th</sup>

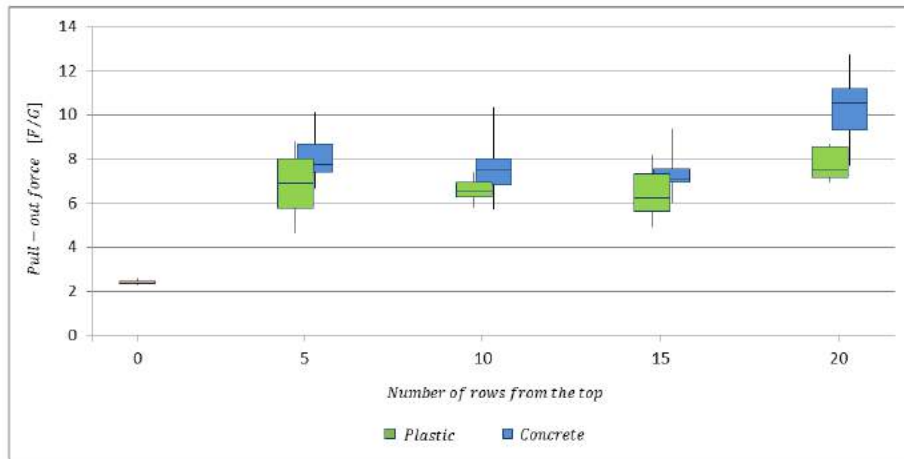


Figure 5.2: Results pull-out series 5 and 6,  $\theta = 45^\circ$ , 3:4 slope,  $1/11$  under layer

Table 5.1: Required dimensionless force as shown in the boxplots

		Plastic					Concrete			
Number of rows above		0	5	10	15	20	5	10	15	20
90°	Minimum	1.30	2.47	3.70	2.71	2.88	4.85	4.85	5.04	5.18
	25th percentile	1.35	2.99	3.81	3.55	3.84	5.69	5.69	5.57	6.04
	Average	1.36	3.53	4.02	4.00	4.77	5.88	5.88	6.46	6.86
	75th percentile	1.46	3.67	4.29	4.20	5.32	5.97	5.97	7.45	8.15
	Maximum	1.59	4.60	5.03	5.82	8.53	7.04	7.04	7.99	9.69
45°	Minimum	2.41	4.66	5.82	4.95	6.93	6.69	5.74	6.03	7.70
	25th percentile	2.47	5.80	6.30	5.62	7.18	7.40	6.82	6.96	9.30
	Average	2.48	6.91	6.54	6.24	7.51	7.76	7.53	7.09	10.56
	75th percentile	2.56	8.02	6.93	7.33	8.56	8.68	8.03	7.56	11.19
	Maximum	2.71	8.80	7.41	8.17	8.70	10.10	10.35	9.39	12.73

percentile of the plastic samples, with a difference ranging from  $0.7G$  to  $2G$ . The difference between the averages ranges from  $1.8G$  to  $2.5G$ , which for the locations up to 15 rows from the top mean a factor of 1.5 between both materials.

The samples that were extracted 20 rows from the top show less difference between the average pull-out force for different materials, but the scatter in the data is significantly larger than for the positions higher on the slope. The scatter within a dataset of units of the same material on the same location only seems to be influenced by the position of the unit on the slope: with increasing elevation the scatter becomes less.

Figure 5.2, depicts the results of the  $45^\circ$ -tests. The differences between the concrete and the plastic samples are smaller, indicating that friction is of less influence here than it was for the perpendicular pull-direction. The average value of the required pull-out force at 5 rows from the top is  $\pm 7.5G$  and decreases to  $\pm 7G$  at 15 rows from the top. The pull-out force at 20 rows from the top (the lowest locations on the slope, close to the toe) is higher again at  $\pm 9G$ .

The average pull-out force for the concrete samples at each elevation on the slope is between  $0.9G$  and  $3.0G$  higher than for the plastic samples. Locations 3 through 8 (5 through 15 rows from the top) all show the same difference of  $0.9G$  and only the lowest locations show a high difference of  $3.0G$ . The 25<sup>th</sup> percentile of the concrete samples approximately corresponds to the 75<sup>th</sup> percentile of the plastic units.

The scatter for each dataset does not seem to be related to the material properties nor to the location on the slope. For both materials as well as for varying locations on the slope the difference between the 75<sup>th</sup> percentile and the 25<sup>th</sup> percentile (height of the boxplot body) ranges from  $0.8G$  to  $2.2G$ .

Compared to the situation in which a model unit had no rows above it, the presence of 5 to 15 subsequent rows above a plastic unit increases the average required force with a factor of 2.6 and for 20 rows this factor increases to 3. For concrete, the increase of the average required force is a factor 3.0 for 5 to 15 rows and 4.3 for 20 rows above the sample.

To directly look at the impact the direction of pulling has on the maximum pull-out force, a third graph has been constructed in which the material properties were disregarded. Figure 5.3 directly relates the direction of pulling and number of rows from the top to the required pull-out force. All samples taken at the same elevation on the slope, pulled out under the same angle, were grouped to form the purple and red boxplots which represent the 90°-tests and the 45°-tests respectively.

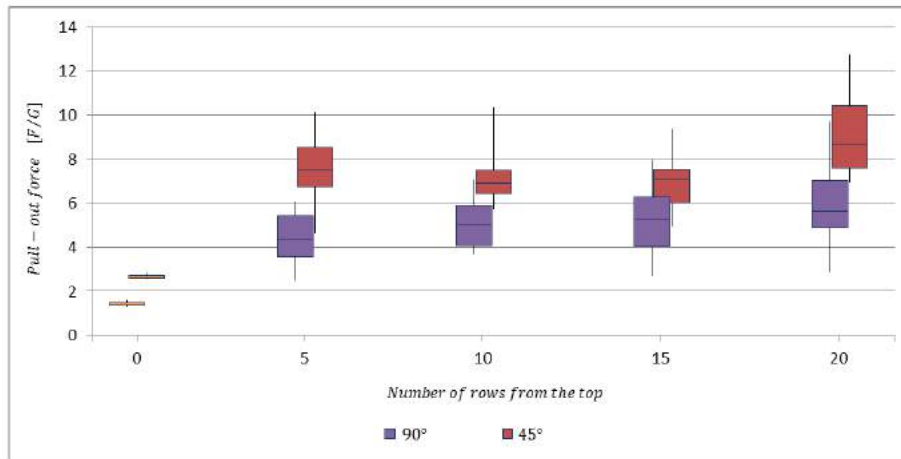


Figure 5.3: Series 3 through 6, 3:4 slope,  $1/11$  under layer, both materials

The purple boxplots show the minimum, average and maximum pull-out forces growing for an increasing number of subsequent rows. The average, 75<sup>th</sup> percentile and maximum forces seem to converge to equilibrium values of  $6G$ ,  $7.5G$  and  $11G$  in case the number of rows was even further increased. The scatter of each dataset increases for an increasing number of rows ( $3.5G$  to  $6.8G$ ) but the height of the boxplot body stays approximately constant at  $2G$ .

The red boxplots do not seem to show a specific trend. The resistance against extraction in a 45° angle is greatest at the lowest location on the slope and least in the middle of the slope. For all four elevations on the slope, the scatter of the datasets is quite large with a minimum of  $4.5G$ .

### 5.1.2 Visual observations

During the execution, observations were made with respect to the placement of the model units, shape of the slope profile after placing, toe construction and pull-out sequence.

#### Placement

At first a coarse under layer was used, which made it difficult to place the model units. The switch to the less coarse under layer made placement easier but still, some inconsistencies were observed which will be explained on the basis of Figure 5.4. The explanation can be quite abstract, therefore a photo series has been enclosed in Appendix D. The following general aspects have been observed on the slopes with respect to the orientation of the units:

1. Unit 6 is only supported by unit 3 and the under layer due to rotation of unit 2 from z-axis to y-axis.
2. Unit 6 is rotated backwards (from x- to z-axis) due to rotation of unit 2 from y-axis to z-axis (around the x-axis).
3. Only the lower chamfers of unit 6 make contact with units 2 and 3 due to rotation of the unit from x-axis to z-axis. This is possible when there is a negative fluctuation in the under layer.



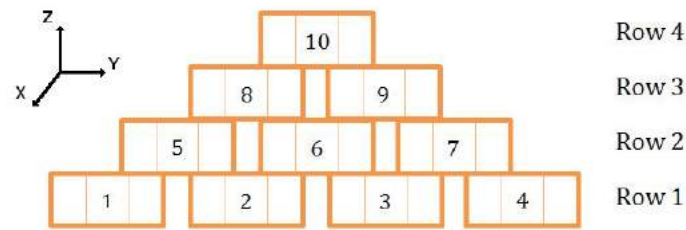


Figure 5.4: Schematic representation of a staggered grid with Xbloc<sup>+</sup> v1

4. Units 2 and 3 have been rotated backwards, unit 6 now also has to be rotated backwards in order for it to make contact with both units and the under layer. Another possibility is that unit 6 is placed with the right orientation but it only makes contact under the nose and tail.
5. Only the nose tip of unit 6 is supported. This is possible when there is a positive fluctuation in the under layer. This is also possible when unit 2 has rotated clockwise and unit 3 anti-clockwise. The wings of the respective units have been rotated downward so unit 6 is rotated forward.
6. Clockwise rotation of units 2 and 3 with an angle  $\beta$  causes unit 6 to have to be rotated anti-clockwise over an angle  $2\beta$  to have the nose supported by both units. This would be a too large rotation so unit 6 is only supported by unit 3. Additionally, the placing distance between 2 and 3 has been increased so unit 6 has possibilities to shift along the y-axis. Consequently, there is less space for units 5 and 7 which implies that they will either be rotated around x-axis or the y-axis.
7. Apart from rotational errors, the units can also shift slightly along the y-axis without being rotated. In the middle of the slope, this will result in larger gaps between the units than supposed to, on the sides of the slope this results in a too dense placement.

The following aspects have been observed on the slopes with respect to under layer and distribution of forces:

- (a) Protruding grains from the under layer that make contact with the bottom of the unit's core cause a unit to have only 2 out of 5 of the low contact points.
- (b) The under layer is placed on a steep and smooth wooden plate which is artificially made more rough by nailing wire mess onto it. The under layer has difficulties transferring force to the wooden slope and sometimes acts more like a sandy layer in which units settle instead of finding a stable position. After, for example, 5 rows have been placed, the profile of the under layer at higher elevations has changed and might no longer fulfill the  $\pm 0.5D_{n50}$  criterion.
- (c) Compaction of the slope as advised by Price [1979] was impossible since no high-frequency vibrating device was on site. Gently shaking of the model set-up resulted in less stable slopes.
- (d) The weight of each row is partially transferred to the under layer and partially to rows underneath. As with other concrete armour units, this weight causes the slope to compact. Armour units in the middle of a row, that have multiple rows above it and also have some of the placement errors as explained above, will slant slightly backwards.

On itself, these kinds of small placement errors are not significant but they influence the accuracy of placement of the other units. On average it takes accurate placing of 2 rows to get rid of the influence of badly placed units in f.e. row 1 on the stability of a unit in row 4. Figure 5.5 gives a few examples of correct and incorrect placed units. In each of the red boxes, numbered 1 through 5, one or several errors can be seen. In the first box error 3 is present, in the second box errors 1 through 3 and d are present, in the third box errors 1 and d are present, in the fourth box, errors 6, 7 and d are present and in the fifth box errors 7 and d are present.

### Slope profile

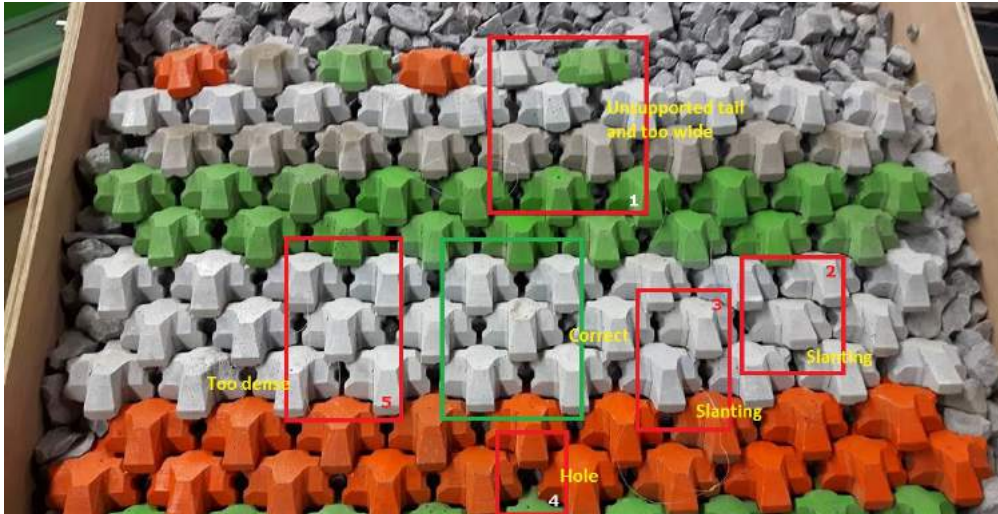


Figure 5.5: Examples of correct and incorrect placement

A slope on which  $Xbloc^{+ v1}$  is placed with its top perfectly level will have an inclination of  $35.3^\circ$ . On a 3:4 slope as used in this research  $Xbloc^{+ v1}$  should be slanting forwards at an angle of  $1.5^\circ$ . For a slope of 2:3 the unit should be slanting backwards at an angle of  $1.6^\circ$ . In the prototype, this is a parameter that can be measured with for example laser technology but in the model the units are too small to notice rotation directly. After a few rows, it becomes apparent that a concave or convex slope is forming due to trouble with finding the foundation on the under layer. When units have been placed with an inclination larger than  $1.5^\circ$  forwards, the slope will become convex. Space forms between the built up slope and the under layer and it becomes harder to place units correctly. When units are placed with an inclination smaller than  $1.5^\circ$  forwards, the slope will become concave. It becomes harder to place the units because it seems like elements are protruding from the under layer and no solid foundation can be found to place the unit with all its contact points on the other units.

### Toe construction

In the pull-out tests, no toe construction was used since it was expected that the slope would be stable on its own. During the 22 tests, failure due to sliding of the first two rows has been observed twice. Sliding off the toe creates spaces between the units in up-slope direction, decreasing the packing density, the weight on a unit and the friction surface.

The placing of the first row was a task that required practising patience. The under layer is never truly smooth, causing each unit to deviate in a different direction. The first row determines the stability of the rest of the slope. If it is placed 2 mm too close to the under layer a convex slope forms. If it is placed 2 mm too far from the under layer a concave slope forms. If the units are placed too far apart, the next rows are also placed too far apart and the appropriate packing density will not be obtained.

### Pull-out sequence

During the test series, in which the units were extracted under a  $90^\circ$  angle, the following mechanism was observed: the load was increased until a sudden start of movement when part of the armour unit slipped out of the surface profile to get stuck 5 mm further. When the load was further increased the unit was fully pulled out. Figure 5.6 displays data obtained with the LSH Load Cell, which measured the pull-out force in voltage. The time series obtained at locations 1, 2 and 4 show a semi-steady increase in voltage which drops vertically and increases again until extraction.

In physics, this is called the "stick-slip phenomenon" which is a "spontaneous jerking motion that can occur while two objects are sliding over each other." The jump occurs when the force on a unit becomes high enough to overcome the friction induced resistance after which the object is launched into the direction of the pulling force. The second gradual increase of the load enables the unit to find a new equilibrium position between the other units but a wave only acts for a few seconds. When the wave reflects off the slope, the unit could be lifted up and put back down, while being pulled out at

the same time. It can take a wave much less force to extract a unit in this way, leading to early failure.

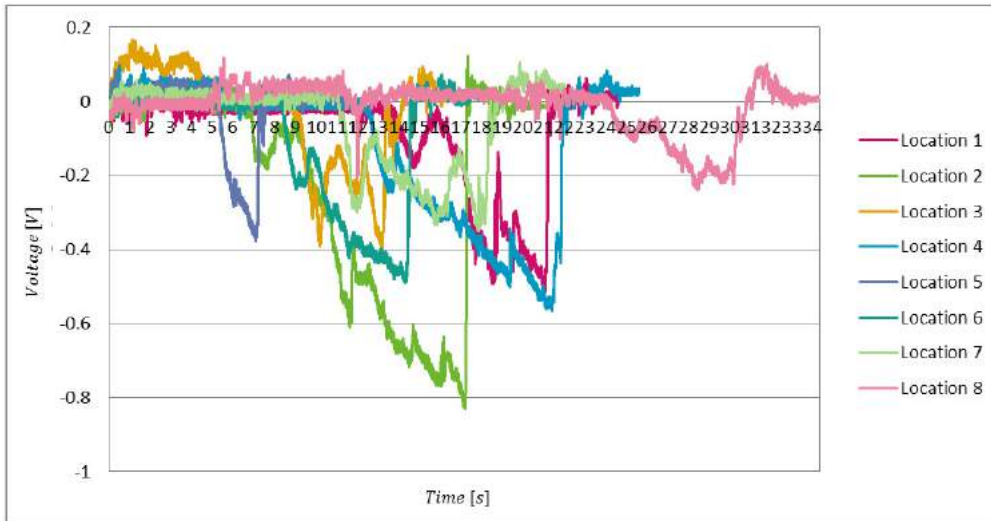


Figure 5.6: Test 7, plastic units,  $\theta = 90^\circ$ ,  $1/11$  under layer

### 5.1.3 Analysis

The above observations give insight into the differences in the results depicted in Figures 5.1 through 5.3. For the  $90^\circ$  pull direction, it is clear that the number of rows has an influence on the stability. Compared to the situation in which a model unit had no rows above it, the presence of 5 to 20 subsequent rows above a plastic unit increases the average required force with a factor of 2.6 to 3.5. For concrete the increase of the average required force is a factor 4.3 to 5. The lowest registered pull-out force is approximately the same for each elevation on the slope:  $3G$  for plastic samples and  $5G$  for concrete samples. This difference could be increased even more if the orientation of the friction planes is perpendicular to the slope in stead of the  $35^\circ$  orientation it is in now, just as is the case for other single layer uniformly oriented armour units (see for example Figures 2.7 and 3.1).

For the  $45^\circ$  pull direction, the results are less clear. An explanation for the dip in stability around 10 and 15 number of rows above in figure 5.3 can be given by the observations. The armour units are very sensitive to placement inaccuracies and, when not placed correctly, the weight of the slope causes units around the middle rows to slant backwards. The situation can be compared to a buckling beam: a slender beam is loaded axially and is on the verge of buckling. Applying a small force on the middle of the beam will let it fail, but if the same force would be applied on either side of the middle, the beam wouldn't fail. When a unit is loaded by a  $45^\circ$  directed force, extra grip is created when the chamfers on the bottom of the unit find grip on the chamfers of the units below it, which in turn gain extra grip from the rows below. Between the 7<sup>th</sup> and 18<sup>th</sup> row, the contact between the chamfers is limited due to the weight of the slope causing units to slant backwards. The reason that the 5<sup>th</sup> row (20 rows from the top) is not affected by this mechanism is that in the first 5 rows the placement inaccuracies have not been developed to the extent of resulting in slanting units.

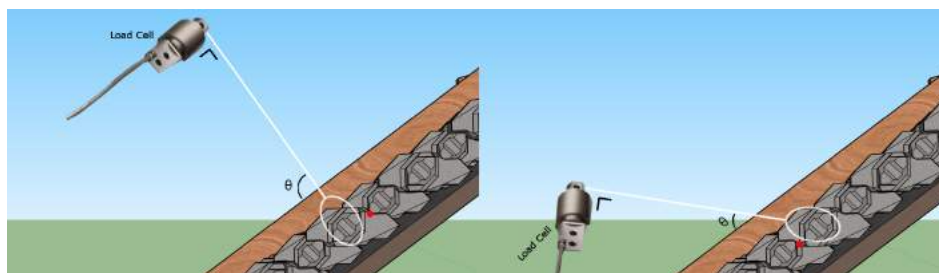


Figure 5.7:  $90^\circ$  and  $45^\circ$  pull directions, model unit rotates around the red dot

A large difference is seen between the pull-out forces in the 90°-series (series 3 and 4, purple boxplots) and the 45°-series (series 5 and 6, red boxplots). This difference is attributed to the interlocking mechanism that plays a role in series 5 and 6 but doesn't play a role in the first series. Figure 5.7 illustrates the (lack of) interlocking mechanism: due to the extraction force, the model unit rotates around the red dot. In the 90° configuration only the presence of the under layer resists this motion, in the 45° configuration the chamfers of units on rows below and the presence of units a row below and a row above prevent this motion.

In Figure 5.8 four photograph's, one representative slope from each series, have been put next to each other. Comparison of the photographs of series 3 with series 5 leads to the conclusion that in the 45°-series the weight of surrounding units is activated when the unit is extracted caused by the interlocking of the chamfers. A change in the orientation of the chamfers, so that they become vertical, might result in a larger degree of interlocking for all pulling directions.



Figure 5.8: Representative slopes from series 3 through 6

When the photographs of series 3 are compared to series 4, or even more obvious when series 5 is compared to series 6, a difference is seen in the amount of damage occurring on the slope during extraction. The concrete-90°-slope shows some damage around locations 1, 3 and 5 where units have been activated during sampling. The other locations the units in the row above show small rotations. The plastic-90°-slope shows almost no activation of units, only the unit just above location 4 on the right is pulled out of its original position. All other units do not seem to have had hindrance of the extractions one row below. The sampled unit did not activate the surrounding units, not by friction nor by interlocking.

The photograph of the concrete-45°-slope indicates that for this direction of the force at all locations the extracted unit has activated the surrounding units. Location 6 is the only location at which no obvious damage is seen. In contrary to this type of damage, the plastic-45°-slope again shows hardly any damage. During extraction the units from rows below were indeed activated but due to the low surface roughness eventually the sampled unit slipped over these units after which they fell back into their original position.

In Section 2.3.3 it has been discussed that pull-out tests can be used for testing armour units and pattern-placed blocks. From the failure mechanisms as depicted in Figure 2.12 the main two failure mechanisms, piston and beam failure, as well as the group-uplift failure have been observed during the pull-out tests. Also, the stick-slip failure mechanism that has been observed is a typical pattern-placed phenomenon. The concrete slopes showed a more interlocking type of behaviour.

To assess whether Xbloc<sup>+</sup> v1 behaves more like a concrete armour unit or like a pattern-placed block data on pull-out tests for concrete armour units (double and single layer, random and uniform orientation) and pattern-placed blocks has been gathered in Table 5.2. This table gives an overview of the performance of each block at a certain slope angle. It states the average required non-dimensional extraction force in a slope-normal direction,  $\mu_{F_{\perp}/G}$ , its standard deviation,  $\sigma_{F_{\perp}/G}$ , and the slope angle on which the test was performed. To be able to compare the different tests, use is made of the average load factor,  $n_{LF} = \frac{F_{\perp}}{G \cos \alpha}$ , which takes into account the slope angle. Each category (double layer



interlocking, single layer uniform, etc.) is displayed from highest to lowest average load factor,  $\mu_{n_{LF}}$ , accompanied by its standard deviation,  $\sigma_{n_{LF}}$ . For Xbloc<sup>+</sup> v1 the data of series 3 and 4 of the 10<sup>th</sup> row (15 rows from the top) have been chosen as representative values.

**Table 5.2:** Data on non-dimensional pull-out force required for extraction for various concrete armour units and pattern-placed blocks

	Unit type	Placement	$\mu_{F_{\perp}/G}$	$\sigma_{F_{\perp}/G}$	Slope	$\mu_{n_{LF}}$	$\sigma_{n_{LF}}$	Conducted by
Double layer interlocking	Stabits - Brickwall pattern	Regular	6.28	0.46	1:2	10.03	0.73	Price [1979]
	Dolosse	Irregular	3.62	1.64	1:2	5.78	2.62	Price [1979]
Double layer bulky	Stone	Irregular	2.14	0.90	1:2	3.42	1.44	Price [1979]
	Stabits - Double	Irregular	1.75	0.60	1:2	2.80	0.96	Price [1979]
	Tetrapods	Irregular	1.53	0.51	1:2	2.44	0.81	Price [1979]
Single layer interlocking	Crablock	Irregular	8.00	5.00	3:4	11.48	7.18	Broere [2015]
	A-jack	Irregular	6.60	2.50	1:2	10.54	3.99	Mickel [1999]
	Xbloc	Irregular	4.22	1.18	1:2	6.74	1.89	de Lange [2010]
	Xbloc	Irregular	4.54	1.35	3:4	6.52	1.94	de Lange [2010]
Single layer uniform	Crablock	Regular	7.20	1.60	3:4	10.33	2.30	Broere [2015]
	Xbloc <sup>+</sup> v1 - Concrete	Regular	6.46	1.04	3:4	9.27	1.49	Present study
	Xbloc <sup>+</sup> v1 - Plastic	Regular	4.00	0.83	3:4	5.74	1.19	Present study
Pattern-placed blocks	Basalt 17 kg - tightly packed	Regular	103.71	75.41	1:3.5	181.22	131.78	Verhagen [1984]
	Basalt 32 kg - tightly packed	Regular	68.06	39.00	1:3.5	118.93	68.15	Verhagen [1984]
	Vilvoord stone - above SWL	Regular	61.18	28.00	1:3.5	106.90	48.93	Verhagen [1984]
	Basalt 35 kg - openly packed	Regular	43.66	29.63	1:3.5	76.29	51.77	Verhagen [1984]
	Vilvoord stone - below SWL	Regular	41.75	23.06	1:3.5	72.95	40.30	Verhagen [1984]
	Haringman block	Regular	20.91	12.19	1:3.5	36.54	21.30	Verhagen [1984]
	Lessin stone	Regular	7.50	7.59	1:3.5	13.11	13.26	Verhagen [1984]

The bulky double layer interlocking armour units show relatively low load factors of  $2.5 < n_{LF} < 3.5$ . This is to be expected since these type of armour units depend mainly on own weight and to a limited extent on interlocking or friction. Dolosse and Stabits (placed in the Brickwall pattern) have a more complex shape than regular stone, Tetrapod and randomly placed Stabits. They depend more on interlocking than the others and therefore have higher load factors of  $6 < n_{LF} < 10$ . The two categories with single layer armour units show values of  $6 < n_{LF} < 12$ , three times as high as the bulky double layer units. Lastly, the pattern-placed blocks show load factor values of  $13 < n_{LF} < 181$ . Lessin stone, which is the least stable pattern-placed block in this table, has a higher resistance against extraction than all concrete armour units.

It has been established that friction plays a large role for Xbloc<sup>+</sup> v1 but the load factors obtained from the model tests do not indicate that this is of the same importance as for pattern-placed blocks. Approximately the same load factors have been obtained for randomly oriented interlocking units in a single layer as for uniformly oriented friction based units in a single layer so the interlocking mechanism cannot be ruled out. If improvements are made to increase the interlocking mechanism, Xbloc<sup>+</sup> v1 will presumably obtain a higher stability against extraction. A higher degree of interlocking might be reached by adapting the orientation of the chamfers on the armour units such that they become vertical. Additionally the contribution of friction to the stability is expected to increase if the orientation of the friction planes is changed to be perpendicular to the slope.

Naturally, Table 5.2 does not include all armour units and placed blocks. Especially data on other single layer uniformly oriented armour units, such as Single Layer Cubes, would be helpful in the assessment of Xbloc<sup>+</sup> v1. Such tests have not been performed and therefore no comparison can be made with other single layer uniformly oriented armour units.

### 5.1.4 Reflection on hypothesis

The hypothesis for the first research question was:

*The stabilizing mechanisms of Xbloc<sup>+</sup> v1 will consist of own weight, interlocking and friction, of which the first two will be the main mechanisms; furthermore, the stability is increased for an increasing number of rows and a decreasing under layer roughness.*

After analysing the pull-out tests, it has been concluded that own weight and friction are the most important stabilising mechanisms. The contact between the bottom chamfers of a unit and the upper chamfers of a unit a row below provides the interlocking mechanism. Surrounding units are only activated when the unit is extracted by a force in down-slope direction, while the peak wave force is exerted in up-slope direction.

An increasing number of rows and decreasing under layer roughness does indeed influence the stability positively.

## 5.2 Hydraulic physical model tests

In total 10 tests (consisting of a minimum of 3 runs each) were conducted on an  $1/11$  under layer. The parameters for each test varied, an overview of the parameters is given in table 5.3 in which also the type of failure mechanism is displayed. In the first 7 tests, large steps were used when increasing the significant wave height for each next run. In tests 8, 9 and 10 small increments were used. Tests 2, 3, 4 and 10 were conducted with concrete units, all other tests with plastic units. For analysing the data the program WaveLab was used which makes use of a spectral analysis and a time series analysis. The time series analysis processes the exact measured data and draws statistics from it. Wavelab also splits the total wave field up into incoming and reflected waves using the Mansard and Funke [1980] method. In the next subsections use will be made of the data as processed by Wavelab. An overview of the actual wave heights, stability numbers and accompanying numbers of damage is enclosed in Appendix G. The presented results will be substantiated by visual observations after which both results and observations will be analysed. A photo-series has been enclosed in Appendix I with a before and after photograph of each slope.

**Table 5.3:** Physical model tests program and failure mechanism

Test nr.	Material	Step size	Failure mechanism
1	Plastic	large	Extraction, pyramid effect
2	Concrete	large	Extraction
3	Concrete	large	Extraction, pyramid effect
4	Concrete	large	Extraction, pyramid effect
5	Plastic	large	Extraction, pyramid effect
6	Plastic	large	Sliding of toe
7	Plastic	large	Extraction
8	Plastic	small	Extraction, pyramid effect
9	Plastic	small	Extraction, pyramid effect
10	Concrete	small	Extraction

### 5.2.1 Presentation of results

#### Damage criteria

For the sake of readability some definitions are repeated here:

- $N_{\#d}$  = the number of units displaced more than  $0.5D_n$
- $N_{od} = \frac{N_{\#d}}{B_a/D_n}$  = "number of displaced units" per a strip of  $1 \cdot D_n$  wide
- "Start of rocking" = The moment at which at least 1 unit is visually observed to move back and forth

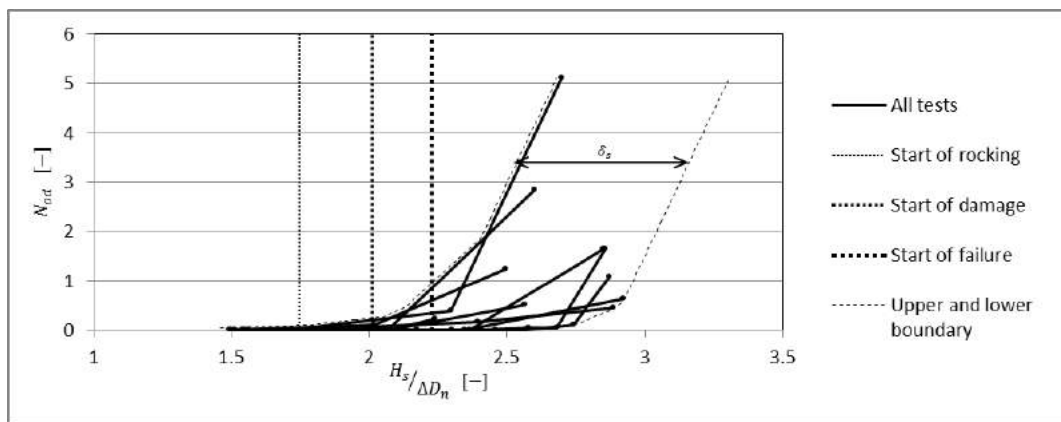
For single layer interlocking armour units Accropode, Core-loc and Xbloc, The Rock Manual (CIRIA et al. [2007]) states that zero damage and only minor rocking is allowed during design conditions. The armour layer may show limited damage during overload conditions of 20%. These strict rules are applied since armour units in a single layer usually fail sudden or brittle and after a unit is extracted the under layer is unprotected. There is no residual strength to withstand the wave attack. The "Start of damage" is defined as  $N_{od} > 0$ , which lies around a stability number of  $\frac{H_s}{\Delta D_n} = 3.7$  for said units. "Failure" is defined as  $N_{od} > 0.5$ , which lies around a stability number of 4.1. Single layer

cubes display rapid damage progression, therefore even stricter rules are applied: "Start of damage" is defined as  $N_{od} = 0$ , which lies around stability number of 3.0, "Failure" is defined as  $N_{od} > 0.2$ , which lies around a stability number of 3.5.

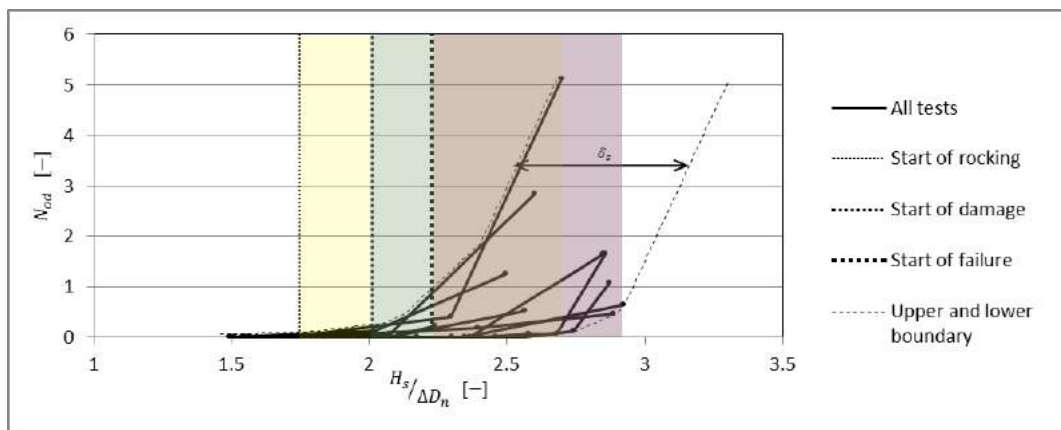
As Xbloc<sup>+</sup> v1 has relatively little interlocking capacity and relies on accurate placement in brick pattern (just like Single layer cubes), brittle failure was expected. It was stated in the methodology (Section 4.2.4) that the slope would be considered failed when 3 or more units were displaced. This corresponds to the definition of "Failure" at  $N_{od} > 0.2$ .

### Overview test results

Figure 5.9a shows the overall performance of Xbloc<sup>+</sup> v1, in this figure all tests and accompanying runs have been plotted. On the vertical axis the Number of displaced units represents the damage to the slope, the horizontal axis displays the stability number as a function of the significant wave height ( $H_s = H_{1/3}$ ). Data-points can be subdivided in categories "no rocking", "rocking", "damage" and "failure". The lowest measured values for start of rocking, damage and failure are indicated by the dotted lines. The spread of the data is indicated by  $\delta_s = 0.61 \frac{H_s}{\Delta D_n}$ .



(a) Relation between stability number and number of displaced units of all tests, for  $H_s$  and the nominal diameter



(b) Regions of "rocking", "damage" and "failure" indicated in yellow, blue and red respectively (overlapping area's indicated by green, brown and purple)

Figure 5.9: All test results

The slopes are completely stable up to  $N_s = 1.75$ . The criterion "no rocking" is observed up to  $N_s < 2.35$ . Rocking was observed for  $1.75 < N_s < 2.68$ . Damage was first observed at  $N_s = 2.01$ , up to  $N_s = 2.92$ . Lastly, failure started at  $N_s = 2.23$  and was observed up to  $N_s = 2.92$ . The data that forms the basis for above graphs has been enclosed in Appendix G. The spread between the lowest and highest values of the three categories is fairly large and the categories overlap for a large part,

indicated in Figure 5.9b by the yellow blue and red areas. **Comparison with other units**

At first glance, Accropode, Core-loc, Xbloc and Single layer cubes perform better than Xbloc<sup>+v1</sup>, Table 5.4. However, the Rock Manual is unclear about the circumstances under which the actual stability numbers of these units were determined. For example the use of a foreshore, the relative water depth at the toe and the type of wave that reaches the structure have not been clearly specified. As has been discussed in Chapter 2, these parameters all have an influence on the stability of the armour layer so the stability numbers of different armour units cannot be compared without taking a critical look at the specific circumstances. It does give an overall estimation of the stability created by Xbloc<sup>+v1</sup> in its current form. In Chapter 3, Hypotheses, a stability number of  $2.0 < \frac{H_s}{\Delta D_n} < 3.3$  was expected and on average a stability number of 2.6 was reached. It should be kept in mind that this is for a situation with deep water and without foreshore, allowing extreme wave heights to reach the structure unaltered. For Xbloc this geometry would lead to a multiplication factor of 2 on the armour unit size.

**Table 5.4:** Stability numbers accompanying the different armour units as stated in the Rock Manual [CIRIA et al., 2007], van Gent and Luis [2013] and as found in this study

	Water depth deep/shallow	Foreshore yes/no	Start of damage $\frac{H_s}{\Delta D_n} [-]$	Failure $\frac{H_s}{\Delta D_n} [-]$
Accropode, Core-loc, Xbloc	shallow	?	3.7 (avg.)	4.1 (avg.)
Single layer cubes	intermediate	no	2.0 to 3.0	3.0 to 3.5
Xbloc <sup>+v1</sup> preliminary test	shallow	yes	3.3	3.3
Xbloc <sup>+v1</sup> current study	deep	no	2.0 (min.)	2.2 (min.)
	deep	no	2.4 (avg.)	2.6 (avg.)

Lastly it has to be noted that the stability number does not solely define the performance of an armour unit. If the stability number of a unit is large but they also have to be placed very densely packed, based on concrete usage it might actually perform less than other units. Also the ease with which a unit can be placed is something that should be taken into account when choosing which armour unit is best suitable for a construction. The next sections will elaborate on the various details and peculiarities of the current study such that the subject "stability" is no longer only described by the parameter  $H_s / \Delta D_n$ .

## 5.2.2 Visual observations

During the hydraulic model testing not only data has been collected but also observations were made with respect to the failure mechanism, damage progression and location of damage.



**Figure 5.10:** Left: wave crest induces high core water level, right: wave through induces outward directed pressures by water wanting to flow out

### Failure mechanism

The failure mechanism dominating Xbloc<sup>+v1</sup> consists of two components: the loosening of armour units and later the extraction of these units. During up-rush the wave loads an armour unit from



below, exerting an upward directed force on the nose and the bottom of the unit. This causes the unit to be loosened from its originally stable position between the other units. With each wave the unit rocks up and down, increasing its surrounding area. Eventually, the unit is tilted with its nose almost vertical, it no longer makes contact with the units a row above. The extraction occurs during the first down rush of a large wave group. A high energy wave group travels towards the structure and the up-rush causes the unit to be detached momentarily, the down-rush initiates the actual extraction. The extraction is caused by the combination of a high water level in the core and a low trough in front of the slope, see Figure 5.10: water accumulates behind the armour layer and an overpressure pushes Xbloc<sup>+</sup> v1 out. Only video footage and no clear photographs including the water level in the core are available of the extraction process, therefore this is visualized step-by-step in Figure 5.11.

There is a warning mechanism: Provided that the steps in wave height between runs are not larger than 1 cm, the slope shows warning signs before extraction. In the first run(s) minor rocking is observed. In the intermediate runs the slope gets the opportunity to find its most stable form, rocking is observed and often leads to tilted blocks that keep rocking. A tilted block still gives stability to the slope since it prevents the sliding down or caving in of the two blocks above. Sometimes a tilted block is rocked into stability again (no movement). In the last run, the run in which failure is determined, rocking and tilted blocks are extracted. As will be discussed in the next section, in 8 out of 10 slopes rocking was observed before failure occurred. In the other 2 cases, rocking could have been missed due to the cloudiness of the water in the flume or due to the large step size speeding up the needed time for failure.

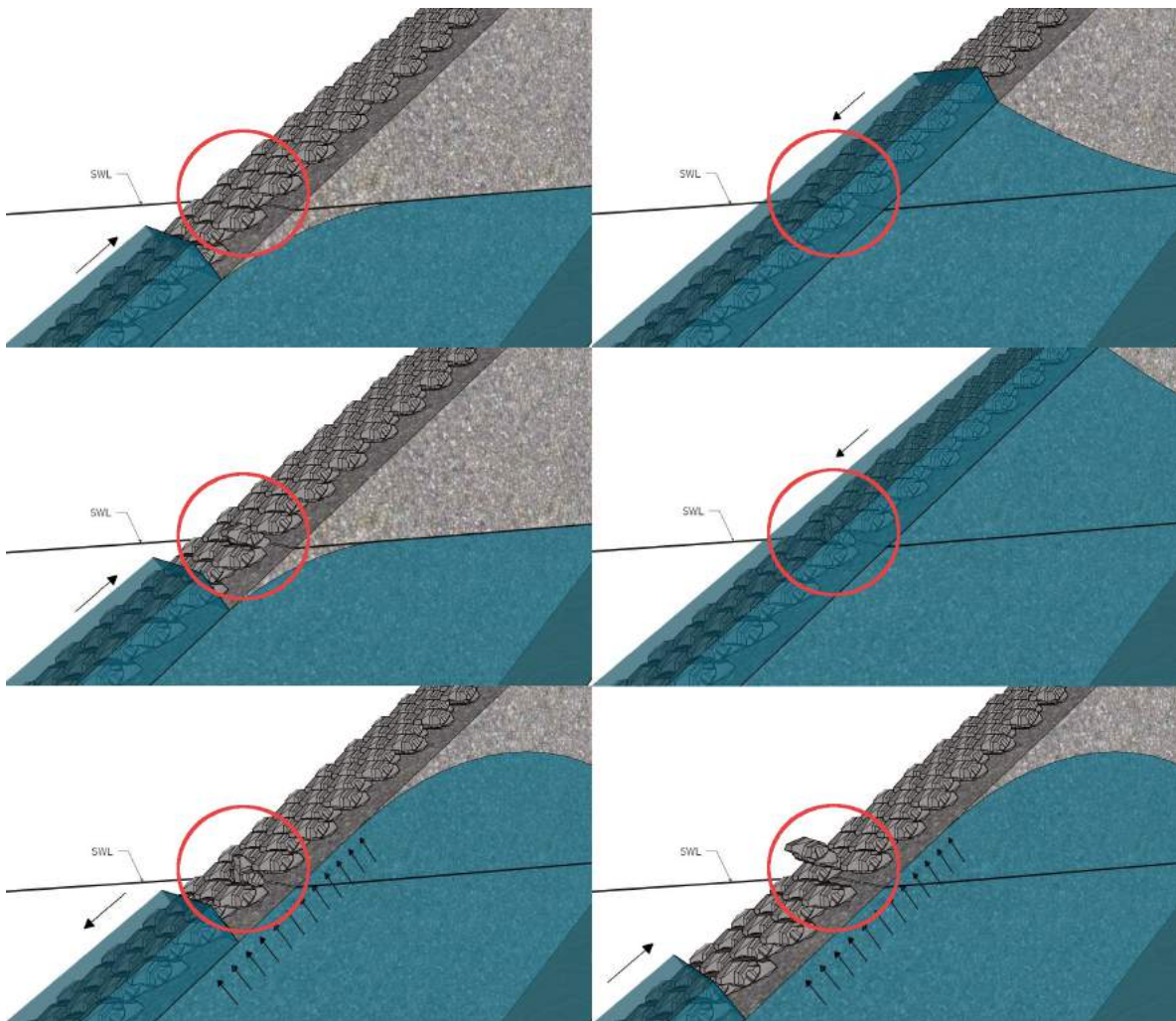


**Figure 5.11:** Extraction of a unit out of the armour layer: loosening and rotation during up- and down-rush after which overpressure pushes Xbloc<sup>+</sup> v1 out during the down-rush of a large energy wave group

If the loosening and rocking of armour units can be prevented, also failure is prevented. This might be achieved by the recommended adaptations with respect to the orientation of the chamfers, as already discussed in Sections 5.1.3 and 6.1.

### Damage progression

A slope with Xbloc<sup>+ v1</sup> is stable as long as all units are in place. Units that remain on their predefined position but with different orientation still contribute to the stability of the slope by preventing the energy of the wave to load other blocks from below and by protecting the under layer from eroding. When a unit is extracted the initial stability of that area depends on the stability of the units on the left, right and above. When these are all placed perfectly no direct damage is observed. With the passing of several high wave groups a semi-stable slope is created again by either of the following mechanisms: the two above units will rotate towards each other into the formed hole, one of the above units slides nose-first into the hole or a unit from the row below is tilted backwards. This has been observed for almost all tests. In 3 out of 10 slopes this situation remained until the end of the run.

When the units surrounding an extracted unit have small rotational errors, lack a decent foundation of the under layer or do not make contact with neighbouring units on all 8 surfaces (see Chapter 3), the damage progresses rapidly. Often at least 3 units are extracted within 1 minute: the initially loose or rocking unit, one of the units to the left or right and the unit a row above which is positioned on these two units. This progresses to form pyramids: triangular shaped voids left by the extraction of multiple units. Pyramids can also form without units being extracted, f.e. when several units are tilted, space is created for the above units to settle. Table 5.3 at the beginning of Section 5.2 states which slopes experienced the formation of pyramids. Additionally, some examples of pyramid formation can be found in the photo series in Appendix I.

### Location of damage

In each test the start of damage was located between the still water level and 4 rows below SWL, and in most cases at 3 rows below SWL. This agrees best with the location of damage as stated in literature for placed blocks and less so for concrete armour units. For example, for Xbloc the initiation of damage is found to be between  $+0.5H_s$  and  $-1.5H_s$  [van Zwicht, 2009], while for placed blocks the damage is found above the maximum run-down  $R_{d,max} = -1.5H_s$  and below the SWL [Schierneck and Verhagen, 2001]. After the initial damage, damage progressed both up and down the slope over a band of 5 rows in total (this could have been more but the run was stopped when a large hole was created).

Damage can, to a certain extent, be predicted: Before the start of the first run of a test, a description was given of the state that the slope was in. Any abnormalities such as slanting blocks or a concave or convex slope, were noted. Slanting blocks had the tendency to slant even more or to start rocking. In 4 out of 10 situations, the damage or extraction in the slope occurred at locations indicated beforehand.

### Placement

The difficulties experienced during the pull-out tests were decreased due to the use of the toe-beam. The positioning of the toe-beam took some effort each test but eventually sped up the process. In contrary to the pull-out tests, the under layer could be compacted and therefore provided more stable support, which was also hypothesised. Lastly, the concrete units were much easier to place than the plastic units, these were so smooth that they would tilt when more rows were placed above.

## 5.2.3 Analysis

The next paragraphs will elaborate on the different aspects of the current study concerning the overall stability, such that the subject "stability" is no longer only described by the parameter  $H_s/\Delta D_n$ .

### 5.2.3.1 Comparison with preliminary test

Jacobs, who's first test with Xbloc<sup>+ v1</sup> has not been documented in a report, showed that the armour unit could be a competitor for other units. The present research is compared with this preliminary test. The background information on the influence of different wave heights on the failure mechanisms, especially the conclusions as stated by Zwanenburg [2012] in Section 2.2.2.4, as well as the behaviour of waves in deep and shallow water, with or without foreshore (Section 2.1.3), are important for this

comparison. In short: Zwanenburg [2012] stated that, for Xbloc, a rocking-based stability relationship  $H_{2\%}$  is the parameter to observe and for an extraction-based stability relationship an extreme or maximum wave height is the best design parameter. Additionally, in shallow water the extreme or maximum wave height is limited due to breaking, while in deep water the extreme wave height can be up to  $\pm 2 \cdot H_s$ . For the same ratio of water depth at the toe over significant wave height, the presence of a foreshore results in a higher ratio of the extreme wave height over the significant wave height. However, when a foreshore is present also the water depth will be much lower, consequently leading to lower extreme wave heights for similar significant wave heights.

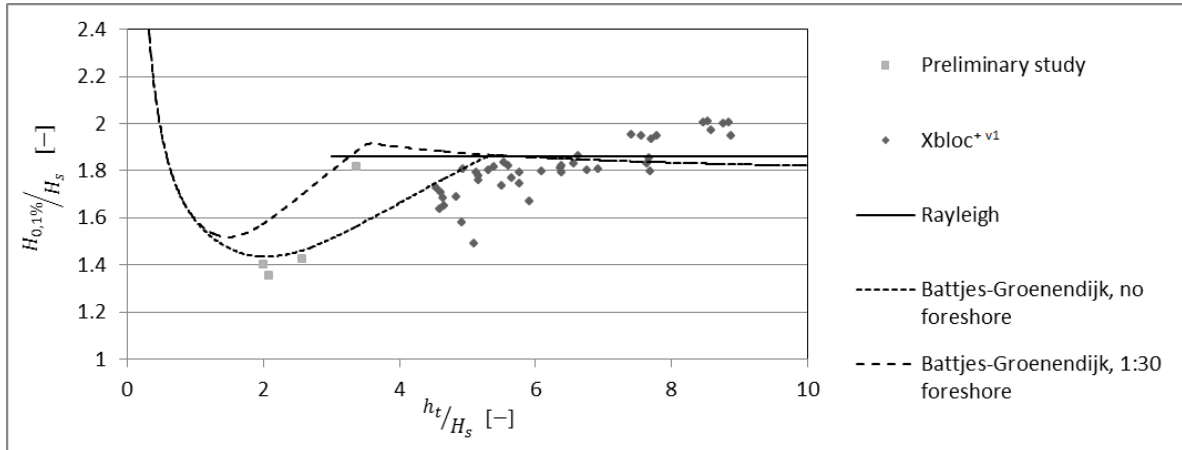


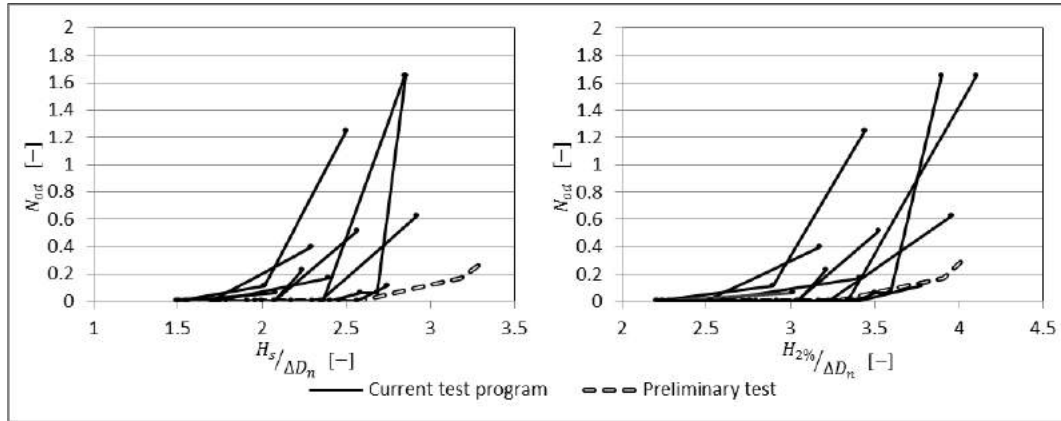
Figure 5.12: Relation between  $H_{0.1\%}$  and  $h_t$  made dimensionless by  $H_s$

The above theory can be explained on the basis of Figure 5.12 which is a duplicate of figure 2.4 with the addition of data-points generated in the preliminary study and in the present study. It shows that the runs of the preliminary study had decreasingly high  $H_{0.1\%}$  to  $H_s$  ratio (from  $\pm 1.8$  to  $\pm 1.4$ ) for increasing  $H_s$ , which corresponds to the visual observations of breaking waves in the flume. In the preliminary study use was made of a 1:30 foreshore, leading to a water depth of 0.25m at the toe. The runs in the present study, without foreshore and a water depth at the toe of 0.50m, experienced only a few breaking waves and only in the last run of each test. The runs started with a  $H_{0.1\%}$  to  $H_s$  ratio of  $\pm 2$  and generally ended with a ratio of  $\pm 1.7$ , the 3 runs in which breaking waves were observed are the vertically largely deviating points around an  $h_t/H_s$  of 5 and 6. These are the Xbloc<sup>+</sup> v1 data-points in the lower left of the dark grey cloud.

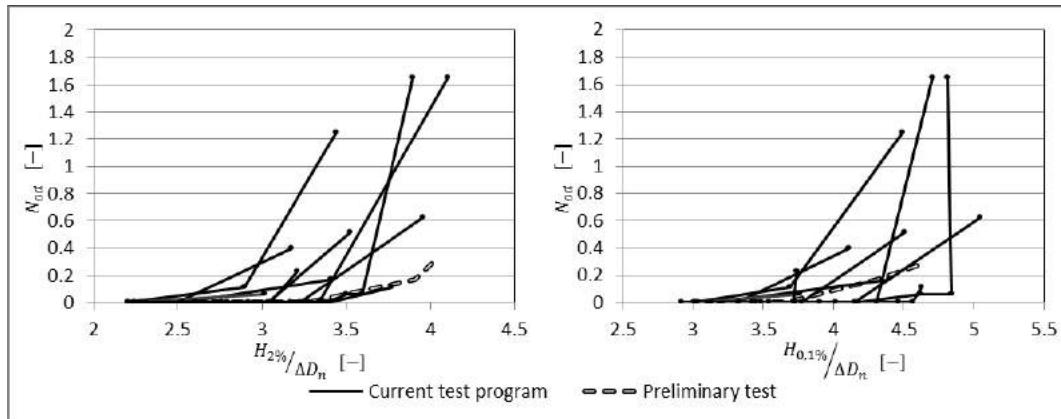
For the comparison of the preliminary and current results, four data-points were omitted:

- 3 data-points were generated on a slope that had already deemed failed (3 or more units were displaced). This caused considerable more damage and should therefore not be analysed in the graphs presented in this section.
- 1 data-point was generated during a run in which the toe slid away from underneath the armour layer, causing failure outside the scope of this thesis.

Figure 5.13a shows the preliminary test and current tests with Xbloc<sup>+</sup> v1 for both the significant wave height and the otherwise commonly used extreme wave height  $H_{2\%}$ . Figure 5.13b compares both studies on basis of the commonly used extreme wave height  $H_{2\%}$  and the maximum wave height present in this study:  $H_{0.1\%}$ . In these combined graphs the horizontal axes show the stability number based on  $H_s$  ( $= H_{1/3}$ ),  $H_{2\%}$  and  $H_{0.1\%}$  and the vertical axes show the damage in Number of displaced units.



(a) Relation between stability and damage for  $H_s$  &  $H_{2\%}$



(b) Relation between stability and damage for  $H_{2\%}$  &  $H_{0.1\%}$

**Figure 5.13:** Comparison of preliminary and present study on basis of  $H_s$ ,  $H_{2\%}$  &  $H_{0.1\%}$

For the same stability number as a function of  $H_s$ , there is less damage in the preliminary test than in all other tests, see Figure 5.13a on the left. The test results obtained by Jacobs cannot be reproduced by comparing on basis of the significant wave height. When the stability number is based on  $H_{2\%}$  it still forms an upper limit for the test results in the present study, see figure 5.13a on the right and 5.13b on the left. Finally, when the stability number is expressed in terms of  $H_{0.1\%}$ , the results obtained in the preliminary test match the results of the current study. This indicates that the maximum wave height is indeed the load that causes the damage, as Zwanenburg [2012] concluded before.

This analysis also confirms that stability cannot be solely expressed based on the stability number defined as  $\frac{H_s}{\Delta D_n}$ , but also the structures geometry and the hydraulic conditions and that physical model testing is still needed to confirm the suitability of a breakwater design.

### 5.2.3.2 Friction properties

One of the main conclusions from the pull-out tests was that friction, caused by for example the material properties, plays a larger role than expected beforehand. During the hydraulic physical model tests both materials were tested under the same conditions. Figures 5.14a, 5.14b and 5.14c show the difference between both materials for the three categories "No rocking", "Rocking" and "Failure". "No rocking" describes the run until which the slope is completely stable, "Rocking" describes the first run in which at least 1 armour unit was visually observed to be moving back and forth and "Failure" describes the run at which 3 or more units were extracted, at which the under layer was visible, or at which the armour layer was unable to fulfill it's function in any other way. The performance comparison of the materials in each category is done based on their appropriate design condition, in analogy to the conclusions of Zwanenburg [2012].

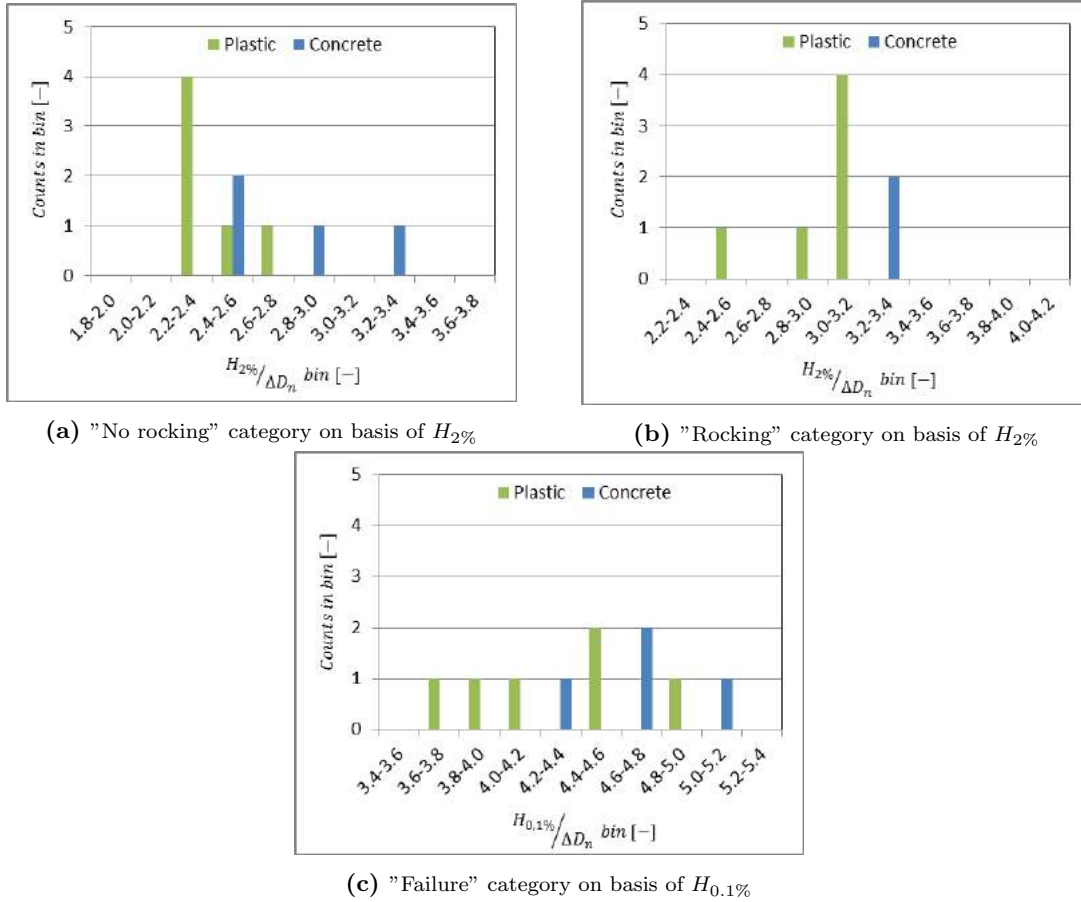


**Figure 5.14:** Comparison of performance of plastic and concrete model units for categories "No rocking", "Rocking" and "Failure" based on stability numbers  $\frac{H_{2\%}}{\Delta D_n}$  and  $\frac{H_{0.1\%}}{\Delta D_n}$

For "No rocking", the highest observed values per test were used. For categories "Rocking" and "Failure", the lowest values at which they occurred were used. All three graphs clearly show a stability difference between the two materials: the concrete units perform better than the plastic units. The average increase of stability of concrete units with respect to the plastic units is  $0.43 \frac{H_{2\%}}{\Delta D_n}$  for "No rocking",  $0.34 \frac{H_{2\%}}{\Delta D_n}$  for "Rocking" and  $0.44 \frac{H_{0.1\%}}{\Delta D_n}$  for "Failure", increases of 18%, 11% and 10% respectively, see also Table 5.5. The influence is largest for when no movement is allowed, which is the main requirement during the lifetime of a breakwater. These results reinforce the conclusion from the pull-out tests that friction contributes largely to the stability of an Xbloc<sup>+</sup> v1 armour layer but due to scale effects it cannot be concluded with 100% certainty.

**Table 5.5:** Stability numbers for comparison concrete and plastic

Based on	No rocking	Rocking	Failure
	$H_{2\%}$	$H_{2\%}$	$H_{0.1\%}$
Plastic, average [-]	2.38	2.97	4.25
Concrete, average [-]	2.81	3.31	4.69
Difference [-]	0.43	0.34	0.44
Relative difference [%]	18	11	10

### 5.2.3.3 Step size

Tests with various step sizes were conducted to determine the influence of compaction on the armour layer stability. By exerting multiple runs with a lower wave height the slope gets the opportunity to compact: all loose armour units find a stable position on the slope. As Price [1979] concluded that

for a double layer of Dolos compaction of the slope lead to a  $\pm 30\%$  increase of stability, and as this is also a common observation for Xbloc, it was expected that compaction would also be favourable for Xbloc<sup>+</sup> v1. Figures 5.15a, 5.15b and 5.15c show the difference between large and small steps for the three categories "No rocking", "Rocking" and "Failure", just as in the previous section.

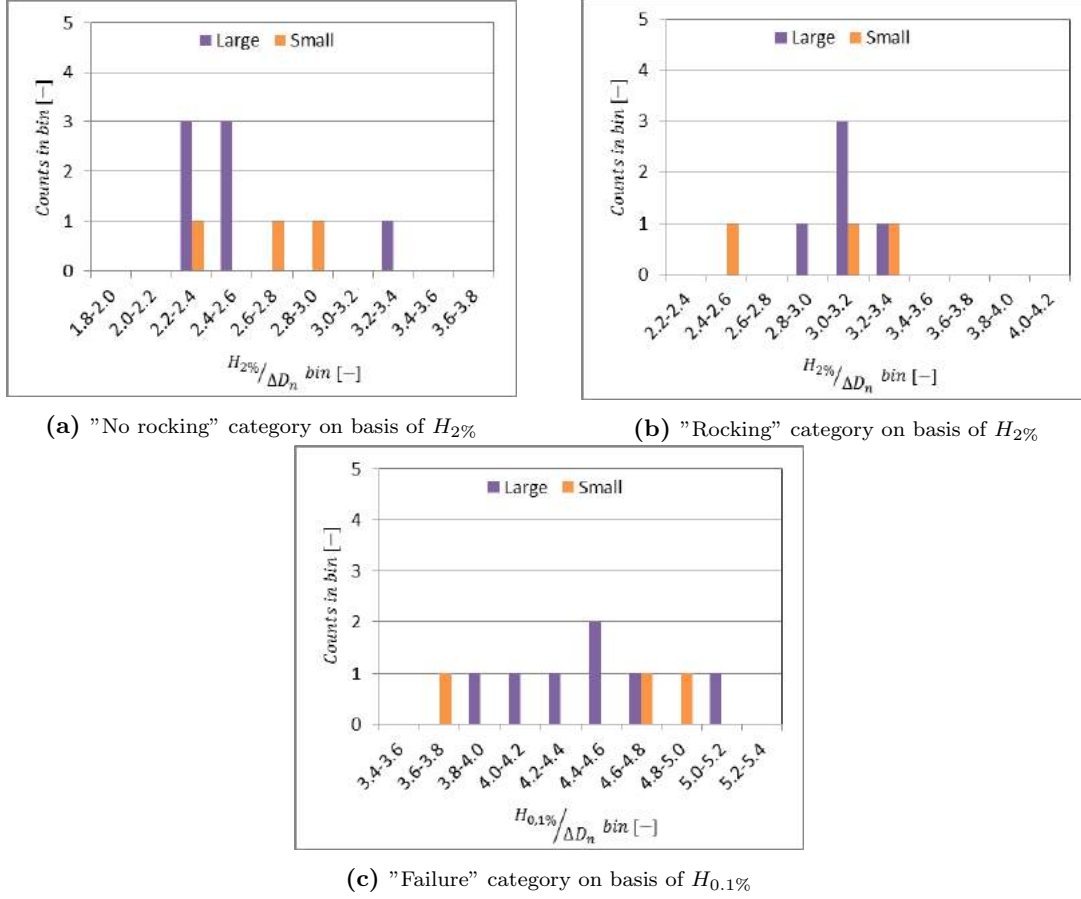


**Figure 5.15:** Comparison of performance of large and small step sizes for categories "No rocking", "Rocking" and "Failure" based on stability numbers  $\frac{H_{2\%}}{\Delta D_n}$  and  $\frac{H_{0.1\%}}{\Delta D_n}$

The category with large step sizes consists of 3 concrete and 4 plastic tests, the category with small step sizes consists of 1 concrete and 2 plastic tests. It must be noted here that one of the tests with plastic model units and small steps, test 8, failed very early. This test is represented by the lowest orange column in each of the 3 figures. The log of this test states "There seems to be a harsh dent between blocks 5R and 6R on row 7 and between 4R and 5R on row 8", which is exactly where 4 units were extracted. For the comparison, the results of test 8 will be left out.

**Table 5.6:** Stability numbers for comparison large and small step size

Based on	No rocking	Rocking	Failure
	$H_{2\%}$	$H_{2\%}$	$H_{0.1\%}$
Large, average [–]	2.51	3.09	4.45
Small, average [–]	2.86	3.22	4.72
Difference [–]	0.35	0.13	0.27
Relative difference [%]	14	4	6

The compaction of the slope leads to an increase of the slope stability of  $0.35 \frac{H_{2\%}}{\Delta D_n}$  for "No rocking",  $0.13 \frac{H_{2\%}}{\Delta D_n}$  for "Rocking" and  $0.27 \frac{H_{0.1\%}}{\Delta D_n}$  for "Failure", increases of 14%, 4% and 6% respectively, see also Table 5.6. On first glance, it is not evident that the approach with a small step size creates a more

stable slope. However, when close attention is paid to the exact numbers of tests 9 and 10 individually (see Appendix G) there are three other things to be remarked:

1. The two remaining tests with small step size - test 9: plastic, test 10: concrete - performed almost exactly the same, while in the previous section it has been shown that the concrete units perform much better. With a small step size the plastic units even reached a higher stability number than the concrete units before failing:  $0.18 \frac{H_{0.1\%}}{\Delta D_n}$  higher.
2. Out of all 6 tests with plastic units, the test with the small step size was by far best. Table 5.7 displays the relative difference of test 9 compared to the average performance of the plastic units. The results of test 9 are similar to the average results of the concrete test series (see Table 5.5). This makes a slope constructed with plastic units, exerted by multiple runs with low wave height, of similar stability as a slope with concrete units.

**Table 5.7:** Stability numbers for comparison of small step size plastic test with other plastic tests

Based on	No rocking	Rocking	Failure
	$H_{2\%}$	$H_{2\%}$	$H_{0.1\%}$
Plastic, average [–]	2.38	2.97	4.25
Plastic, small step size [–]	2.79	3.17	4.81
Difference [–]	0.41	0.20	0.56
Relative difference [%]	17	7	13

With the addition of the above two aspects it can be concluded that the compaction of the slope by exerting a favourable wave climate (multiple runs with lower wave heights) does have a positive influence on the armour layer stability, and seems to remove the differences between smooth (plastic) and rough (concrete) armour units. The favourable wave climate rearranges the precise location and orientation of each unit such that it is placed in its most stable position. The contribution of friction has become less and the contribution of weight and interlocking has become more due to better alignment of the units.

#### 5.2.3.4 Concrete armour unit or Pattern placed block

Based on the observed failure mechanisms of overpressure from inside the structure, it is apparent that the armour layer is not porous enough. Due to a low interlocking mechanism, armour units can easily be rotated during up-rush. After losing their stable foundation on the under layer, they start to rock. When a large wave disintegrates on the slope, water stays relatively long inside the structure and the head difference over the structure creates overpressure. This pressure reduces the capability of the armour units dead weight to build up friction. As concluded from the pull-out tests, the stability of Xbloc<sup>+ v1</sup> is mainly based on friction, subsequently, lose armour units are pushed out. This is described as uplift.

In Section 2.2.2.4 the expression for the leakage length has been introduced, see Equation 2.19 and the accompanying paragraph for an explanation of the parameters. The leakage length is a measure of the permeability of the armour layer and thus a measure of the vulnerability to uplift. The formula is intended for revetments but can also grant insight into the porosity of an Xbloc<sup>+ v1</sup> armour layer. For  $\Lambda \ll L$  the water level inside the structure can follow the instantaneous water level with ease and there are no differences across the top layer, which is the case for relatively permeable armour layers such as constructed with rock or armour units. For  $\Lambda \approx L$  the water level inside the breakwater has difficulties following the instantaneous water level which is the case for relatively impermeable armour layers, such as constructed with pattern-placed blocks. It has already been observed that for the construction tested in this research, the latter is more suitable than the first (see Section 5.2.2) which is an indication that Xbloc<sup>+ v1</sup> experiences some of the same problems as pattern-placed blocks do.

The permeability is a measure of the ease with which water can move through a porous medium, such as an armour layer. The porosity indicates how much of a porous medium is open space. An



armour layer with a high porosity is more permeable than an armour layer with a low porosity, and, subsequently, less vulnerable to uplift.

The porosity is estimated in two ways:

- By calculating the volumetric porosity from the bulk volume, as is practice for concrete armour units
- By considering the armour layer as a placed block revetment and estimating the porosity from photographs

If  $Xbloc^{+v1}$  is assumed to be a concrete armour unit, the porosity can be estimated by the volumetric porosity,  $n_v$ . The Rock Manual [CIRIA et al., 2007] states that the volumetric porosity can be calculated by Equation 5.1. In this equation an imaginary box around the armour layer is drawn. The volumetric porosity is expressed as the total volume minus the volume of rock or concrete, relative to the total volume. For  $Xbloc^{+v1}$ , this results in a volumetric porosity of 58%. The same has been done for  $Xbloc$  and Single layer cubes.

If  $Xbloc^{+v1}$  is assumed to be a pattern placed block, the porosity can be estimated by measuring the surface of voids on a photograph. The built up pressure under the armour layer is dissipated through these voids. When voids are measured for the photographs as depicted in Figures 5.16a and 5.16b, the porosity comes out to be  $\pm 8\%$ . The same has been done for  $Xbloc$  in Figures 5.16c and 5.16d and for Single layer Cubes in Figure 2.19b. These the volumetric and photographic porosities of armouring concepts  $Xbloc$ ,  $Xbloc^{+v1}$ , Single layer cube, Rock and Pattern-placed blocks are shown in Table 5.8.

$$n_v = \frac{V_b - V_r}{V_b} \quad (5.1)$$

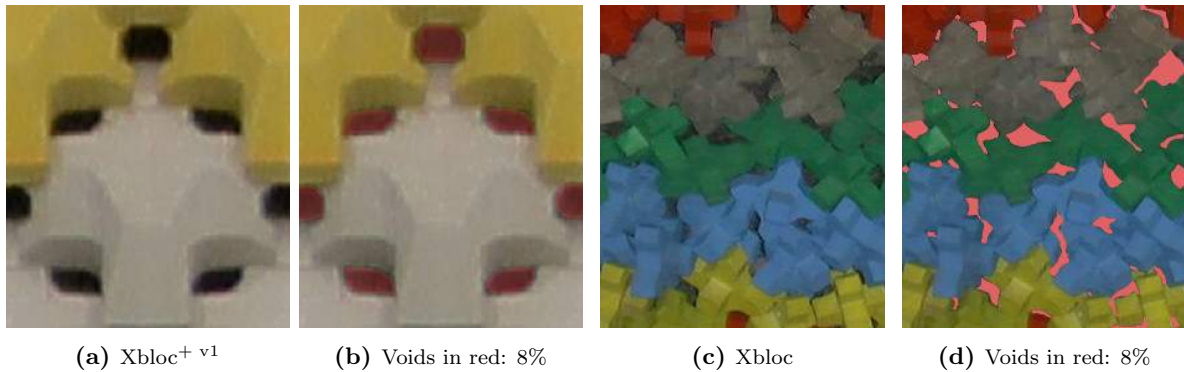


Figure 5.16: Porosity of  $Xbloc^{+v1}$  and  $Xbloc$  by computing surfaces on a photograph

Table 5.8: Porosity of various armouring concepts

	Xbloc	$Xbloc^{+v1}$	Single layer cubes	Rock	Pattern-placed blocks
Volumetric porosity [%]	58	58	25	40	-
Photographic porosity [%]	8	8	25	-	$\sim 5$

The permeability based on the volumetric porosity can be seen as an upper limit: all void volume on the outer half of the armour layer, within the imaginary box, contributes to the volumetric porosity but not to the amount of water that is able to penetrate the armour layer from the inside. This holds for both  $Xbloc$  and  $Xbloc^{+v1}$ . The permeability based on the photographic porosity can be seen as a lower limit: not only the channels perpendicular to the slope contribute to the porosity but also the channels parallel to the slope contribute. This holds for  $Xbloc^{+v1}$  and even more so for  $Xbloc$  as an  $Xbloc$  armour layer has channels in all directions instead of only perpendicular and parallel. For Single layer cubes the volumetric and photographic porosity are the exact porosity.



Based on the values in the table,  $\text{Xbloc}^{+v1}$  theoretically has the same permeability properties as  $\text{Xbloc}$  and should, therefore, be classified as a concrete armour unit. However, far less armour units are extracted in tests with  $\text{Xbloc}$ , therefore an  $\text{Xbloc}^{+v1}$  armour layer is much more sensitive to uplift than an  $\text{Xbloc}$  armour layer. The main difference in both armour units is that the bottom of  $\text{Xbloc}^{+v1}$  is a flat surface under which water pressure can build up which is released when it reaches one of the holes in-between units, while the bottom of  $\text{Xbloc}$  has protruding elements and much more channels through which the water can flow out of the structure easily. Single layer cubes also have a bottom with a flat surface but the porosity of the armour layer is much larger than that of  $\text{Xbloc}^{+v1}$ .

The permeability of an  $\text{Xbloc}^{+v1}$  armour layer seems to be somewhere in-between that of placed blocks and concrete armour units: it is lower than that of  $\text{Xbloc}$  and Single layer cubes but larger than that of placed blocks. The vulnerability of the armour layer to uplift is therefore also in-between that of both armouring types.

The uplift can easily be decreased by increasing the permeability perpendicular to the slope. This can be done by increasing the length of nose, tail and wings or by making the armour unit hollow, such as is the case for other uniformly oriented armour units like *SeaBee* and *Haro*.

### 5.2.3.5 Slope angle

Even though only one slope angle has been tested, the influence of the slope angle can be analysed through reasoning. In Section 2.3.3 the stability was depicted as a function of the slope angle together with the stability mechanism, see Figure 2.14. The contribution from gravity decreases with increasing slope angle. The contribution from interlocking and surface friction is different for interlocking and bulky units but the general tendency is that it increases with increasing slope angle. For interlocking units this is because the protruding elements of the unit interlock to form interwoven connections. For bulky units this is because the surfaces perpendicular to the slope are pressed tightly together, increasing the friction force activated during wave attack.

When  $\text{Xbloc}^{+v1}$  is placed on a 2:3 or 1:2 slope the unit slants  $3.18^\circ$  or  $7.19^\circ$  backwards with respect to the 3:4 slope, see Figure 5.17. This rotates the planes that create the interlocking and friction forces, indicated in red, such that the  $90^\circ$  angle of pulling on a 2:3 or 1:2 slope is similar to an  $86.82^\circ$  or  $82.81^\circ$  angle of pulling on a 3:4 slope. As was shown in the pull-out tests, by pulling the unit at a  $90^\circ$  angle, the weight of few surrounding units was activated. By pulling at a  $45^\circ$  angle, several of the surrounding units were activated through the chamfers of units on lower rows and the pull out force was much larger: the interlocking mechanism was improved. For a backwards slanting unit on a less steep slope the interlocking mechanism will improve as well, however, there will be less weight of subsequent rows loading the unit. As a result, the friction force will decrease.

Lastly, the wave action needs to be taken into account. A less steep slope is subjected to less severe wave attack since energy is dissipated on the longer slope, also represented by the Iribarren number in Section 2.1.1. The backwards rotation of the armour units, however, increases the units bottom surface on which the up-rushing wave exerts the load that will cause rocking.

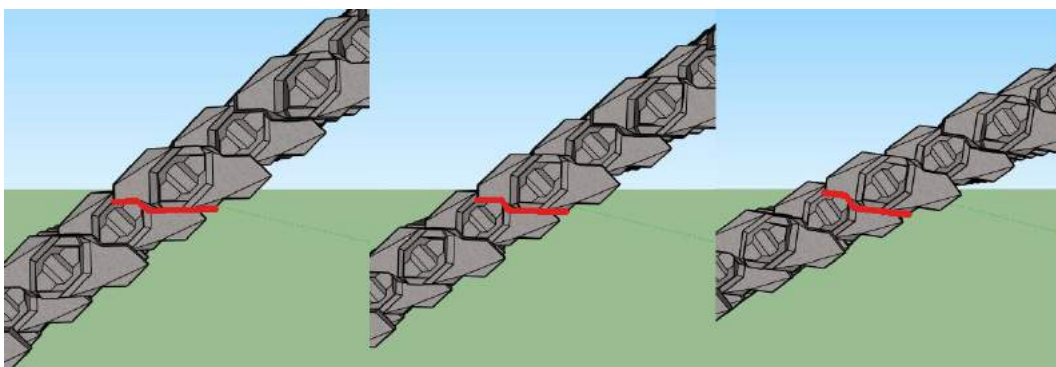


**Figure 5.17:**  $\text{Xbloc}^{+v1}$  on a 3:4, 2:3 and 1:2 slope, friction planes and chamfers indicated in red

The use of Xbloc<sup>+ v1</sup> on a less steep slope improves the interlocking mechanism, decreases the friction force, decreases the severity of the general type of wave attack and increases the surface vulnerable to wave action resulting in rocking. As it is unknown to what degree each aspect will influence the stability, tests should be done with a variety of slope angles. From these tests the influence of the slope angle on the stability of an Xbloc<sup>+ v1</sup> armour layer can be determined.

#### 5.2.4 Reflection on hypothesis

The hypothesis for the second research question was:

*There will be a large difference between the performance of the plastic and concrete armour units since, in the absence of a strong interlocking mechanism, friction plays a large role. Any irregularities in the surface profile can be an indication for weak spots; at those locations there is not enough surface contact to create the needed friction. The stability number of Xbloc<sup>+ v1</sup> will be*

$$2.0 < \frac{H_s}{\Delta D_n} < 3.3 \text{ for failure.}$$

The plastic and concrete model units performed differently: the concrete units created a more stable slope than the plastic units. However, decreasing the step size of the wave height for subsequent runs leads to similar results for both materials. The locations at which irregularities were visible were often the locations at or around which rocking or damage started. The overall performance of Xbloc<sup>+ v1</sup> was in the expected range based on  $H_s$  and similar to the previous test in terms of the stability number based on  $H_{0.1\%}$ .

# Chapter 6: Conclusions and Recommendations

This chapter finalizes this report by giving the conclusions and recommendations as experienced throughout the research. Firstly, the conclusions and recommendations of the pull-out tests will be given. The conclusions and recommendations following the results of the hydraulic model tests will be stated in the second section. The last section focusses on the main question and research goal stated in Chapter 2. It gives the combined conclusions and recommendations for the future development of Xbloc<sup>+</sup>. The conclusions and recommendations are given for a specific design and combination of parameters and should only be used in this specific context.

## 6.1 Pull-out tests

The following conclusions and recommendations will give an answer to the first research question: *How does Xbloc<sup>+</sup> v1 achieve its stability?*. The pull-out tests were conducted prior to the hydraulic model tests, therefore the conclusions and recommendations in this section have been formulated independent of the hydraulic model test results.

### 6.1.1 Conclusions

#### Resistance against extraction

The 3 most destabilizing forces on the slope are the peak force in vertical/up-slope direction ( $F_{up}$ , representing up-rush), the force normal to the slope ( $F_{normal} = 0.45F_{up}$ , representing outflow of water) and the force in horizontal/down-slope direction ( $F_{down} = 0.35F_{up}$ , representing outflow of water) [Hald, 1998]. Xbloc<sup>+</sup> v1 has a higher stability against the down-slope directed force, which is the weaker destabilizing force, than against the slope-normal directed force which is the stronger destabilizing force.

The influence of the surface roughness is larger than anticipated: both the 90° and the 45°-series show large differences when comparing concrete units with plastic units. The interlocking mechanism contributes to Xbloc<sup>+</sup> v1 stability to a far lesser extent than expected: the direction of the extraction force determines the interlocking degree. The observed stick-slip phenomenon indicates that, at first, friction governs the stability. When the friction force is overcome, interlocking prevents the unit from being pulled out directly.

Armour units lowest on the slope had the highest resistance against extraction and unit highest on the slope had the lowest resistance against extraction. The weight of the upper part of the armour layer pushes on the lowest and middle rows. The lowest rows are secured by the toe construction but the middle rows are not secured. Depending on the direction of pulling, the middle part of the slope is less (45°) or more (90°) stable than the upper part.

#### Placement

Xbloc<sup>+</sup> v1 is very sensitive to placement inaccuracies, especially the first few rows are vulnerable to bad placement. Once these rows are placed correctly, the rest of the slope is relatively easy to place. A  $1/6$  under layer will have a larger  $D_{n50}$  and therefore allows larger fluctuations ( $\pm 0.5D_{n50}$  is allowed). These fluctuations result in a very difficult to place armour layer. A smaller under layer will result in a more stable construction, as long as the material cannot be washed out through the voids in the armour layer. During the pull-out tests the under layer was less stable than it would be in prototype due to the difficulties in transferring forces to the wooden slab.

**Supporting structures**

The stability of the underlying constructions such as the toe and the under layer have a high influence on the total stability. A large percentage of the weight of the armour layer is transferred to the toe so failure of this element leads directly to loss of contact of the above armour units, and, consequently, to loss of friction and interlocking. The stability of a single unit then only depends on the own weight.

**Comparison with other units**

The comparison of the average load factor for various armouring concepts has shown that the resistance against extraction of Xbloc<sup>+v1</sup> lies in the range of those of concrete armour units. The obtained values are common for both friction and interlocking dominated armour units. Unfortunately, no pull-out data is available on well-known uniformly placed single layer armour units such as Single Layer Cubes, Diahitis, SeaBee and Haro. Xbloc<sup>+v1</sup> does show some of the same failure characteristics as pattern-placed blocks and also experiences some of the same problems with respect to under layer smoothness and placement.

**6.1.2 Recommendations****Use of a larger scale**

The difference in pull-out force in slope-normal direction has been attributed to the inter-block friction. When model units are scaled geometrically the influence of friction cannot be scaled correctly and scale effects arise. Due to these effects, the difference in pull-out force in slope-normal direction cannot be attributed to the inter-block friction with certainty. Pull-out tests for single layer armour units should be carried out on the largest scale reasonably possible to reduce the scale-effects involving friction. The outcome of pull-out tests should only be interpreted as indicative due to the many schematisations (f.e. wave direction being unidirectional and uniform, compaction).

**Reference studies**

Xbloc and Crablock rely very little on friction to create armour layer stability. Pull-out tests with these 2 armour units in concrete and plastic will give insight into the results of the present research. If for Xbloc and Crablock no difference is found in pull-out force for both materials, it can be concluded with certainty that the stability of an Xbloc<sup>+v1</sup> armour layer depends largely on friction. If the differences are large, as they were for Xbloc<sup>+v1</sup>, no conclusion can be formed about friction being a stabilising mechanism for Xbloc<sup>+v1</sup>. Additionally, it will prove that the material used in model testing influences the armour layer stability and any model tests done with concrete instead of plastic units results in an overestimation of the stability.

The roughness of the under layer has a large impact on the correct placement of this armour unit. Pull-out tests as well as hydraulic tests should be conducted with under layers 1/15 and 1/20 to determine which under layer creates the most stable armour layer without being washed out.

**Increase interlocking**

Independent of the discussion if friction is the main contributor to stability, the interlocking capacity should be enlarged. There are no scale effects concerning interlocking, it is therefore the safest way of increasing the units resistance against extraction. It can easily be realized by changing the inclination of the chamfers on the top and bottom of Xbloc<sup>+v1</sup> until they are almost vertical.

**Rotate planes of contact**

The rotation of the planes on which the armour units make contact from 35° to 90° has a two-fold effect. Armour units can be placed more easily and the force normal to the friction plane increases, therefore the required force to extract a unit increases.

**Toe construction**

To create a more stable first row a type of (concrete) beam could be used on which the first row of blocks are secured, limiting their movement. For the physical model tests it is recommended that a sturdy toe-beam is used, the toe can also be reinforced by using a rock berm. The advantage of a toe-beam is that it also ensures that all units are aligned and have the same forward and backward rotation.

## 6.2 Hydraulic physical model tests

The following conclusions and recommendations will give an answer to the second research question: *How does Xbloc<sup>+ v1</sup> respond to wave loading?*. The conclusions and recommendations of the pull-out tests have been implemented in the hydraulic model tests.

### 6.2.1 Conclusions

#### Performance Xbloc<sup>+ v1</sup>

The performance of an armour unit with respect to failure is usually expressed in the stability number but this is subject to geometrical configurations and armour unit specific characteristics such as packing density. It has to be noted that the stability number does not solely define the performance of an armour unit. If the stability number of a unit is large but they also have to be placed very densely packed, based on concrete usage it might actually perform less than other units. A direct comparison with other units is therefore not possible. Compared on a qualitative basis, Xbloc<sup>+ v1</sup> is on the right track of becoming a good competitor.

The results of the preliminary test by Jacobs (1:30 foreshore and shallow water) were matched by the results of the present study (no foreshore and deep water) when a comparison was made based on the stability number based on the extreme wave height  $H_{0.1\%}$ , which substantiates the conclusions as stated in the thesis of Zwanenburg [2012]. Xbloc<sup>+ v1</sup> fails at an average of  $4.43 \frac{H_{0.1\%}}{\Delta D_n}$ . The plastic units reached  $4.25 \frac{H_{0.1\%}}{\Delta D_n}$  on average and the concrete units performed better at  $4.69 \frac{H_{0.1\%}}{\Delta D_n}$  on average, an increase of 10%. By decreasing the step size between subsequent runs the slope is compacted by low waves and the stability is increased such that the plastic units perform similar to the concrete units. The hydraulic physical model tests were done under conservative conditions (no foreshore, large water depth, long slope so no dissipation by overtopping), therefore the results can be considered a lower limit for the stability (when working with plastic blocks).

#### Resistance against extraction

Due to a low interlocking mechanism, armour units can easily be rotated during up-rush, and, after losing their stable foundation on the under layer, they start to rock. When a large wave disintegrates on the slope and water flows out of the core and armour layer, the rocking units are pushed out. This has been contributed to the combined influence of a low interlocking mechanism and low porosity of the armour layer. The porosity of an Xbloc<sup>+ v1</sup> is smaller than that of Xbloc and Single layer cubes but larger than that of placed blocks. The vulnerability of the armour layer to uplift is therefore also in-between that of both armouring types.

#### Damage

When Xbloc<sup>+ v1</sup> starts to rock, it creates space around it. After the unit is extracted, surrounding units will either slide into the void left by the extracted unit or be extracted their selves: a pyramid shape of voids will form. The location of damage is between SWL and 4 rows below SWL. The location of damage can be predicted on forehand by inspecting the uniformity of the slope.

#### Supporting structures and placement

The aluminium toe-beam was a good tool in ensuring the correct placing and packing density of the first few rows. Again, the importance of a stable toe construction is proven to be very important: failure due to horizontal sliding of the toe was observed. The plastic units were harder to place: the units in the middle rows slanted backward due to the weight of the rows above them and the lack of inter-block friction.

#### Slope angle

The use of Xbloc<sup>+ v1</sup> on a less steep slope improves the interlocking mechanism, decreases the friction force, decreases the severity of the general type of wave attack and increases the surface vulnerable to wave action resulting in rocking. The interaction of these 4 aspects makes it, at this moment, impossible to determine the influence of the slope angle.

## 6.2.2 Recommendations

### Reference studies

There are too many differences in the way armour units are tested by different facilities for them to be directly compared. It is advised that a large test program is set-up in which the most widely used armour units are all tested for the exact same model configuration and wave load.

For Xbloc<sup>+ v1</sup> specifically it is advised that other slope angles are tested to get more insight into the contribution of each stabilising mechanism. As the start of damage and start of failure are very close to each other, the step size should be minimized to 1cm  $H_{0.1\%}$  for the current unit size.

The results of the preliminary and current study and the theses of Moreno [2017] & Rada [2017] should be compared so that the improvements on the stability during various designs can be monitored. If a change in stability can directly be attributed to an element of the unit then more targeted improvements can be applied.

### Increase porosity armour layer

Uplift due to overpressure should be prevented. It is recommended that the porosity of the armour layer is increased, this can be done by increasing the gaps between the blocks or by designing a gap or hole in the block similar to those in Haro or SeaBee. In this way the overpressure can be relieved.

### Increase interlocking

The armour units are rotated out of their original position due to the wave force during up-rush pushing on the bottom of the unit. When a unit is rotated it can rock back and forth and will eventually be extracted. The units can be prevented from rotating by improving the interlocking mechanism.

## 6.3 Final conclusions and recommendations

The main question was: *How does the shape of the uniformly placed single layer concrete armour unit Xbloc<sup>+ v1</sup> affect the armour layer stability?*. The goal was: *To find the failure mechanism(s) that dominate Xbloc<sup>+ v1</sup> and modify its shape such that an armour layer made out of Xbloc<sup>+ v2</sup> armour units will be more stable.* The conclusion and recommendations of the pull-out and hydraulic model tests together have resulted in the following conclusions and recommendations with respect to improvement of the shape and stability of Xbloc<sup>+ v1</sup>.

### 6.3.1 Conclusions and recommendations

The stability of an Xbloc<sup>+ v1</sup> armour layer relies on its own weight, the friction between neighbouring units and, due to its shape, also some interlocking. This is unlike other single layer uniformly oriented concrete armour units whose stability depend on own weight and friction. It is, so to speak, a hybrid form of the two main armouring concepts. Due to the specific test configuration, Xbloc<sup>+ v1</sup> cannot be compared to other units on a quantitative basis, but compared on a qualitative basis, Xbloc<sup>+ v1</sup> is on the right track of becoming a good competitor.

The degree of interlocking is mainly dependent on the direction of the force but also on the placement accuracy, the slope profile (convex or concave) and the elevation along the slope. The interlocking capacity can be increased easily by rotating the chamfers such that they are almost vertical. The degree in which friction contributes depends on the elevation along the slope, the direction of the force and the surface roughness of the unit. This can be increased by rotating the planes of contact (friction surfaces) such that they are perpendicular to the slope, just as they are for other uniformly oriented units and pattern-placed blocks. The rotation of these planes from 35° to 90° has a two-fold effect: armour units can be placed more easily and the force normal to the friction plane increases, therefore the required force to extract a unit increases. If the friction planes are not rotated, it should at least be made easier to check whether Xbloc<sup>+ v2</sup> units are placed with the right orientation and that all friction planes are making contact. Lastly, the permeability of the armour layer is too low, making the armour layer vulnerable to uplift. This can be counteracted by incorporating a hole through the armour unit, perpendicular to the slope.

The placement of Xbloc<sup>+ v1</sup> is a time consuming process. It is facilitated by a finer and smoother under layer which is well-compacted, as well as a toe-beam which guarantees the horizontal placing

distance as well as the angular orientation of the first row.

From both the pull-out and hydraulic model tests it was concluded that the surface roughness of the units has a large impact on the results. It has also been found that the smooth units can perform similar to the rough units if the wave load is slowly increased. For reference, pull-out and hydraulic tests for a simple reference case should be done with both concrete and plastic Crablock (uniformly placed but influenced by friction as well as by interlocking) and Xbloc (interlocking dominated). If there is a large difference between plastic and concrete in these tests, any hydraulic model tests executed with concrete units might have given an overestimation of the stability, both for friction and interlocking dominated armour units.

# Bibliography

- Bakker, P., Klabbers, M., Muttray, M., and van den Berge, A. (2005). Hydraulic performance of xbloc armour units. Technical report, PDF from [www.Xbloc.com](http://www.Xbloc.com).
- Battjes, J. A. and Groenendijk, H. W. (2000). Wave height distributions on shallow foreshores. *Journal of Coastal Engineering*, 40(3):161–182.
- Bonfantini, F. (2014). Set-up to design guidance for the Crablock armour unit - Comparison of single layer armour units investigation. Technical report, UNESCO-IHE Institute for Water Education, The Netherlands.
- Broere, A. (2015). Physical model tests on stability and interlocking of new breakwater armour block CrablockTM. Master's thesis, Delft University of Technology, The Netherlands.
- Brouwer, M. (2013). The influence of the under layer on the stability of single layer armour units. Master's thesis, Delft University of Technology, The Netherlands.
- Burcharth, H. F. (1992). Reliability evaluation of a structure at sea. In *Proceedings of the Short Course on Design and Reliability of Coastal Structures, ICCE*. Department of Civil Engineering, Aalborg University, Denmark.
- Burcharth, H. F. and Andersen, O. H. (1995). On the One-Dimensional Unsteady Porous Flow Equation. *Journal of Coastal Engineering*, 24(3-4):233–257.
- Burcharth, H. F., Liu, Z., and Troch, P. (1999). Scaling of core material in rubble mound breakwater model tests. In *Proceedings of the Fifth International Conference on Coastal and Port Engineering in Developing Countries, Cape Town, South Africa*, pages 1518–1528.
- CIRIA, CUR, and CETMEF (2007). *The Rock Manual. The use of rock in hydraulic engineering*. C683, CIRIA, London, 2nd edition.
- d'Angremond, K., van Roode, F. C., and Verhagen, H. J. (2001). *Breakwaters and closure dams - Engineering the interface of soil and water*. Delft Academic Press, The Netherlands, 2nd edition.
- de Lange, M. (2010). Extraction force Xbloc: Model tests - Taking into account the influence of the slope angle, the density of the concrete of the Xbloc, the vertical position of the Xbloc and the roughness of the under layer on the extraction force of an Xbloc armour unit. Master's thesis, Delft University of Technology, The Netherlands.
- Gier, F., Schuttrumpf, H., Munnich, J., and van der Meer, J. (2012). Stability of interlocked pattern placed block revetments. In *Proceedings of the 33rd Conference on Coastal Engineering, Santander, Spain*.
- Hald, T. (1998). *Wave Induced Loading and Stability of Rubble Mound Breakwaters*. PhD thesis, Hydraulics & Coastal Engineering Laboratory, Department of Civil Engineering, Aalborg University, Denmark.
- Holthuijsen, L. H. (2007). *Waves in oceanic and coastal waters*. Cambridge University Press, United Kingdom.
- Holthuijsen, L. H. and Herbers, T. H. C. (1986). Statistics of breaking waves observed as whitecaps in the open sea. *Journal of Physical Oceanography*, 16(8):290–297.
- Hovestad, M. (2005). Breakwaters on steep foreshores - the influence of the foreshore steepness on armour stability. Master's thesis, Delft University of Technology, The Netherlands.
- Hughes, S. A. (1993). *Physical models and laboratory techniques in Coastal Engineering*, volume 7. World Scientific Publishing Co. Pte. Ltd., Singapore.



- Jacobs, R. P. M. (2015). Ibloc Model Tests, 2D Hydraulic Model Tests - Factual Report. Internal document from BAM Infra Consultants, DMC.
- Mansard, E. P. D. and Funke, E. R. (1980). The measurement of incident and reflected spectra using a least squares method. In *Proceedings of the 17<sup>th</sup> International Conference on Coastal Engineering*, volume 1, pages 154–172. ASCE, New York, N.Y.
- Mickel, J. J. (1999). A-Jacks Matrix Stability: Deflection Due to Static Normal Loads. Master's thesis, Oregon State University, United States of America.
- Moreno, A. J. (2017). Experimental study on the wave overtopping performance of Xbloc<sup>+</sup> armour unit. Master's thesis, Delft University of Technology, The Netherlands.
- Muttray, M. and Reedijk, J. S. (2008). Design of concrete armour layers. Technical report, PDF from [www.Xbloc.com](http://www.Xbloc.com).
- Oortman, N. J. (2006). Influence of foreshore steepness on wave velocity and acceleration at the breakwater interface. Master's thesis, Delft University of Technology, The Netherlands.
- Peters, D. J. (2017). *Design of Pattern-placed Revetments*. PhD thesis, Delft University of Technology, The Netherlands.
- PIANC, WG36 (2005). Catalogue of prefabricated elements. Technical report, International Navigation Association.
- Price, W. A. (1979). *Static stability of rubble mound breakwaters*, volume 60. The Dock & Harbour Authority, Hydraulics Research Station, United Kingdom.
- Rada, B. (2017). Hydraulic performance of Xbloc<sup>+</sup> armor unit. Master's thesis, Delft University of Technology, The Netherlands.
- Reedijk, J. S., Muttray, M., van den Berge, A., and de Rover, R. (2008). Effect of core permeability on armour layer stability. Technical report, PDF from [www.Xbloc.com](http://www.Xbloc.com).
- Salaudhin, M. (2015). Physical model tests on new armour block Crablock for breakwaters to come to preliminary design guidance. Master's thesis, Delft University of Technology, The Netherlands.
- Schiereck, G. J. and Verhagen, H. J. (2001). *Introduction to Bed, Bank and Shore protection - Engineering the interface of soil and water*. Delft Academic Press, The Netherlands.
- ten Oever, E. (2006). Theoretical and experimental study on the placement of Xbloc. Master's thesis, Delft University of Technology, The Netherlands.
- US Army Corps of Engineers (1984). *Shore Protection Manual*, volume 2. Coastal Engineering Research Center, USACE, Washington DC, United States.
- van de Koppel, M. A. (2012). Static and dynamic loads on the first row of interlocking, single layer armour units. Master's thesis, Delft University of Technology, The Netherlands.
- van der Meer, J. W. (1987). Stability of Breakwater Armour Layers - Design Formulae. *Journal of Coastal Engineering*, 11:219–239.
- van der Meer, J. W. and Heydra, G. (1991). Rocking armour units: Number, location and impact velocity. *Journal of Coastal Engineering*, 15:21–39.
- van Gent, M. R. A. and Luis, L. (2013). Application of Cubes in a single layer. In *Proceedings of the 6<sup>th</sup> International Conference on Applied Coastal Research, Lisbon, Portugal*.
- van Gent, M. R. A., Plate, S. E., Berendsen, E., Spaan, G. B. H., van der Meer, J. W., and d'Angremond, K. (1999). Single-layer rubble mound breakwaters. In *Proceedings of the International Conference on Coastal Structures, Santander, Spain*, pages 231–239.
- van Zwicht, B. N. M. (2009). Effect of the concrete density on the stability of Xbloc armour units. Master's thesis, Delft University of Technology, The Netherlands.

- Verhagen, H. J. (1984). Trekproeven op glooiingsconstructies in de Oosterschelde. Technical report, Rijkswaterstaat Adviesdienst Vlissingen, WWKZ-84,V002.
- Verhagen, H. J. (2016). Bed, bank and shoreline protection - chapter 7. Powerpoint presentation, Delft University of Technology, The Netherlands.
- Zwanenburg, S. A. A. (2012). The influence of the wave height distribution on single layer concrete armour units. Master's thesis, Delft University of Technology, The Netherlands.

# List of Figures

1.1	Difference between Xbloc and Xbloc <sup>+</sup> . . . . .	2
1.2	Thesis Outline . . . . .	5
2.1	H/T diagram, d'Angremond et al. [2001] . . . . .	7
2.2	Breaker types as defined by the breaker parameter, Verhagen [2016] . . . . .	8
2.3	Rayleigh distribution for deep water . . . . .	10
2.4	Relation between $H_{0.1\%}$ and $h_t$ made dimensionless by $H_s$ . . . . .	10
2.5	Experimental data on wave induced loading by Hald [1998] . . . . .	11
2.6	Important structural parameters in breakwater design [CIRIA et al., 2007] . . . . .	12
2.7	Overview of the most used armour units, supplemented with Cubipod, Crablock and Xbloc <sup>+</sup> v1, after [Muttray and Reedijk, 2008] . . . . .	13
2.8	Relation between $K_D$ and $N_s$ for a safe design, start of damage and failure [Bakker et al., 2005] . . . . .	15
2.9	Damage progression for increasing wave height . . . . .	16
2.10	Possible failure mechanisms with red failure mechanisms being most important for this research [Burcharth, 1992] . . . . .	17
2.11	Examples of placed blocks: Basalt, Basalton, Ronaton, Verkalit (interlocking), Hillblok and Hydroblok . . . . .	19
2.12	Failure mechanisms of pattern-placed blocks, after Peters [2017] . . . . .	21
2.13	Full-scale pull-out test on Verkalit interlocking placed block, chronological sequence [Gier et al., 2012] . . . . .	22
2.14	Influence of the slope angle on stabilisation mechanisms for complex interlocking units and bulky type of units, after Price [1979] . . . . .	23
2.15	Becoming familiar with Xbloc <sup>+</sup> v1 . . . . .	24
2.16	Definitions Xbloc <sup>+</sup> . . . . .	24
2.17	Definition of $D_{cu}$ . . . . .	25
2.18	Introduction to Crablock . . . . .	26
2.19	Pattern placement of cubes in a single layer [van Gent and Luis, 2013] . . . . .	27
3.1	3D and topview of SeaBee, Diahitis, Cube, Cob, Shed and Xbloc <sup>+</sup> v1. Indication of colours: blue = vertical friction plane ( $\perp$ to slope), red = horizontal friction plane atop ( $\parallel$ to slope), green = horizontal friction plane below ( $\parallel$ to slope) . . . . .	28
4.1	Model set-up . . . . .	31
4.2	Methods of securing fishing line: "Simple", "3 loops" and "Cross" . . . . .	32
4.3	Measuring method . . . . .	33
4.4	Overview of the model set-up . . . . .	35
4.5	Overview breakwater set-up . . . . .	36
4.6	Relation between wave steepness and stability number for varying slopes [d'Angremond et al., 2001] . . . . .	36
4.7	Toe-beam . . . . .	37
5.1	Results pull-out series 3 and 4, $\theta = 90^\circ$ , 3:4 slope, $1/11$ under layer . . . . .	40
5.2	Results pull-out series 5 and 6, $\theta = 45^\circ$ , 3:4 slope, $1/11$ under layer . . . . .	41
5.3	Series 3 through 6, 3:4 slope, $1/11$ under layer, both materials . . . . .	42
5.4	Schematic representation of a staggered grid with Xbloc <sup>+</sup> v1 . . . . .	43

5.5	Examples of correct and incorrect placement . . . . .	44
5.6	Test 7, plastic units, $\theta = 90^\circ$ , $1/11$ under layer . . . . .	45
5.7	$90^\circ$ and $45^\circ$ pull directions, model unit rotates around the red dot . . . . .	45
5.8	Representative slopes from series 3 through 6 . . . . .	46
5.9	All test results . . . . .	49
5.10	Left: wave crest induces high core water level, right: wave through induces outward directed pressures by water wanting to flow out . . . . .	50
5.11	Extraction of a unit out of the armour layer: loosening and rotation during up- and down-rush after which overpressure pushes Xbloc <sup>+ v1</sup> out during the down-rush of a large energy wave group . . . . .	51
5.12	Relation between $H_{0.1\%}$ and $h_t$ made dimensionless by $H_s$ . . . . .	53
5.13	Comparison of preliminary and present study on basis of $H_s$ , $H_{2\%}$ & $H_{0.1\%}$ . . . . .	54
5.14	Comparison of performance of plastic and concrete model units for categories "No rocking", "Rocking" and "Failure" based on stability numbers $\frac{H_{2\%}}{\Delta D_n}$ and $\frac{H_{0.1\%}}{\Delta D_n}$ . . . . .	55
5.15	Comparison of performance of large and small step sizes for categories "No rocking", "Rocking" and "Failure" based on stability numbers $\frac{H_{2\%}}{\Delta D_n}$ and $\frac{H_{0.1\%}}{\Delta D_n}$ . . . . .	56
5.16	Porosity of Xbloc <sup>+ v1</sup> and Xbloc by computing surfaces on a photograph . . . . .	58
5.17	Xbloc <sup>+ v1</sup> on a 3:4, 2:3 and 1:2 slope, friction planes and chamfers indicated in red . . . . .	59
A.1	Density model units . . . . .	ii
A.2	Difference between concrete and plastic densities . . . . .	ii
C.1	Overview of the model set-up . . . . .	v
D.1	Concave slope profile, increasing the stability . . . . .	vi
D.2	Influence of under layer on placement of model units . . . . .	vi
D.3	Placement errors row underneath . . . . .	vi
D.4	Model unit slanted backwards . . . . .	vii
D.5	Placement distance . . . . .	vii
E.1	Applicable theory, after Holthuijsen [2007], modified . . . . .	ix
F.1	Cumulative distribution curve of the applied core of the breakwater model . . . . .	xi
I.1	Hydraulic physical model tests: test 1 . . . . .	xviii
I.2	Hydraulic physical model tests: test 1 extra, $H_s = 11.22$ cm . . . . .	xviii
I.3	Hydraulic physical model tests: test 2 . . . . .	xviii
I.4	Hydraulic physical model tests: test 3 . . . . .	xix
I.5	Hydraulic physical model tests: test 4 . . . . .	xix
I.6	Hydraulic physical model tests: test 5 . . . . .	xix
I.7	Hydraulic physical model tests: test 6 . . . . .	xx
I.8	Hydraulic physical model tests: test 7 . . . . .	xx
I.9	Hydraulic physical model tests: test 8 . . . . .	xx
I.10	Hydraulic physical model tests: test 9 . . . . .	xxi
I.11	Hydraulic physical model tests: test 10 . . . . .	xxi
I.12	Hydraulic physical model tests: test 10 extra, $H_s = 10.80$ cm . . . . .	xxi

# List of Tables

- 1 List of Latin Symbols . . . . . x
- 2 List of Greek symbols . . . . . xi
  
- 2.1 Characteristics Xbloc<sup>+</sup> v1 and Xbloc expressed as function of the unit size . . . . . 25
  
- 4.1 Test program pull-out tests . . . . . 32
- 4.2 Required distances for wave gauges . . . . . 34
- 4.3 Overview of model elements . . . . . 35
- 4.4 Test program hydraulic model tests . . . . . 38
- 4.5 Targeted significant wave height and peak period per test run . . . . . 38
  
- 5.1 Required dimensionless force as shown in the boxplots . . . . . 41
- 5.2 Data on non-dimensional pull-out force required for extraction for various concrete armour units and pattern-placed blocks . . . . . 47
- 5.3 Physical model tests program and failure mechanism . . . . . 48
- 5.4 Stability numbers accompanying the different armour units as stated in the Rock Manual [CIRIA et al., 2007], van Gent and Luis [2013] and as found in this study . . . . . 50
- 5.5 Stability numbers for comparison concrete and plastic . . . . . 55
- 5.6 Stability numbers for comparison large and small step size . . . . . 56
- 5.7 Stability numbers for comparison of small step size plastic test with other plastic tests . . . . . 57
- 5.8 Porosity of various armouring concepts . . . . . 58
  
- A.1 Average data model units . . . . . ii
- A.2 Measurements model units . . . . . iii
  
- E.1 Applicable wave theory determined by the Ursell number and the graph by Le Mehaute . . . . . viii
  
- G.1 My caption . . . . . xii
  
- H.1 Test 1, Plastic, large steps . . . . . xiii
- H.2 Test 2, Concrete, large steps . . . . . xiii
- H.3 Test 3, Concrete, large steps . . . . . xiii
- H.4 Test 4, Concrete, large steps . . . . . xiv
- H.5 Test 5, Plastic, large steps . . . . . xiv
- H.6 Test 6, Plastic, large steps . . . . . xv
- H.7 Test 7, Plastic, large steps . . . . . xv
- H.8 Test 8, Plastic, small steps . . . . . xv
- H.9 Test 9, Concrete, small steps . . . . . xvi
- H.10 Test 10, Concrete, small steps . . . . . xvii

# Appendix A: Model Units

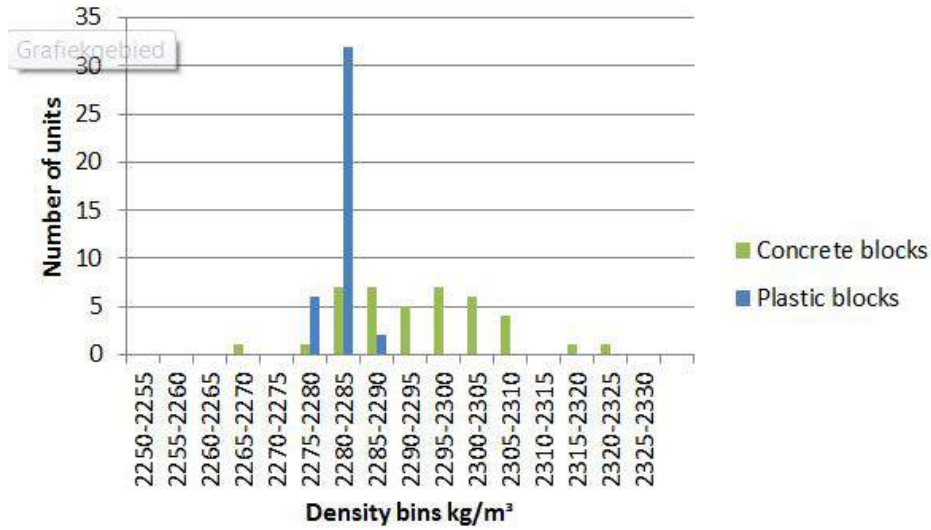
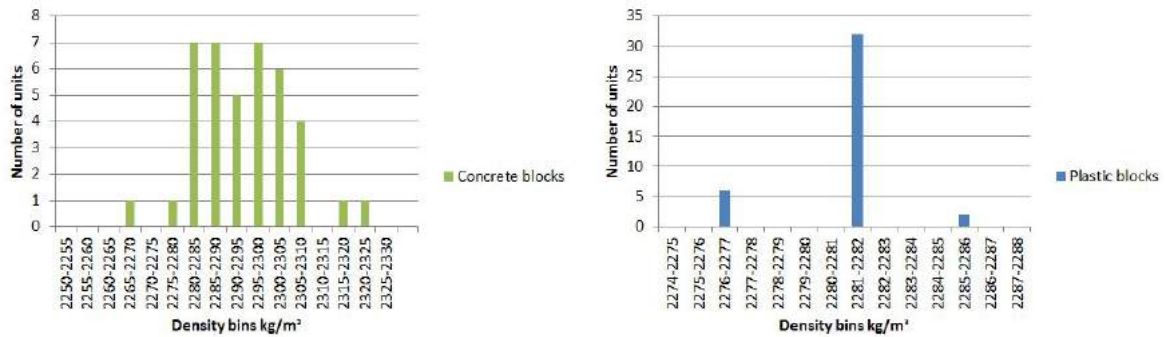


Figure A.1: Density model units



(a) Density concrete model units

(b) Density plastic model units

Figure A.2: Difference between concrete and plastic densities

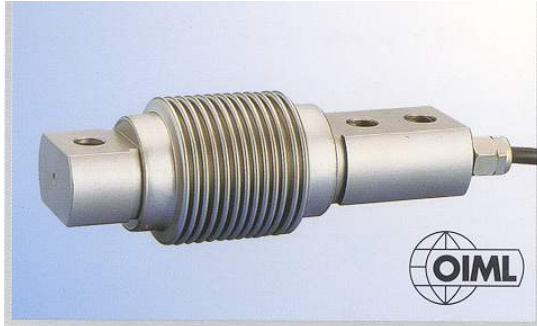
Table A.1: Average data model units

	Plastic			Concrete		
	Minimum	Average	Maximum	Minimum	Average	Maximum
Width [mm]	48,1	48,135	48,2	46,5	47,6525	48,2
Weight [gr]	58,4	58,42	58,5	55,1	57,2475	59,1
$\rho$ [ $\text{kg/m}^3$ ]	2276	2281	2285	2261	2289	2317
St.dev. [ $\text{kg/m}^3$ ]		2,046			11,119	

Table A.2: Measurements model units

Plastic		Direct under water			Concrete		Direct under water			After a few hours under water				
D [mm]	W_dry [gr]	W_wet [gr]	V [ml]	$\rho$ [kg/m]	D [mm]	W_dry [gr]	W_wet [gr]	V [ml]	$\rho$ [kg/m]	W_sat [gr]	W_wet [gr]	V [ml]	$\rho$ [kg/m]	
48,1	58,4	32,8	25,6	2281	47,5	56,6	31,9	24,7	2291	57,6	32,9	24,7	2332	
48,1	58,4	32,8	25,6	2281	47,8	57,1	32,1	25,0	2284	58,1	33,1	25,0	2324	
48,2	58,4	32,8	25,6	2281	48,1	58,5	33,0	25,5	2294	59,5	34,0	25,5	2333	
48,2	58,4	32,8	25,6	2281	47,9	57,2	32,1	25,1	2279	58,2	33,1	25,1	2319	
48,1	58,4	32,8	25,6	2281	47,1	56,9	32,1	24,8	2294	57,9	33,1	24,8	2335	
48,1	58,4	32,8	25,6	2281	46,5	55,5	31,2	24,3	2284	56,5	32,2	24,3	2325	
48,1	58,4	32,8	25,6	2281	47,8	57,1	32,1	25,0	2284	58,1	33,1	25,0	2324	
48,1	58,4	32,8	25,6	2281	46,9	55,1	30,9	24,2	2277	56,1	31,9	24,2	2318	
48,2	58,5	32,9	25,6	2285	48,1	58,1	32,8	25,3	2296	59,1	33,8	25,3	2336	
48,1	58,4	32,8	25,6	2281	47,8	56,6	31,8	24,8	2282	57,6	32,8	24,8	2323	
48,2	58,4	32,8	25,6	2281	48,0	58,1	32,8	25,3	2296	59,1	33,8	25,3	2336	
48,1	58,4	32,8	25,6	2281	47,1	56,8	32,0	24,8	2290	57,8	33,0	24,8	2331	
48,1	58,5	32,8	25,7	2276	47,8	56,3	31,6	24,7	2279	57,3	32,6	24,7	2320	
48,1	58,4	32,8	25,6	2281	47,9	58,1	32,8	25,3	2296	59,1	33,8	25,3	2336	
48,1	58,4	32,8	25,6	2281	47,0	56,6	31,8	24,8	2282	57,6	32,8	24,8	2323	
48,1	58,4	32,8	25,6	2281	47,8	56,9	31,9	25,0	2276	57,9	32,9	25,0	2316	
48,2	58,4	32,8	25,6	2281	47,4	56,6	31,8	24,8	2282	57,6	32,8	24,8	2323	
48,1	58,4	32,8	25,6	2281	47,3	56,3	31,7	24,6	2289	57,3	32,7	24,6	2329	
48,2	58,4	32,8	25,6	2281	48,1	58,3	33,0	25,3	2304	59,3	34,0	25,3	2344	
48,1	58,5	32,8	25,7	2276	47,6	57,0	32,4	24,6	2317	58,0	33,4	24,6	2358	
48,1	58,4	32,8	25,6	2281	47,2	58,0	32,7	25,3	2292	59,0	33,7	25,3	2332	
48,2	58,4	32,8	25,6	2281	47,9	56,8	31,8	25,0	2272	57,8	32,8	25,0	2312	
48,1	58,4	32,8	25,6	2281	47,8	57,0	32,1	24,9	2289	58,0	33,1	24,9	2329	
48,2	58,5	32,8	25,7	2276	47,2	58,1	32,7	25,4	2287	59,1	33,7	25,4	2327	
48,1	58,4	32,8	25,6	2281	48,1	59,1	33,4	25,7	2300	60,1	34,4	25,7	2339	
48,2	58,5	32,8	25,7	2276	47,7	57,1	32,3	24,8	2302	58,1	33,3	24,8	2343	
48,1	58,4	32,8	25,6	2281	48,1	57,5	32,3	25,2	2282	58,5	33,3	25,2	2321	
48,2	58,4	32,8	25,6	2281	48,1	57,9	32,6	25,3	2289	58,9	33,6	25,3	2328	
48,1	58,4	32,8	25,6	2281	47,2	57,5	32,5	25,0	2300	58,5	33,5	25,0	2340	
48,2	58,5	32,9	25,6	2285	47,6	56,2	31,5	24,7	2275	57,2	32,5	24,7	2316	
48,1	58,4	32,8	25,6	2281	47,0	56,9	32,3	24,6	2313	57,9	33,3	24,6	2354	
48,1	58,4	32,8	25,6	2281	48,2	58,3	32,9	25,4	2295	59,3	33,9	25,4	2335	
48,2	58,4	32,8	25,6	2281	47,8	56,5	31,7	24,8	2278	57,5	32,7	24,8	2319	
48,1	58,4	32,8	25,6	2281	48,0	58,0	32,7	25,3	2292	59,0	33,7	25,3	2332	
48,1	58,4	32,8	25,6	2281	47,3	57,7	32,6	25,1	2299	58,7	33,6	25,1	2339	
48,1	58,5	32,8	25,7	2276	47,8	57,6	32,6	25,0	2304	58,6	33,6	25,0	2344	
48,1	58,4	32,8	25,6	2281	48,0	56,7	31,8	24,9	2277	57,7	32,8	24,9	2317	
48,2	58,4	32,8	25,6	2281	48,1	58,1	32,4	25,7	2261	59,1	33,4	25,7	2300	
48,1	58,4	32,8	25,6	2281	47,7	57,0	32,1	24,9	2289	58,0	33,1	24,9	2329	
48,2	58,5	32,8	25,7	2276	47,8	58,2	32,8	25,4	2291	59,2	33,8	25,4	2331	
Average	48,14	58,42	32,81	25,62	2281	47,65	57,25	32,24	25,01	2289	58,25	33,24	25,01	2329

# Appendix B: LSH Load Cell



## LSH Load Cell

- Stainless Steel construction
- Capacities from 10 Kg to 200 Kg
- 2 mv/v output
- High accuracy
- Interchangeable to most brands
- OIML Approved Class C4

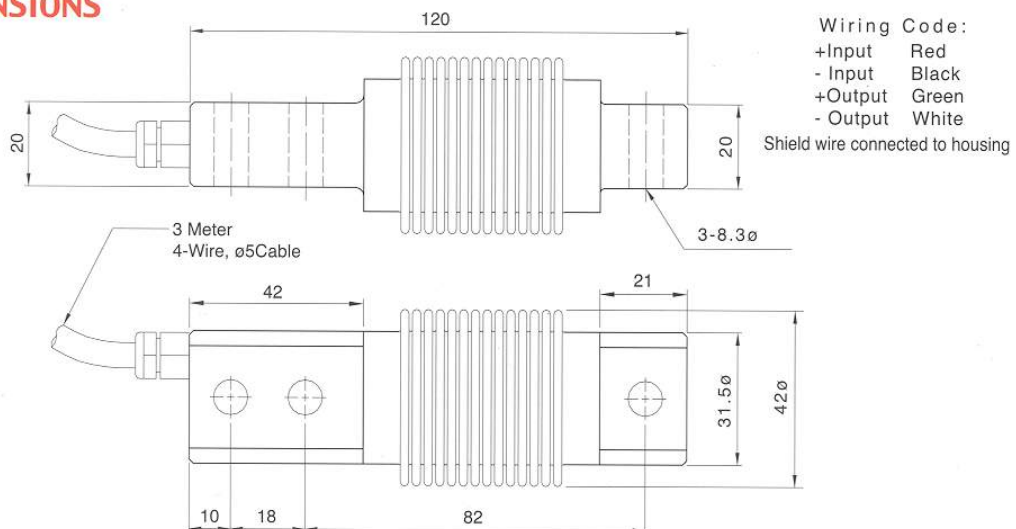
Certificate No. R60/2000-NL-00.11

## SPECIFICATIONS

Accuracy Class (max. number of intervals)	C1 (1000)	C3 (3000)	C4 (4000)
Rated Capacities(Kg)	10,20,50,100,200		
Combined Error (% of R.O.)	0.035	0.017	0.010
Non-Repeatability (% of R.O.)	0.015	0.010	0.008
Minimum Division Size (v min., % of R.O.)	0.030	0.010	0.008
Temperature Coefficient			
Output (ppm/°C, of load)	16	5	3
Zero (ppm/°C, of R.O.)	42	14	11
Creep Return (% of load, 30 Min.)	0.050	0.017	0.013
Rated Output (mv/v)	2 ± 0.25%		
Zero Balance (% of R.O.)	± 2		
Excitation (Volt)	10 recommended, 15 Max.		
Input Impedance (Ω)	385 ± 10		
Output Impedance (Ω)	356 ± 1%		
Operating Temperature Range (°C)	-40 to +60		
Environmental Protection (DIN)	IP 68		
Safe Overload (% of R.O.)	150		
Deflection (mm, @ Rated Capacity)	0.25, 0.25, 0.29, 0.32, 0.44		

Example for Order Number: **LSH-10-C4**, **LSH**: load cell type, **10**: capacity in kg, **C4**: accuracy class, OIML Class C 4000 divisions.

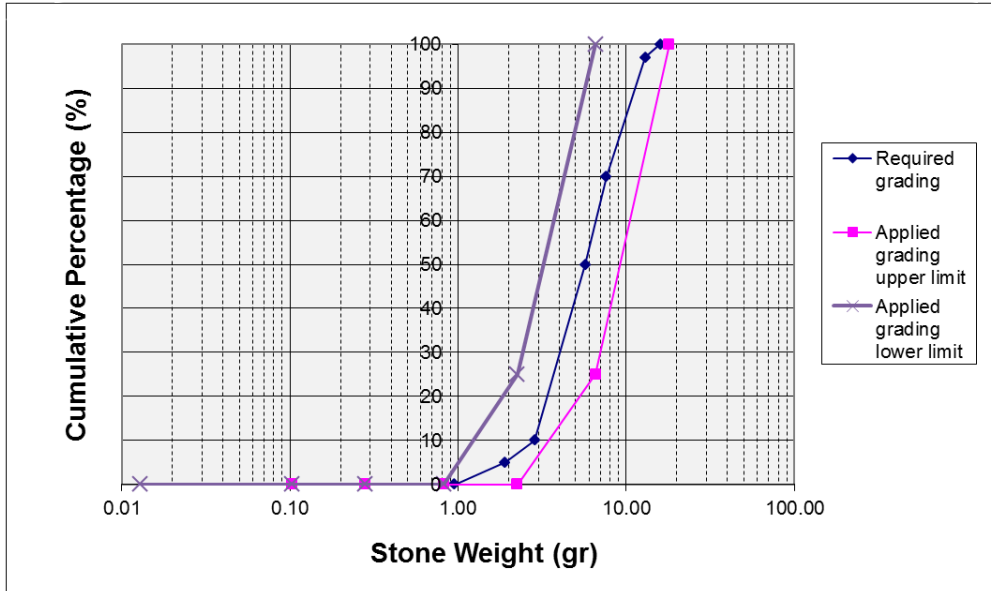
## DIMENSIONS



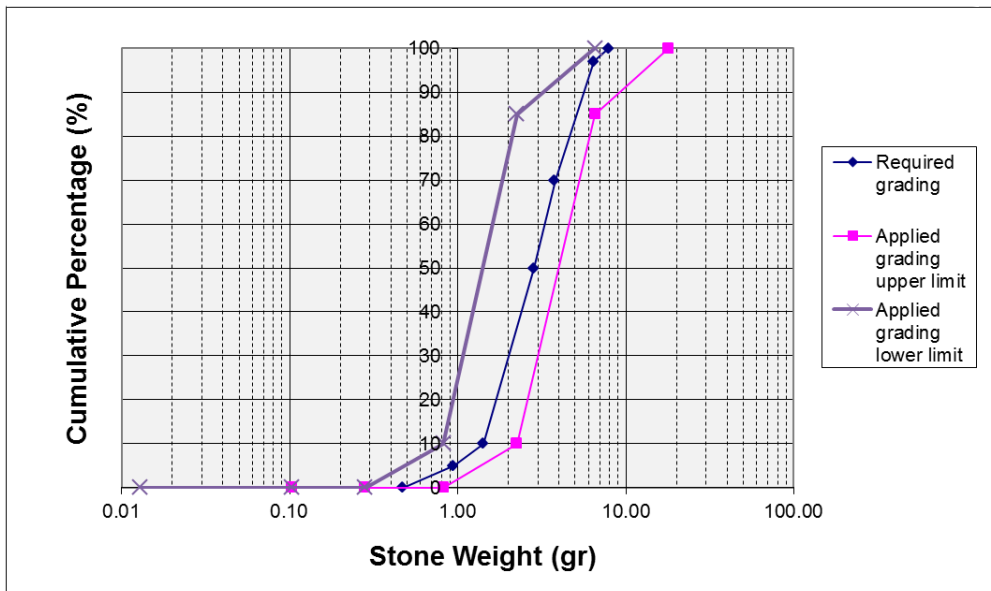


# Appendix C: Under layer composition(s)

Determination of the under layers that were used in both the pull-out tests and the hydraulic physical tests.



(a)  $1/6$  Under layer used for pull-out tests 1 through 3



(b)  $1/11$  Under layer used for pull-out tests 4 through 22 and all hydraulic model tests

Figure C.1: Overview of the model set-up

# Appendix D: Photo series Pull-out tests



Figure D.1: Concave slope profile, increasing the stability



(a) Correct placement      (b) Negative fluctuation: tail unsupported      (c) Positive fluctuation: wing unsupported

Figure D.2: Influence of under layer on placement of model units



(a) Only chamfers make contact      (b) Nose supported on one side only

Figure D.3: Placement errors row underneath



Figure D.4: Model unit slanted backwards



(a) Unit can move sideways

(b) Unit doesn't have enough space sideways, leads to errors in the above row

Figure D.5: Placement distance

# Appendix E: Applicable wave theory

A good indicator of the degree of non-linearity of the waves is the Ursell number given by equation E.1, which is the ratio of the wave steepness over the relative water depth. When the Ursell number is small (say below 5), Linear Wave Theory may be used. For larger values of the Ursell number a non-linear theory such as Stokes theory (adding 1, 3 or 5 sine components) or cnoidal theory should be used. The applicability of theories can also be graphically determined with use of Figure E.1. In this figure the vertical axis represents the influence of the wave steepness and the horizontal axis represents the influence of the relative water depth. The waves as proposed by the test programme of the physical model tests, have an Ursell number ranging from 0.96 to 4.26, indicating that in the beginning the waves are linear but in the end they have become non-linear and 2<sup>nd</sup> order Stokes theory *should* be used. In the Figure this is depicted with the black arrow.

$$N_{Ursell} = \frac{H}{d} \frac{L^2}{d^2} = \frac{HL^2}{d^3} \begin{cases} N_{Ursell} = small, & \text{Linear Wave Theory applicable} \\ N_{Ursell} < 10, & \text{Stokes theory applicable} \\ 10 < N_{Ursell} < 26, & \text{Stokes and cnoidal theory applicable} \\ N_{Ursell} > 26, & \text{cnoidal theory applicable} \end{cases} \quad (E.1)$$

**Table E.1:** Applicable wave theory determined by the Ursell number and the graph by Le Mehaute

H	L	d	T	$N_{Ursell}$	Theory	$\frac{d}{gT^2}$	$\frac{H}{gT^2}$	Applicable Theory
0.0589	1.4367	0.5000	0.971438	0.9732	LWT	0.05401	0.006366	2 <sup>nd</sup> Order Stokes
0.0638	1.5427	0.5000	1.011104	1.2156	Stokes	0.049855	0.006366	2 <sup>nd</sup> Order Stokes
0.0688	1.6451	0.5000	1.049273	1.4887	Stokes	0.046294	0.006366	2 <sup>nd</sup> Order Stokes
0.0737	1.7440	0.5000	1.0861	1.7926	Stokes	0.043208	0.006366	2 <sup>nd</sup> Order Stokes
0.0786	1.8395	0.5000	1.12172	2.1273	Stokes	0.040507	0.006366	2 <sup>nd</sup> Order Stokes
0.0835	1.9318	0.5000	1.156242	2.4927	Stokes	0.038124	0.006366	2 <sup>nd</sup> Order Stokes
0.0884	2.0211	0.5000	1.189763	2.8890	Stokes	0.036006	0.006366	2 <sup>nd</sup> Order Stokes
0.0933	2.1075	0.5000	1.222366	3.3159	Stokes	0.034111	0.006366	2 <sup>nd</sup> Order Stokes
0.0982	2.1913	0.5000	1.254121	3.7734	Stokes	0.032406	0.006366	2 <sup>nd</sup> Order Stokes
0.1031	2.2726	0.5000	1.285091	4.2614	Stokes	0.030863	0.006366	2 <sup>nd</sup> Order Stokes
0.1080	2.3515	0.5000	1.315333	4.7797	Stokes	0.02946	0.006366	2 <sup>nd</sup> Order Stokes
0.1130	2.4288	0.5000	1.344895	5.3307	Stokes	0.028179	0.006366	2 <sup>nd</sup> Order Stokes
0.1179	2.5037	0.5000	1.37382	5.9109	Stokes	0.027005	0.006366	2 <sup>nd</sup> Order Stokes
0.1238	2.5911	0.5000	1.407747	6.6474	Stokes	0.025719	0.006366	2 <sup>nd</sup> Order Stokes
0.1297	2.6760	0.5000	1.440875	7.4278	Stokes	0.02455	0.006366	2 <sup>nd</sup> Order Stokes
0.1356	2.7586	0.5000	1.473258	8.2521	Stokes	0.023482	0.006366	2 <sup>nd</sup> Order Stokes
0.1375	2.7856	0.5000	1.483896	8.5367	Stokes	0.023147	0.006366	2 <sup>nd</sup> Order Stokes
0.1572	3.0440	0.5000	1.586351	11.6498	Stokes	0.020254	0.006366	2 <sup>nd</sup> Order Stokes

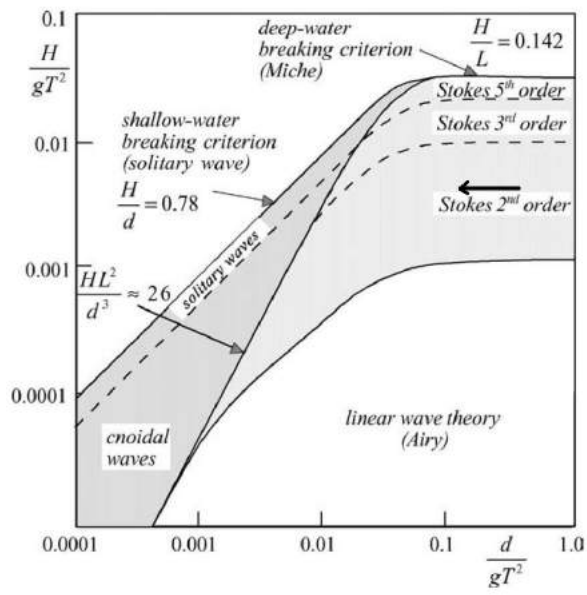


Figure E.1: Applicable theory, after Holthuijsen [2007], modified

# Appendix F: Core Material

## F.1 Theory on Core Scaling

Burcharth et al. [1999] stated that the characteristic pore velocity be chosen as an average of the velocities at 6 locations in the core:

- At the height of the SWL: in the centre of the core, on the interface between core and under layer at the seaward side and in the middle
- At  $1H_s$  below SWL: in the centre of the core, on the interface between core and under layer at the seaward side and in the middle

The horizontal pressure gradient can be calculated with the Forchheimer equation as given in Burcharth and Andersen [1995]:

$$I_x = \alpha \left( \frac{1-n}{n} \right)^2 \frac{\nu}{gd_{50}^2} \left( \frac{U}{n} \right) + \beta \left( \frac{1-n}{n} \right) \frac{1}{gd_{50}} \left( \frac{U}{n} \right)^2 \quad (\text{F.1})$$

In this equation,  $\alpha$  and  $\beta$  are coefficients depending on the Reynolds number (Equation 2.21), grain shape and grading,  $n$  is the porosity of the breakwater and  $U$  is the pore velocity.

By equation the Forchheimer equation to the instantaneous horizontal pressure gradient in prototype, each pore velocity is found. After time-averaging it has to be checked if this pore velocity justifies the applied coefficients  $\alpha$  and  $\beta$  by calculating the Reynolds number.

Now the pore velocity in prototype is known, Froude scaling ( $U_{model} = \frac{U_{prototype}}{\sqrt{N}}$ ) can be applied to find what the characteristic pore velocity in the model should be. With help of Equation F.1 an stone diameter can be chosen. Lastly it has to be checked if the models Reynolds number still justifies the choices for  $\alpha$  and  $\beta$ .

Unfortunately, the tables available for  $\alpha$  and  $\beta$  have been discovered to be not very accurate. The choice for these values is not very straight-forward and the outcome of the approach is very sensitive for these parameters. Additionally, it's difficult to pinpoint the exact porosity of the structure. Therefore, for the calculation of the stability of breakwaters, the lack of knowledge about core scaling is still a major problem.

## F.2 Core composition

It is unclear what kind of grading should be applied around the nominal diameter of 8.8 mm. A Rosin Rammler curve, as described by CIRIA et al. [2007], was created to present a general breakwater core of 1-500 kg and the shape of this curve was fitted around the wanted  $D_{n50}$ . The curve was steepened to exclude fines smaller than 4 mm and to exclude grains with a diameter larger than 16 mm. The first has to do with the permeability of the core becoming to low and the second has to do with the ease of placement. Figure F.1 shows the core grading as used in the hydraulic model tests. The turquoise graph displays the core applied for the preliminary model test by Jacobs [2015], the purple graph represents the Rosin Rammler curve around  $D_{n50} = 8.8$  mm and the pink and blue graphs represent the upper and lower limit of the applied core grading respectively.

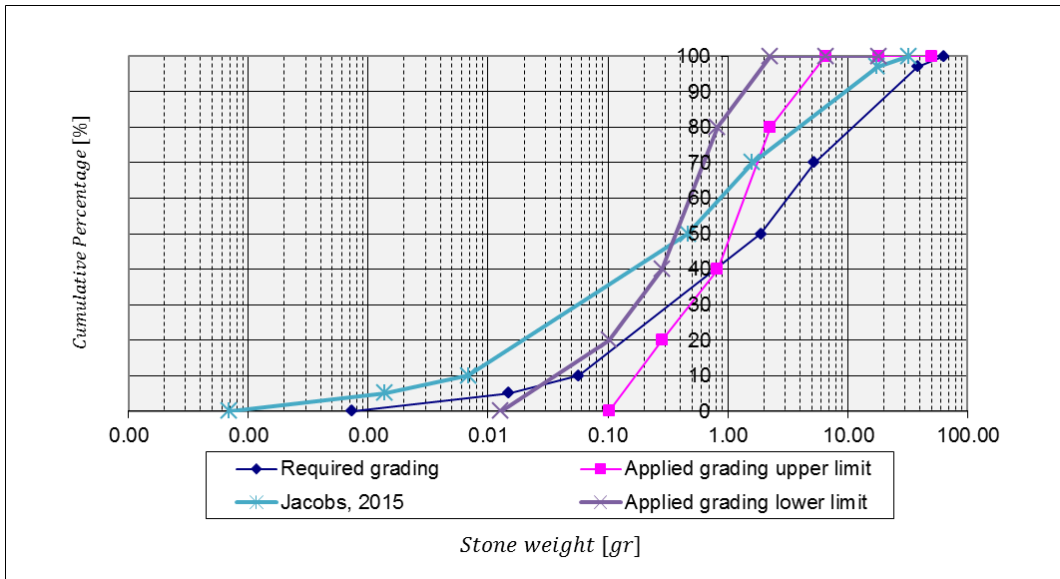


Figure F.1: Cumulative distribution curve of the applied core of the breakwater model

# Appendix G: Actual wave heights

Table G.1: My caption

File name	Hs	T.Hs	H.2%	H.0.1%	Hs/(delta*Dn)	H2%/(delta*Dn)	H0.1%/(delta*Dn)	No rocking	Rocking	Damage	Failure	Nod
Talud 1 - Plastic - Target 0.0673.txt	0.06426	1.003	0.09438	0.1252	1.702143	2.4999728	3.3163446	x				0
Talud 1 - Plastic - Target 0.0898.txt	0.08665	1.146	0.1198	0.1551	2.2952177	3.1733073	4.108347		x	x	x	0.39753168
Talud 1 - Plastic - Target 0.1122.txt	0.1018	1.273	0.1517	0.1609	2.6965166	4.0182865	4.2619796					5.11112161
Talud 2 - Concrete - Target 0.0673.txt	0.06551	1.003	0.09602	0.12	1.7376477	2.5469231	3.1829907	x				0
Talud 2 - Concrete - Target 0.0898.txt	0.09031	1.144	0.1285	0.1658	2.3954658	3.4084526	4.3978322			x	x	0.17037072
Talud 2 - Concrete - Target 0.1122.txt	0.1088	1.248	0.1611	0.1779	2.8859116	4.2731651	4.7187838					0.45432192
Talud 3 - Concrete - Target 0.0673.txt	0.06501	0.998	0.09732	0.1168	1.7243852	2.5814055	3.098111	x				0
Talud 3 - Concrete - Target 0.0898.txt	0.08843	1.144	0.1216	0.1564	2.3455989	3.2254306	4.1484979	x				0
Talud 3 - Concrete - Target 0.1122.txt	0.1101	1.277	0.149	0.1903	2.920394	3.9522135	5.0476928			x	x	0.62469264
Talud 4 - Concrete - Target 0.0673.txt	0.06522	0.9991	0.09625	0.121	1.7299555	2.5530238	3.2095157	x				0
Talud 4 - Concrete - Target 0.0898.txt	0.08912	1.14	0.126	0.1624	2.3639011	3.3421403	4.3076475		x			0
Talud 4 - Concrete - Target 0.1122.txt	0.1074	1.274	0.1546	0.1773	2.8487767	4.1007531	4.7028688			x	x	1.64691696
Talud 5 - Plastic - Target 0.0589.txt	0.05656	0.9343	0.08311	0.1134	1.4981825	2.2014489	3.0037817	x				0
Talud 5 - Plastic - Target 0.0786.txt	0.07613	1.063	0.1093	0.1392	2.01656	2.8951794	3.6871818		x	x		0.11358048
Talud 5 - Plastic - Target 0.0982.txt	0.09426	1.174	0.1299	0.1696	2.4967942	3.4408399	4.4924284				x	1.24938528
Talud 6 - Plastic - Target 0.0589.txt	0.05707	0.9365	0.08448	0.114	1.5116916	2.2377379	3.0196748	x				0
Talud 6 - Plastic - Target 0.0786.txt	0.07841	1.068	0.1138	0.1419	2.0769535	3.0143771	3.7587004		x	x		0.05679024
Talud 6 - Plastic - Target 0.0982.txt	0.09812	1.168	0.1346	0.1461	2.5990394	3.5653353	3.8699516				x	2.83951201
Talud 7 - Plastic - Target 0.0589.txt	0.05859	0.9368	0.08713	0.1178	1.5519539	2.3079321	3.1203306	x				0
Talud 7 - Plastic - Target 0.0786.txt	0.07828	1.064	0.1146	0.1425	2.07351	3.0355678	3.7745935		x			0
Talud 7 - Plastic - Target 0.0982.txt	0.09674	1.181	0.1329	0.1702	2.5624854	3.5203051	4.5083214			x	x	0.51111216
Talud 8 - Plastic - Target 0.0589.txt	0.0582	0.9339	0.08481	0.1146	1.5416234	2.2464791	3.0355678	x				0
Talud 8 - Plastic - Target 0.0688.txt	0.06616	1.011	0.09542	0.129	1.7524709	2.5275208	3.4170004		x			0
Talud 8 - Plastic - Target 0.0737.txt	0.07215	1.047	0.1042	0.1302	1.9111363	2.7600887	3.4487864		x			0
Talud 8 - Plastic - Target 0.0786.txt	0.07832	1.058	0.1152	0.1403	2.0745695	3.0514608	3.716319		x	x		0
Talud 8 - Plastic - Target 0.0835.txt	0.08451	1.104	0.1211	0.1411	2.2385326	3.2077422	3.7375097				x	0.22716096
Talud 9 - Plastic - Target 0.0589.txt	0.05902	0.9337	0.08611	0.1184	1.5633439	2.280914	3.1362236	x				0
Talud 9 - Plastic - Target 0.0688.txt	0.06745	1.008	0.09833	0.1316	1.7866409	2.6046019	3.4858702	x				0
Talud 9 - Plastic - Target 0.0737.txt	0.07403	1.046	0.1055	0.1335	1.9609344	2.7945236	3.5361981	x				0
Talud 9 - Plastic - Target 0.0835.txt	0.08201	1.097	0.1196	0.1472	2.1723116	3.1680097	3.8990888		x	x		0
Talud 9 - Plastic - Target 0.0884.txt	0.09081	1.134	0.1284	0.1577	2.4054093	3.4011074	4.1772168		x	x		0
Talud 9 - Plastic - Target 0.0933.txt	0.09739	1.169	0.1321	0.1745	2.5797029	3.4991144	4.6222215		x	x		0.05679024
Talud 9 - Plastic - Target 0.0982.txt	0.1012	1.187	0.1357	0.1828	2.6806236	3.5944725	4.842075		x	x		0.05679024
Talud 9 - Plastic - Target 0.1031.txt	0.1078	1.222	0.1471	0.1817	2.8554468	3.89644	4.8129378				x	1.64691696
Talud 10 - Concrete - Target 0.0589.txt	0.05633	0.9354	0.08331	0.1098	1.4941489	2.2097913	2.9124365	x				0
Talud 10 - Concrete - Target 0.0688.txt	0.06486	1.01	0.09523	0.1254	1.7204065	2.5259684	3.3262253	x				0
Talud 10 - Concrete - Target 0.0786.txt	0.07538	1.063	0.11	0.1401	1.9994487	2.9177415	3.7294041	x				0
Talud 10 - Concrete - Target 0.0884.txt	0.08675	1.131	0.1235	0.1513	2.301037	3.275828	4.0132208		x			0
Talud 10 - Concrete - Target 0.0933.txt	0.09274	1.166	0.1272	0.1682	2.4599213	3.3739702	4.461492		x			0
Talud 10 - Concrete - Target 0.0982.txt	0.09668	1.188	0.1284	0.172	2.5644295	3.4058001	4.5622867		x			0
Talud 10 - Concrete - Target 0.1031.txt	0.1033	1.222	0.1421	0.1745	2.7400245	3.7691915	4.628599			x	x	0.11358048
Talud 10 - Concrete - Target 0.1080.txt	0.1083	1.247	0.1465	0.1851	2.8726491	3.8859012	4.9097632			x	x	1.07901456



# Appendix H: Log physical hydraulic model tests

This Appendix gives an overview of all observations done for each run. Armour units are referred by their location. The rows are counted from the toe up and each unit is counted either from the left or the right, f.e. 3L row 8 indicates the 3<sup>rd</sup> block from the left side of the flume in row 8. Orange colored runs have been excluded from the data analysis because the slope had already failed or they were otherwise not representative.

**Table H.1:** Test 1, Plastic, large steps

Run	Target $H_s$ [cm]	Time [min]	Observations
-	-	start	No specific initial observations
1	6.73	-	No disturbances
2	8.98	2nd 3rd 4th 6th  12th  16th	Rocking of 3L in row 13 and 14 Considered blocks tilted Extraction of 4 blocks on rows 13 and 14 (or 12 and 13) 3, 3, 2, 1 blocks on rows 12, 13, 14, 15 respectively are caving in Everything is calving in, stones of sublayer are being extracted Extraction of 2 blocks in row 16
3	11.22	1st	Total destruction, stop test

**Table H.2:** Test 2, Concrete, large steps

Run	Target $H_s$ [cm]	Time [min]	Observations
-	-	start	1L on row 11 is not placed firmly, 2L on row 15 is slanting
1	6.73	-	No disturbances
2	8.98	4th 8th 13th	Extraction of 2 blocks in rows 7 and 8 Stabilised Redistribution of blocks to fill the gap
3	11.22	2nd 3rd	Rocking of green block for 3 waves, then extraction Enough failure, stop test.

**Table H.3:** Test 3, Concrete, large steps

Run	Target $H_s$ [cm]	Time [min]	Observations
-	-	start	Slope looks firm/solid
1	6.73	-	No disturbances
2	8.98	5th 10th 15th	No disturbances No disturbances No disturbances
3	11.22	- 3rd 4th	5L row 8 seems to be loose 2L row 8 seems looser 2L row 8 is slanting, no rocking

*Continued on next page*

Table H.3 – Continued from previous page

Run	Target $H_s$ [cm]	Time [min]	Observations
		6th	Extraction of considered block
		7th	Tilting of 2L and 3L row 7, redistribution of blocks to fill gap
		9th	Stable, no rocking
		10th	Extraction of 2L row 9
		12th	Extraction of another block on row 7/8
		13th	Stable, no rocking, 5L row 7 is slanting
		14th	Extraction of 2L row 11, exposing hole
		15th-18th	Stable
		19th	Sliding of loose blocks, stop test

Table H.4: Test 4, Concrete, large steps

Run	Target $H_s$ [cm]	Time [min]	Observations
-	-	start	Robert placed the first 16 rows. 4R and 5R row 11, 3R and 4R row 12 and 4R row 18 are slanting. Around rows 15 and 16 left the slope is concave (hollow)
1	6.73	-	No disturbances. 4R row 11 seems to be slanting less but 6R seems to be slanting more
2	8.98	5th 10th 12th 16th	No disturbances 4L row 8 is slanting and rocks with high energy waves Rocking but stable No rocking, stable.
3	11.22	3rd 4th 5th 6th 7th	Extraction of 6L and 7L rows 6 and 7 4R row 9 half extracted Extraction of multiple blocks in rows 5 and at high energy waves Large pyramid extracted, waiting for redistribution to fill gap No redistribution, test stopped

Table H.5: Test 5, Plastic, large steps

Run	Target $H_s$ [cm]	Time [min]	Observations
-	-	start	Over mid-section of height the slope is slightly convex on the left and concave in the middle
1	5.89	-	No disturbances
2	7.86	4th 9th 11th 13th 13:30	Rocking of 2R and 3R row 7 Also rocking of surrounding block(s) row 8 Also rocking of surrounding block(s) row 9 Rocking and almost extraction of 2R and 3R row 7 At last 2 waves a slid pyramid based at row 7 was created
3	9.82	3rd 9th	3R and 4R row 6 tilted Sudden extraction of 4 blocks in rows 6, 7 and 8. Test stopped

**Table H.6:** Test 6, Plastic, large steps

Run	Target $H_s$ [cm]	Time [min]	Observations
-	-	start	Had a lot of trouble with the sublayer, decided to take off the toe and reconstruct sublayer. Toe was replaced a tad higher. Slope looks firm, 5L row 6 slightly slanted.
1	5.89	-	No disturbances
2	7.86	- 4th 15th -	4L and 5L row 6 seem to be slightly slanted 4L row 6 rocks at high energy waves only (4 times) Last 5 waves caused 5L row 6 to tilt
3	9.82	1st 2nd 3rd 03:25 -	2R row 6 and 3R row 5 tilted Row 7 left falls in gap On the right <u>whole section</u> is rocking Extraction of 2 blocks, test stopped The whole right section was rocking because the toe-beam slid approximately 5 cm to the front, allowing a lot of space between the blocks. <u>Failure because of instability of the toe!</u>

**Table H.7:** Test 7, Plastic, large steps

Run	Target $H_s$ [cm]	Time [min]	Observations
-	-	start	The toe had to be reconstructed again. Issues with the angle of the first 7 rows, it was quite convex [I put the spatula on the bumpy part and knocked it a few times to get it into the right angle]. 3L row 12 is slightly slanted.
1	5.89	-	No disturbances
2	7.86	2nd 5th  12th 15th	3L row 8 rocking at high energy waves Rocking of 3 blocks on the left on rows 7 and 8 at high energy waves 4L row 7 rocking and slanting Slight rocking at row 6
3	9.82	3rd  5th 05:49 8th 09:21 10:21 11:20	Constant rocking rows 6 and 7, 3L row 12 seems slightly slanted 3L row 6 tilted and rocking, row 7 also rocking, 3R on rows 5 and 6 tilted Extraction of 3L row 6 and 2 blocks right on rows 5 and 6, redistribution on the left and arching on the right 2x arching Extraction of 2 blocks right on rows 5 and 6 Heavy rocking left in redistributed part Stones of sublayer right are extracted. Test stopped

**Table H.8:** Test 8, Plastic, small steps

Run	Target $H_s$ [cm]	Time [min]	Observations
-	-	start	There seems to be a harsh dent between blocks 5R and 6R on row 7 and between 4R and 5R on row 8.
1	5.89	-	No disturbances
2	6.87	8th 14th	2L row 7 slight rocking 2L row 7 slanted slightly and constant rocking

*Continued on next page*

Table H.8 – Continued from previous page

Run	Target $H_s$ [cm]	Time [min]	Observations
3	7.37	5th 10th 14:01 15th	No disturbances (no rocking either) No disturbances 2L row 7 slight rocking 4R row 8 seems slightly slanted but could also be the initial dent
4	7.86	2nd 5th 8th 10:38  13th 13:55 14:30 15:20	2L row 7 rocking 2L row 6 also rocking Half extraction 2L row 6 Heavy rocking on those 2 blocks and slightly extracted with each rocking move Rocking stopped Rocking resumed row 7 High energy waves, 2L rows 6 and 7 slanted 2L row 7 tilted
5	8.35	1st 3rd  6th 10th  11th  13th 15th	Rocking on row 8 Rocking only on row 7 and with high energy waves on rows 8 and 9 Redistribution in rows 7, 8 and 9. Stable again Sudden extraction of 4R row 6, this is the block under the initial dent Extraction of 1 block right on row 7 or 8, the 2 blocks above fill in gap Redistribution is still stable Not enough suction force for the blocks to be extracted but examination of the photographs from above points to failure since this is defined as “number of extracted elements from armour layer >1”

Table H.9: Test 9, Concrete, small steps

Run	Target $H_s$ [cm]	Time [min]	Observations
-	-	start	Slope looks firm/solid
1	5.89	-	No disturbances
2	6.87	-	No disturbances
3	7.37	-	4L row 4 slightly slanted
5	8.35	11th 13th	2R row 8 slanting, and rocking. 3R also seems to be slanting 2R row 8 tilted and rocking, seems to be caused by poor inclination of the blocks on the edge
6	8.84	1st 2nd 04:04 04:25  07:15 10:09 16:30	4L row 7 slightly slanted 2R row 9 slightly slanted 3L row 8 rocking at high energy waves High energy wave group caused 4L row 7 to tilt and are forcing 3L and 4L on row 8 out with each passing wave 4L row 7 still present and tilted Stable situation has formed on both the left and the right No extractions yet!
7	9.33	00:58 1:53 07:34 10:50 15:09	3L and 4L row 8 rocking by high energy wave group 4L row 9 fills gap 4L row 6 tilted and rocking, filling the gap Still stable Slope doesnt want to fail

Continued on next page

Table H.9 – Continued from previous page

Run	Target $H_s$ [cm]	Time [min]	Observations
8	9.82	04:24 05:30 09:10	4R row 6 almost tilted 5R row 7 almost tilted, 4L row 8 and 4L row 6 are loose and can be picked up and taken away by waves but hasn't happened 4R row 6 almost out
9	10.31	04:20 05:00 07:20 10:27 15:54 -	High energy wave group causes more blocks to be loose on the left side, on the right side 2 blocks are extracted Slope has stabilised Extraction of 1 block Whole left area moves up and down with high waves Gap left has closed up again In total 3 blocks have been extracted so the slope has failed

Table H.10: Test 10, Concrete, small steps

Run	Target $H_s$ [cm]	Time [min]	Observations
-	-	start	Slope looks firm/solid, 2L row 7 and 4L row 17 slightly slanted
1	5.89	-	No disturbances
2	6.87	-	4R row 6 slightly slanted
4	7.86	-	No disturbances, 1.5 minutes longer than should have been
6	8.84	09:20 11:26	R6 row 7 slanting R6 row 7 rocking
7	9.33	5th 11:02	R6 row 7 rocking slightly only R6 row 7 stopped rocking, no movements at all
8	9.82	- 12:22	Not even at high waves rocking 3R row 5 rocking, slanted
9	10.31	05:30 06:20 06:55 07:30 08:40 10:20 11:55 16:00 16:30	4R row 6 is slowly being pulled out 4R row 6 pulled out and tilted, 5R row 7 fills in gap, both rocking 3R row 5 is being pulled out 3R row 5 tilted and rocking (as are 4R row 6 and 5R row 7) 4R and 5R row 8 is filling gap, 3R row 5 not rocking anymore, is being held in place by 3R row 6 4R row 7 also in gap, pyramid is formed, most blocks in pyramid are rocking 5R row 9 is top of pyramid No extractions yet but 3R row 5 dangerously loose Extraction of 3R row 5 at high energy group
10	10.80	- 02:00 09:30 11:09 12:36	Pyramid is still stable 4R row 6, 2R row 8 and 5R row 7 are rocking Sudden extraction of 6R row 8 Extraction of 4 blocks on the right side, pyramid has evolved to row 11 Test stopped

# Appendix I: Before and after photographs hydraulic physical model tests



(a) Before

(b) After,  $H_s = 8.98$  cm

Figure I.1: Hydraulic physical model tests: test 1



Figure I.2: Hydraulic physical model tests: test 1 extra,  $H_s = 11.22$  cm

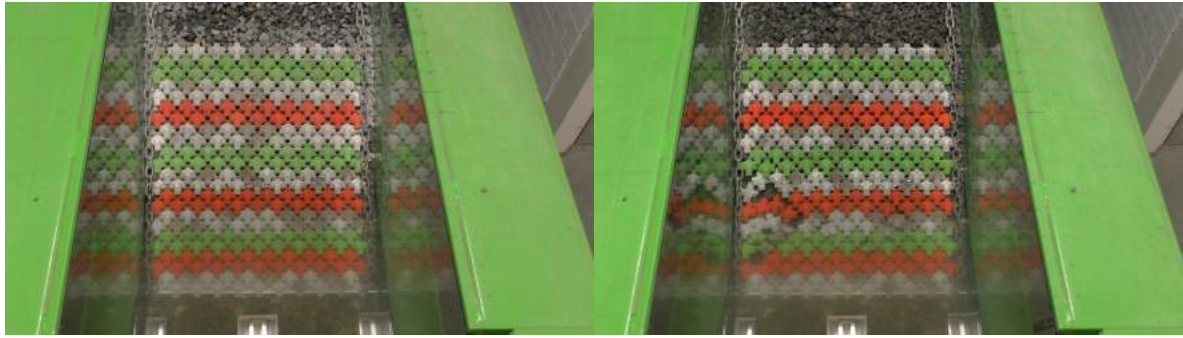


(a) Before

(b) After,  $H_s = 8.98$  cm

Figure I.3: Hydraulic physical model tests: test 2





(a) Before

(b) After,  $H_s = 11.22$  cm

**Figure I.4:** Hydraulic physical model tests: test 3



(a) Before

(b) After,  $H_s = 11.22$  cm

**Figure I.5:** Hydraulic physical model tests: test 4



(a) Before

(b) After,  $H_s = 9.82$  cm

**Figure I.6:** Hydraulic physical model tests: test 5



(a) Before

(b) After,  $H_s = 9.82$  cm

Figure I.7: Hydraulic physical model tests: test 6



(a) Before

(b) After,  $H_s = 9.82$  cm

Figure I.8: Hydraulic physical model tests: test 7



(a) Before

(b) After,  $H_s = 8.35$  cm

Figure I.9: Hydraulic physical model tests: test 8





(a) Before

(b) After,  $H_s = 10.31$  cm

**Figure I.10:** Hydraulic physical model tests: test 9



(a) Before

(b) After,  $H_s = 10.31$  cm

**Figure I.11:** Hydraulic physical model tests: test 10

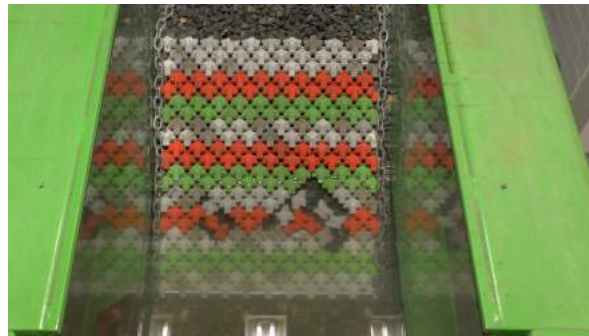


**Figure I.12:** Hydraulic physical model tests: test 10 extra,  $H_s = 10.80$  cm